



ARISTOTLE UNIVERSITY OF THESSALONIKI
Interinstitutional Program of Postgraduate Studies in
PALAEONTOLOGY - GEOBIOLOGY



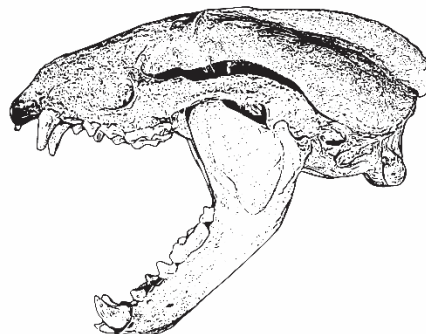
ANNA SAVVIDOU
Geologist

FUNCTIONAL MORPHOLOGY OF THE SKULL IN FOSSIL AND
EXTANT MELINAE

MASTER THESIS

Direction: Macropalaeontology

Directed by Aristotle University of Thessaloniki



THESSALONIKI

2021





Interinstitutional
Program of
Postgraduate
Studies in
PALAEOLOGY – GEOBIOLOGY

supported by:



Τμήμα Γεωλογίας ΑΠΘ
School of Geology A.U.Th



school of biology

Τμήμα Βιολογίας ΑΠΘ
School of Biology A.U.Th



**National and
Kapodistrian
University of Athens**
Faculty of Geology and
Geoenvironment

Τμήμα Γεωλογίας & Γεωπεριβάλλοντος ΕΚΠΑ
Faculty of Geology & Geoenvironment NKUA



Τμήμα Γεωλογίας Παν/μίου Πατρών
Department of Geology, Patras Univ.



UNIVERSITY OF THE AEGEAN

Τμήμα Γεωγραφίας Παν/μίου Αιγαίου
Department of Geography, Aegean Univ.





ANNA SAVVIDOU
ANNA ΣΑΒΒΙΔΟΥ
Πτυχιούχος Γεωλόγος

FUNCTIONAL MORPHOLOGY OF THE SKULL IN FOSSIL AND EXTANT MELINAE

ΜΟΡΦΟΛΕΙΤΟΥΡΓΙΚΗ ΑΝΑΛΥΣΗ ΤΟΥ ΚΡΑΝΙΟΥ ΑΠΟΛΙΘΩΜΕΝΩΝ ΚΑΙ
ΣΥΓΧΡΟΝΩΝ MELINAE

Υποβλήθηκε στο ΔΠΜΣ Παλαιοντολογία-Γεωβιολογία

Ημερομηνία Προφορικής Εξέτασης: 20/05/2021
Oral Examination Date: 20/05/2021

Three-member Examining Board

Professor Dionisios Youlatos, Supervisor
Professor Dimitrios S. Kostopoulos, Member
Professor Nikolai Spassov, Member

Τριμελής Εξεταστική Επιτροπή

Καθηγητής Διονύσιος Γιουλάτος, Επιβλέπων
Καθηγητής Δημήτριος Κωστόπουλος, Μέλος Τριμελούς Εξεταστικής Επιτροπής
Καθηγητής Nikolai Spassov, Μέλος Τριμελούς Εξεταστικής Επιτροπής



© Anna Savvidou, Geologist, 2021

All rights reserved.

FUNCTIONAL MORPHOLOGY OF THE SKULL IN FOSSIL AND EXTANT MELINAE
– *Master Thesis*

© Άννα Σαββίδου, Γεωλόγος, 2021

Με επιφύλαξη παντός δικαιώματος.

ΜΟΡΦΟΛΕΙΤΟΥΡΓΙΚΗ ΑΝΑΛΥΣΗ ΤΟΥ ΚΡΑΝΙΟΥ ΑΠΟΛΙΘΩΜΕΝΩΝ ΚΑΙ
ΣΥΓΧΡΟΝΩΝ MELINAE – *Μεταπτυχιακή Διπλωματική Εργασία*

Citation:

Savvidou A., 2021. – Functional morphology of the skull in fossil and extant Melinae. Master Thesis, Interinstitutional Program of Postgraduate Studies in Palaeontology-Geobiology. School of Geology, Aristotle University of Thessaloniki, 112 pp.

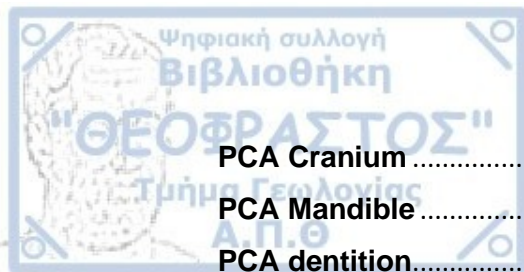
It is forbidden to copy, store and distribute this work, in whole or in part, for commercial purposes. Reproduction, storage and distribution are permitted for non-profit, educational or research purposes, provided the source of origin is indicated. Questions concerning the use of work for profit-making purposes should be addressed to the author.

The views and conclusions contained in this document express the author and should not be interpreted as expressing the official positions of the Aristotle University of Thessaloniki.

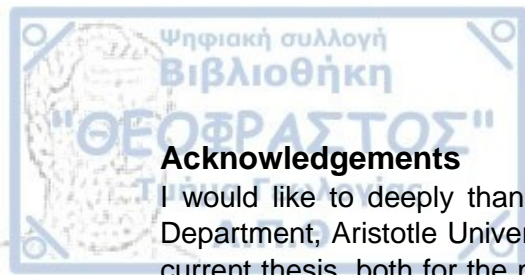


Content

Acknowledgements	9
ABSTRACT	10
ΠΕΡΙΛΗΨΗ	11
INTRODUCTION	12
The genus <i>Meles</i> : origin, systematics, evolution	12
<i>Meles dimitrius</i> Koufos, 1992	13
Extant representative <i>Meles</i> Brisson, 1762	14
MATERIAL	20
METHODS	23
Morphometric measurements and indices	23
Cranial measurements and indices	24
Mandibular measurements and indices	26
Dental measurements and indices	29
HSB structures	31
Dry skull method, computation of bite force and endocranial volume	32
Body mass	34
Myological analysis	34
Dissection	36
PCSA (muscle volume, fascicle length, pennation angle)	36
RESULTS	38
Myological analysis	38
Digastricus	38
Masseter	39
Pterygoids	40
Temporalis	41
Non-metric descriptive comparison of the fossil <i>Meles dimitrius</i> and the extant <i>Meles</i> [<i>Meles meles</i> , <i>Meles canescens</i> (Crete), <i>Meles anakuma</i> , <i>Meles leucurus</i>]	47
Cranium	47
Mandible	51
Dentition	52
HSB structures	54
Metric comparisons	55
PCAs	55



PCA Cranium	56
PCA Mandible	63
PCA dentition	69
Dry skull method; Bite force and Endocranial volume	77
Muscle accommodation	79
PCSA, Bite force and comparison of wet and gross method	83
Body mass	84
DISCUSSION	86
PCA, Non – metric descriptive and Myological remarks	86
Cranium	86
Mandible	90
Dentition	91
Dry skull method / Endocranial volume	93
Dissection / Muscle accommodation	93
PCSA Bite Forces / Comparison of dry method and PCSA (gross) method ..	94
Synthesis / Conclusion	94
Hypothesis for the fossil <i>Meles dimitrius</i>	96
REFERENCES	98
APPENDIX	109



Acknowledgements

I would like to deeply thank my supervisor, Professor Dionisios Youlatos (Biology Department, Aristotle University of Thessaloniki), for his guidance and advice on the current thesis, both for the methodological part as well as for his suggestions on the text. I would also like to express my sincere appreciation to Professor Dimitrios Kostopoulos (Geology Department, Aristotle University of Thessaloniki), member of my examining board, for entrusting me with the studied material which is part of the collection of the Museum of Geology Paleontology and Paleoanthropology, Aristotle University of Thessaloniki (LGPOT), as well as for his helpful advice and suggestions on the text. I deeply thank Professor Nikolai Spassov (Bulgarian Academy of Sciences), member of my examining board, for providing specimens for comparative material, part of the collection of the National Museum of Natural History of Sofia (NMNHS) as well as for his extremely helpful suggestions on the text. My deep thanks to Dr. Petros Lymperakis (curator of the Vertebrate department of the Natural History Museum of Crete), for providing comparative material part of the collection of the Natural History Museum of Crete (NHMC). I also kindly thank Dr. Aleksandra Panyutina (Russian Academy of Sciences, Severtsov Institute of Ecology and Evolution, Moscow, Russia), Ph. D. Professor Senior Engineer Song Li (Kunming Natural History Museum of Zoology, Kunming Institute of Zoology, Chinese Academy of Sciences, No.32 Jiachang Donglu, Kunming, Yunnan, China), Associate Professor Yamato Tsuji (Ishinomaki Senshu University, Ishinomaki, Miyagi, Japan) and Associate Professor Eishi Hirasaki (Kyoto University, Primate Research Institute, Inuyama, Japan) for providing photographic material of specimens crucial for the completion of the current thesis. Also, I thank all those who participated in the excavations of the Mygdonia Basin and especially Professor George D. Koufos (Geology Department, Aristotle University of Thessaloniki) for all his work and contribution to the paleontological excavations. Finally, I wish to thank my friends and family for their unceasing encouragement.



ABSTRACT

The present thesis investigates the functional morphology of the skull of representatives of the subfamily Melinae Bonaparte, 1838. Specifically, it examines the extant genus *Meles* from several localities of Europe and Asia, as well as the fossil species *Meles dimitrius* from the Early Pleistocene of Greece.

This study is composed of three main parts. Firstly, descriptive observations of both myological and osteological nature are presented. The myological analysis examines the skull of *Meles meles* with the purpose of inferring certain information about the masticatory system, creating a 'muscle map' of all the significant muscles included in the feeding procedure and capturing of prey. A muscle map is also created for the extinct species by observing the analogous muscle scars on the cranium and mandible of *Meles dimitrius*. Osteological observations concern morphological features of the cranium, mandible, and teeth, which refer to possible ecomorphological adaptations. Secondly, a quantitative analysis has been conducted, including the computation of several measurements and indices related to functional characteristics in order to concur if there are ecological characters which can be attributed to different ecomorphs. In the third part, a combination of data from the myological analysis and bibliographical method contribute to the computation of bite force (using the Physiological Cross-Sectional Area) of both the gross and dry method, while the results of each method are compared. Hunter Schreger Bands, endocranial volume and body mass were also examined in order to infer additional information about the ecology of the species. It is examined whether there are significant differences in the species of a generalist / omnivorous animal such as the badger.

This analysis aims to the better understanding of the ecomorphology and ecology of *Meles dimitrius*, a close but extinct relative of recent *Meles*. The utter purpose is to create an ecological profile of both the extant badger and of *Meles dimitrius*.

The main findings of the study suggest that the species of *Meles* present certain traits which separate them ecomorphologically in two main groups. The first one includes the mainland species (*M. meles*, *M. leucurus*) and the second one the insular species (*M. canescens* (Crete), *M. anakuma*). *Meles dimitrius* is placed closer to the insular group, which is characterized by relatively more developed masticatory system and specifically by a well-developed temporalis muscle, increased bite forces, increased endocranial volume and a possible better adaptation to consuming and processing meat.

ΠΕΡΙΛΗΨΗ

Η παρούσα εργασία μελετά τη λειτουργική μορφολογία του κρανίου και της γνάθου των αντιπροσώπων της υποκογένειας *Melinae*, Bonaparte, 1938. Συγκεκριμένα εξετάζεται το σύγχρονο γένος *Meles* από διαφορετικές τοποθεσίες της Ευρώπης και της Ασίας, καθώς και το απολιθωμένο είδος *Meles dimitrius* από το Κάτω Πλειστόκαινο του ελληνικού χώρου.

Η ανάλυση που πραγματοποιήθηκε αποτελείται από τρία κύρια μέρη. Αρχικά, πραγματοποιήθηκαν κάποιες μυολογικές και οστεολογικές παρατηρήσεις. Η μυολογική ανάλυση, με την ανατομία κρανίων του είδους *Meles meles*, αποσκοπεί στην παρατήρηση του μασητικού μυολογικού συστήματος καθώς και στη δημιουργία ενός «μυολογικού χάρτη» όλων των κύριων μυών που χρησιμοποιούνται κατά την κατανάλωση τροφής και αιχμαλώτιση του εκάστοτε θηράματος. Ένας «μυολογικός χάρτης» δημιουργήθηκε επίσης και για τον απολιθωμένο αντιπρόσωπο, *M. dimitrius*, με την παρατήρηση των αντίστοιχων μυϊκών αποτυπωμάτων στο κρανίο και τη γνάθο των δειγμάτων. Οι οστεολογικές παρατηρήσεις σχετίζονται με συγκεκριμένα μορφολογικά χαρακτηριστικά του κρανίου, της γνάθου και των δοντιών τα οποία αντιστοιχούν σε πιθανές οικομορφολογικές προσαρμογές. Επιπλέον, πραγματοποιήθηκε μια ποσοτική ανάλυση, η οποία περιλαμβάνει ορισμένες μετρήσεις και δείκτες σχετιζόμενους με λειτουργικά χαρακτηριστικά. Σκοπός ήταν η αναγνώριση ορισμένων λειτουργικών χαρακτήρων, οι οποίοι μπορούν να αποδοθούν σε διαφορετικές οικομορφές. Τέλος, συνδυάζοντας δεδομένα από την επεξεργασία υλικού από τη μυολογική ανάλυση και από βιβλιογραφικές μεθόδους, υπολογίστηκε η δύναμη δαγκώματος. Αυτό πραγματοποιήθηκε με τον υπολογισμό της φυσιολογικής διατομής επιφάνειας (Physiological Cross-Sectional Area), τόσο με τη χρήση μυολογικών δεδομένων (gross method) όσο και από κρανιομετρικά δεδομένα (dry method). Τα αποτελέσματα των δύο μεθόδων συγκρίθηκαν. Επίσης υπολογίστηκε ο όγκος της εγκεφαλικής κάψας, το σωματικό βάρος, ενώ εξετάστηκαν και οι Hunter Schreger Bands γραμμές ώστε να συγκεντρωθούν περισσότερες πληροφορίες σχετικές με την οικολογία των ειδών. Εξετάζεται εάν υπάρχουν σημαντικές διαφοροποιήσεις στα είδη ενός οργανισμού όπως ο ασβός, ο οποίος θεωρείται παμφάγος / γενικευτής.

Αυτή η προσπάθεια στοχεύει στην κατανόηση της οικομορφολογίας και οικολογίας του *Meles dimitrius*, του κοντινού αλλά εξαφανισμένου συγγενή των σύγχρονων *Meles*. Ο τελικός σκοπός είναι η δημιουργία οικολογικών προφίλ τόσο για τα είδη του σύγχρονου ασβού όσο και για τον απολιθωμένο αντιπρόσωπο.

Τα κύρια ευρήματα της έρευνας συνοψίζονται στον διαχωρισμό των ειδών του *Meles* σε δύο οικομορφολογικές ομάδες. Η πρώτη περιλαμβάνει τα είδη της ενδοχώρας (*M. meles*, *M. leucurus*) και η δεύτερη τα νησιωτικά είδη [*M. canescens* (Crete), *M. anakuma*]. Το *Meles dimitrius* τοποθετείται πιο κοντά στη νησιωτική ομάδα, η οποία χαρακτηρίζεται από σχετικώς πιο ανεπτυγμένο μασητικό μυϊκό σύστημα και συγκεκριμένα από έναν καλά ανεπτυγμένο κροταφικό μυ, αυξημένες δυνάμεις κατά το δάγκωμα καθώς και αυξημένο ενδοκρανιακό μέγεθος και πιθανώς μια καλύτερη προσαρμογή στην κατανάλωση και επεξεργασία του κρέατος.

INTRODUCTION

The genus *Meles*: origin, systematics, evolution

The genus *Meles* Brisson, 1762 attributed to the Melinae Bonaparte, 1838 subfamily, of the Mustelidae Fischer de Waldheim, 1817 family, is said to have originated in Asia, from a marten – like ancestor which occurred in the Early – Middle Miocene (Roper, 2010). The tropical forests of SE Asia gave rise to an arboreal, mainly carnivorous predator which gradually abandoned the forested areas for a more open environment. It finally adapted to a terrestrial lifestyle, enhancing its ability to dig burrows (semi – fossorial lifestyle) for protection from potential predators, while also shifting to a more omnivorous diet (Roper, 2010). The consequent genus *Meles* (further deriving from *Melodon* at about 4.4 – 3.6 Ma) (Madurell-Malapeira et al., 2011) dispersed from East to West and finally reached Europe.

The genus is present in faunas dating back to the early Villafranchian while managing to survive until the present day. The badger (*Meles* spp.) is spread throughout the whole Palaearctic region (Madurell-Malapeira et al., 2011 and references therein). The genus *Meles* is represented by six taxa in the fossil record of Europe (*M. thorali*, *M. thorali spelaeus*, *M. iberica*, *M. dimitrius*, *M. hollitzeri* and *M. meles atavus*). The extant representatives of the genus are further separated in *Meles meles* for Europe and SW – Central Asia and *Meles anakuma* for the rest of the Asia including Japan (Baryshnikov et al., 2003). However, several authors support the existence of a third species, *Meles leucurus*, of continental Asia while *Meles anakuma* is confined mainly to Japan. A later hypothesis proposes the existence of a fourth species, *Meles canescens* (Abramov and Puzachenko, 2013). This taxon was firstly recognized as a subspecies of *Meles meles* but upgraded to the species rank since then. *Meles canescens* is distributed throughout Southwest Asia (Sato, 2016). Interestingly, the representatives of *Meles* from the island of Crete and Rhodes Island (Greece) are attributed to *M. canescens* and specifically to the subspecies *M. c. arcalus* (Proulx, 2016). Genetic analyses (Del Cerro et al., 2010; Ibiş et al., 2015; Marmi et al., 2006) place this specific population of the Greek islands closer to *M. canescens* (of SW Asia) rather than to *M. meles* (Europe). Marmi et al. (2006) propose that *Meles* in Crete is linked with the human migration from Asia Minor, as Crete was not connected with the mainland during the Pleistocene.

At an evolutionary context, Abramov and Puzachenko (2013; and references therein) suggest that the beginning of the lineage with *Melodon* (4.4 – 3.6 Ma) led to an ancestor of the genus *Meles* (~2.5 Ma) from which an Asian and a European clade originated at about 1.8 Ma ago (Madurell-Malapeira et al., 2011). *Meles chiai*, of the Late Pleistocene (China) is the first recorded specimen of the Asian clade which later (1.09 - 0.22 Ma) led to two consequent species, those of *M. leucurus* (mainland Asia) and *M. anakuma* (Japan). In the European record, *M. thorali* is firstly described from the Pleistocene of France and is said to combine both Asiatic and European characters. Madurell-Malapeira et al. (2011) suggest that the Spanish *M. iberica* and *M. dimitrius* (from Gerakarou, Greece) should be attributed to *M. thorali*. *Meles thorali* is said to have evolved to *M. m. atavus* (which was proposed to be almost identical to *M. hollitzeri* from Germany, Austria and *M. dimitrius* from Apollonia by Madurell-Malapeira et al., 2011). Nonetheless these suggestions for the union of the subsequent species have not been confirmed and revisions are yet to be made. *Meles m. atavus*

is suggested to have led to two clades of the European badger: *M. meles* (mainland Europe) and *M. canescens* (SW Asia). This separation is believed to have occurred due to palaeogeographic changes and isolation of certain populations.

***Meles dimitrius* Koufos, 1992**

The fossil taxon *Meles dimitrius* was discovered in Greece (localities of Apollonia and Gerakarou). Its taxonomy is controversial as some researchers believe that it consists of two forms (ancestral and derived) with the former including samples from Gerakarou attributed to the ancestral *Meles thoralis* (early – middle Villafranchian) and samples from Apollonia attributed to a more derived form, that of *Meles meles atavus* (Epivillafranchian) (Madurell-Malapeira et al., 2011). Waiting for more material and studies on the taxonomy of the Greek taxon, the examined samples will continue to be referred to here as *Meles dimitrius*.

Localities

The current study examines fossil samples from both Apollonia and Gerakarou localities in Mygdonia Basin (Fig. 1).

Apollonia – 1 (APL) fossil locality belongs to the Platanochori Formation of sands, sandstones, conglomerates, clays, marls, marly limestones, silts and silty sands (Koufos et al. 1995, Konidaris et al., 2015, 2020). The rich mammal fauna revealed is of Early Pleistocene (Epivillafranchian) age, dated indirectly between 1.2 and 1.0 Ma (Koufos, 2018; Spassov, 2003).

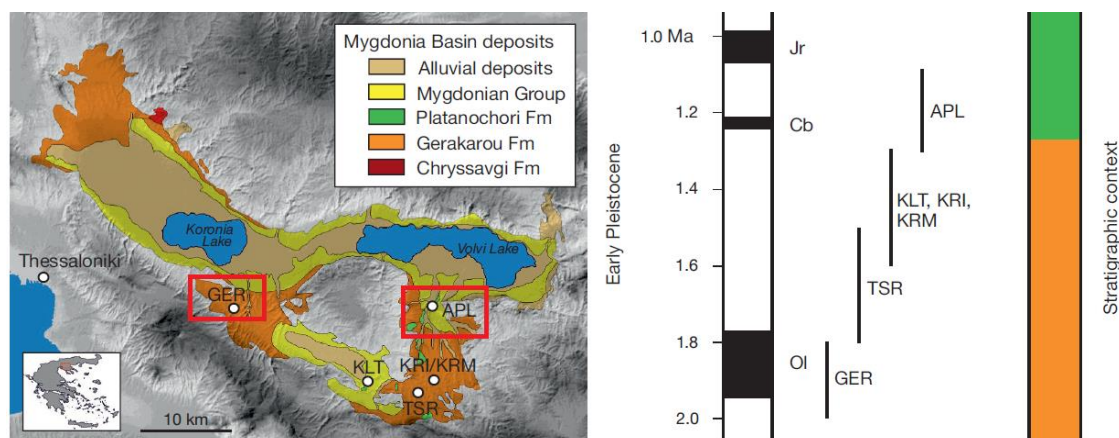


Figure 1. Map of the Mygdonia basin modified from (Kostopoulos et al., 2018). The two localities (GER, APL) are highlighted in red boxes. The stratigraphy of the area is also depicted.

The APL vertebrate fauna consists of the following taxa: *Mammuthus meridionalis*, *Canis etruscus*, *Canis arvensis*, *Canis apolloniensis*, *Lycaon* (=Xenocyon) sp., *Vulpes alopecoides*, *Ursus etruscus*, *Mustela* sp., *Pachycrocuta brevirostris*, *Megantereon cultridens*, *Lynx issiodorensis*, *Equus apolloniensis*, *Stephanorhinus* sp., *Praemegaceros pliotarantoides*, *Arvernoceros* cf. *veretschagini*, *Pontoceros ambiguous mediterraneus*, *Soergelia brigittae*, *Praeovibos mediterraneus*, *Bison* cf. *degiulii*, *Ovis* sp. and *Hemitragus orientalis* (Konidaris et al., 2020; Kostopoulos et al., 2018; Koufos et al., 1992; Koufos and Kostopoulos, 2016)

Gerakarou-1 (GER-1) is also located in the Mygdonia Basin (Fig. 1) and takes part of the upper levels of the homonymous Gerakarou Formation consisting of red brown

sands, gravels, sandy silts and clays characteristic of a fluvio – terrestrial depositional environment (Konidaris et al., 2015; Koufos et al., 1995). The Late Villafranchian Gerakarou fauna is indirectly dated around 1.8Ma and likely before the Olduvai subchron of the Early Pleistocene (Konidaris et al., 2021; Koufos, 2014; Spassov, 2003).

The GER vertebrate fauna includes cf. *Borsodia*, *Apodemus* cf. *mystacinus*, *Hystrix refossa*, *Canis etruscus*, *Canis arnensis*, *Pliohyena perrieri*, *Pachycrocuta brevirostris*, *Panthera gombaszoegensis*, *Mammuthus meridionalis*, *Equus stenonis mygdoniensis*, *Sus strozii*, *Eucladoceros ctenoides*, *Metacervoceros* aff. *rhenanus*, *Croizetoceros ramosus gerakarensis*, *Leptobos* cf. *etruscus*, ?*Gazellospira* sp., *Gazella bouvraine*, and *Antelope koufosi*, (Koufos, 2006; Koufos and Kostopoulos, 2016; Lazaridis et al., 2019).

Studies concerning the APL faunal assemblage of both the carnivorous and herbivorous association show similar results about the palaeoenvironment. As far as carnivores are concerned, a significant abundance of terrestrial and cursorial taxa has been observed while there seems to be a lack of arboreal ones. Moreover, the presence of canids (grassland specialists), felids, hyaenids and mustelids indicates an open environment (Koufos, 2014). Analyses concerning the mesowear of herbivorous teeth as well as morphometric analyses of the metapodials of certain taxa (*Bison*) (Koufos, 2018; Maniakas and Kostopoulos, 2017) indicate mainly grazing-mixed feeding behavior and open to patchy environments. The presence of limited forested areas is also supported by certain taxa (i.e. *Mammuthus meridionalis*, large cervids) (Koufos, 2018). Consequently, the environment should be considered as an open/mixed grassland, comparable to that of a woodland-grassland, with a domination of steppe fauna and elements of open woodland/bushland (Spassov, 2016). These results are in accordance with the existing evidence about the Mediterranean at Epivillafranchian times where alternations between open and forested conditions were typical due to the beginning of the Pleistocene glacial and interglacial oscillations (Kahlke et al., 2011; Vislobokova and Agadjanian, 2016)

The above data suggest that the ecological context of *Meles dimitrius* can be described as a relatively open environment (open grassland) with limited forested patches. A previous analysis of *M. dimitrius* by Kargopoulos (2019) based on several ecomorphological features (such as dental mesowear/morphology, bite force -dry method-, bending strength of canines/incisors and endocranial volume), focusing on an evolutionary context, proposed that *M. dimitrius* had a possibly increased percentage of plant material in its diet compared to the extant *M. meles*, though, these two species were suggested to be quite similar ecomorphologically.

Extant representative *Meles* Brisson, 1762

Meles is found in a vast variety of environments and latitudes due to its extreme adaptability in its variable diet as well as its high endurance in a wide range of climates. For example, in higher latitudes and colder environments it possesses the ability of torpor remaining inactive during the colder months (Elmeros et al., 2018). Another important adaptation is the shift to omnivory, and specifically to opportunistic foraging, making good use of all the available food resources.

The genus *Meles* is also observed in insular environments throughout the Palaearctic region. Specifically, it has an obvious presence in Japan (*M. anakuma*), Korea, Crete (*M. c. arcalus*), Rhodes (*M. c. rhodius*), Sicily and the NW European islands of Britain and Ireland (*M. meles*) (Iurino, 2014; Lynch et al., 1997; Sleeman et al., 2009). Insular badgers are characterized by a smaller size when compared to the mainland populations as well as by an absence of the first upper premolar P1 (Iurino, 2014; Sleeman et al., 2009), adaptations connected to the insular and isolated environments. The endemic fauna of the Holocene islands is believed to have a lowered expression of endemism due to the little time that has passed since the isolation of the taxa (Masseti, 1998), nonetheless differences with the mainland representatives are apparent.

Carnivores are quite rare in insular environments as the majority of them are not efficient swimmers. There is also no standard rule or pattern of features characterizing insular carnivores and changes occurring, are mainly unpredictable in the carnivoran clade. The most common and notable characteristic observed in insular populations is the reduction of size. Such a case could possibly be attributed to ecological release, available food resources (Meiri et al., 2004) and other environmental or ecological factors, which are not yet clearly understood as there are a lot of unpredictable variables and interactions among the taxa. Insular ecosystems are considered to be ecologically unbalanced (Palombo, 2018). It has been noticed that a decrease in size occurs in larger animals when fewer predators and competitors are present (Meiri et al., 2004). This could also be the case for the Cretan badger as it is suggested to be the largest predator on the island (Sfenthourakis and Triantis, 2017) and appears to have reduced its size when compared to the mainland badgers. Since there are no larger predators to compete for the available food resources or to prey on the badgers, size as a defense mechanism is no longer important. Furthermore, limited food resources could also be a reason for size reduction, as original sizes could not be supported by limited food (Sleeman et al., 2009).

Description

The badger (genus *Meles*) is a medium-sized, robust animal (BW = 8 – 15kg, HBL = 56 – 90 cm, with females usually being a little smaller than males). When compared to other carnivores, it is considered one of the largest representatives of the family. It is short limbed and short tailed with a relatively small skull, lengthened snout, and elongated body shape (Roper, 2010).

It possesses powerful non-retractable claws used for digging, while the forelimbs are somewhat stronger and longer than the hindlimbs due to their extensive use for digging (either for burrows or for acquisition of food). Consequently, the morphology of the scapula is typical of that of a semi – fossorial animal (prominent ridge acromion process and deltoid ridge) (Loy, 2018). The front part of the body seems concentrate the majority of the strength (concentration of muscles) making it quite powerful. While not specifically adapted to it, it has the ability to climb and swim (Roper, 2010; Heptner and Sludskii, 2001).

The skull (small in size but elongated in snout length compared to its body size) is characterized by small eyes, and ears and a large nasal cavity, indicating a greater sense of smell compared to sight and hearing (Ewer, 1986; Roper, 2010).

The Melinae possess an extra carnassial cusp, which is diagnostic of the subfamily. The first premolars are residual (and not always present) as a consequence of the enlargement of the first molars and reduction (in size and number) of the rest of the teeth (Hancox, 1988). The dental formula of the European badger is I3/3, C1/1, P4/4, M1/2. Asian badgers are distinguished by European badgers due to the lack of p1 and p2 of the lower dentition and P1 of the upper (Baryshnikov et al., 2003). The dentition is typical of an omnivorous diet. The teeth are equally adapted to crushing, grinding and slicing, as is shown by the reduced blade (when compared to strictly carnivorous taxa), the enlarged protocone of the carnassials and the flat broadened multicusped molars (Ewer, 1986; Loy, 2018).

Habitat use

Meles can survive in a variety of habitats making the best use of their environment. The most suitable environments are temperate climates with sufficient food resources, little competition from other predators (mainly foxes and racoon dogs with which they overlap in diet) and appropriate ground to dig burrows. Deciduous mixed forests with sparse undergrowth, open fields, grasslands, riverine habitats, and steppes are usual habitats for a badger. These conditions may be the ideal however, badgers can and do thrive in the majority of habitats (Roper, 2010).

For their setts, that consist of burrows, they prefer places where they can easily dig, which have tree or rock coverage near the entrance, well drained soils and are mainly isolated in order to avoid predators and possible dangers (Byrne et al., 2012).

Dietary preferences

Despite being described as a carnivore, the badger is adapted to a more omnivorous diet which changes in accordance with the availability of food at a specific place and time of the year. Their omnivorous diet allows them to take advantage of a variety of ecosystems (including urban) (Gomes et al., 2020) making their distribution and survival successful.

The food consumed by badgers varies at different places and periods of the year (seasonal variation). *Meles meles* is described as a generalist predator with opportunistic foraging behavior (Li et al., 2013) despite the fact that many authors have proposed the idea of it being an earthworm specialist (hypothesis that was rejected later) or locally specializing in certain types of food (controversial hypothesis as it has not been fully established) (Roper, 1994).

Multiple studies conclude that badgers feed on almost anything, from plant material, arthropods and invertebrates to carrion, small mammals, amphibians and birds, with the contribution of each food varying in different climates and places (Revilla and Palomares, 2002). More specifically, their diet is composed of fruit, vegetables, cereal, insects, earthworms, invertebrates (like snails, slugs or mollusks), small mammals (rodents, juvenile rabbits), birds, amphibians, reptiles, fish and carrion.

The locality where they reside plays an important role in their diet. It has been found that the diet of the Mediterranean badger compared to that of the Central and Northern Europe presents several differences. In the North small vertebrates are consumed at

a higher rate, whereas in the South insects are preferred as a main protein source (Goszczyński et al., 2000).

In the Mediterranean, the diet of *M. meles* is mainly composed of rabbits, olives, figs and insects (Barea-Azcon et al., 2010; Boesi and Biancardi, 2002; Pigozzi, 1991; Rosalino et al., 2005) with different percentages of each category in different places. For example, in Spain the main source appears to be juvenile rabbits and figs while in Italy, olives constitute a high proportion of their diet (Barea-Azcon et al., 2010). Seasonal variations also exist with fruits consumed more often in the summer and autumn, small mammals in autumn/winter and insects in winter and spring. However, this pattern changes whenever there is abundance in a specific type of food (it is consumed at increased rates due to easier access) (Pigozzi, 1991). Additionally in more humid areas of the Mediterranean there is an increase in the consumption of earthworms (Virgós et al., 2004).

In central Europe the main source seems to be insects and small mammals (less plant material and increased percentages of meat). Fruit also appears to be an important part of their diet (seasonally and not among all localities) (Roper and Mickevicius, 1995). In Britain badgers rely mostly on cereal (Roper, 1994) while there are certain areas where earthworms seem to be a large part of their diet (mainly in humid northern and central Europe where forested areas exist) (Li et al., 2013).

Altitude also seems to play an important role. A study in the Swiss Alpes showed a limit of the dispersal of badgers at 1600-1700m, and they are never found above the tree line (due to limited food resources) (Daiiana, 1995). Another study in the Swiss Jura mountains (Fischer et al., 2005) showed a zonation where, as the altitude increases and the cultivated crops decrease the dietary preferences change (soil management seems to be crucial). In high mountains, mammals, cereal and invertebrates are mostly consumed. In intermediate areas the main food source is maize and mammals. Lastly, in lower altitudes maize, cereal, fruit and mammals (small rodents, lagomorphs) are preferred.

Foraging/feeding Behavior:

Meles is a nocturnal or crepuscular animal (Byrne et al., 2012). It is usually solitary, but when food resources are abundant it may form groups (Carpenter et al., 2005), however, always hunts and forages alone.

Badgers use at an extensive rate their ability to dig, usually by burrowing and rooting in the soil, to acquire their food. While digging, they place their paws to the desired place and rotate their bodies around it. As a generalist forager, it places its nose close to the ground and consumes all that is edible. If food is found in a specific area badgers continue the search in close vicinity of the area (Roper, 2010). They seem to be quite skillful at other strategies too. While not active predators they commonly prey on slowly moving animals killing them with a single powerful bite (Ewer, 1986).

Badgers have developed several feeding tactics. As they are too slow to capture adult rabbits, they feed on the young by locating their sett (usually by smell) and digging vertically down, eating the located prey inside the nest (Roper, 2010). As far as hedgehogs and toads are concerned, badgers turn them on their back, immobilizing them with one paw opening up the prey's belly eating the soft parts while leaving the

skin intact so as to avoid spikes and poisonous skin glands respectively (Roper, 2010). Insects and larvae are unearthed using their front legs, while cow dung is turned upside down in order to find beetles (Ewer, 1986). While feeding on earthworms, badgers plunge their snout on the ground and capture prey with their incisors.

Competition, predators and defense

The Eurasian badger (*Meles meles*), the racoon dog (*Nyctereutes procyonoides*) and the red fox (*Vulpes vulpes*) show an overlap in their diets (similar habitat use), mainly during the winter when resources are limited. However, this overlap is of minor importance as the competition does not appear to be high. Moreover, the amount of overlap decreases as food resources increase (Elmeros et al., 2018; Kauhala and Ihalainen, 2014).

Badgers do not seem to have natural predators however, bears, lynxes and wolves may often hunt them. They defend themselves by hiding in their burrows, but also appear to be quite aggressive when intrigued, a crucial behavior which helps them when encountering enemies. Their strategy of defense is that of stand and fight as they are quite slow animals lacking the ability to outrun all possible predators. Their developed musculature (mainly of the neck) is an advantage while fighting with an enemy (badger or other), as it helps prevent dislocating and breakage of the individual's neck. The usual fighting tactics include face to face biting and snapping at the neck and head of the enemy (Roper, 2010).

An interesting adaptation is that of their skin which is loose and not overstretched, so that predators are unable to have a firm grip on them while lessening the damage inflicted to the underlying tissues. This trait has a secondary use of storing fat during autumn in order to be used during torpor at winter when badgers remain inactive at cold climates (Roper, 2010).

Other threats to badgers are mainly anthropogenic activities such as urbanization, habitat modification, hunting, and road kills. Despite the fact that diseases seem to be quite common in the life of a badger (rabies, bovine tuberculosis, ectoparasites), they are of minor importance as no serious cases have been recorded of a disease killing a vast number of badgers. On the contrary they pose a serious threat to humans and cattle, as vectors.

Aims of the study

The aim of this study is to examine the skull of extinct and extant species of the genus *Meles* from a morphofunctional and ecomorphological perspective. In this way, the skull of the fossil *Meles dimitrius* from Greece will be compared to that of extant species, including *M. meles* (mainland Europe), *M. leucurus* (mainland Asia), the insular *M. canescens* (Crete) and *M. anakuma* (Japan) The study focuses on the analysis of the cranium, mandible, and dentition, in relation to the masticatory abilities and functions. This analysis includes qualitative descriptive (non – metric) and quantitative (metric) univariate and multivariate approaches. The non – metric approaches include observations and comparisons concerning the osteological and myological morphology, related to ecomorphological adaptations of the skull. Firstly, there will be a detailed comparative description of the fossil specimen in terms of functional aspects. Moreover, based on dissections of skulls of extant *M. meles* and

on comparative approaches from the literature (e. g., Ercoli, 2017; Ercoli et al., 2017; Perry, 2018; Sasaki et al., 2000) there will be an attempt to reconstruct the muscular system of the skull and mandible of the fossil *M. dimitrius*. Finally, the structure of the tooth enamel by the Hunter - Schreger Bands (HSB) will also be analyzed, using approaches by Ferretti (2007), Stefen (1999) and Tseng (2012), who have used the HSB structures on carnivores to examine the hardness of consumed food.

The quantitative (metric) approaches include the use of standard distance measurements and indices, related to functional aspects of the cranium, mandible and dentition. These measurements and indices are based on ecomorphological studies of carnivores (Christiansen and Adolfssen, 2005; Cox, 2008; Ellis et al., 2009; Friscia et al., 2007; Friscia and Van Valkenburgh, 2010; Gittleman, 1986; Kieser, 1995; Law et al., 2018; Meachen-Samuels and van Valkenburgh, 2009; Meloro, 2011; Popowics, 2003; Radinsky, 1981; Romaniuk, 2018; Sacco and Van Valkenburgh, 2004; Sicuro and Oliveira, 2002, 2011; Timm-Davis et al., 2015; Zhang et al., 2007) and are related to functional adaptations such as relative development of muscles, induced forces, morphologies correlating to specific behaviors and food preferences. These data will be analyzed via multivariate (Principal Component Analysis) and univariate (ANOVA, Kruskal – Wallis) analyses.

Additionally, endocranial volume, body mass, and bite forces will be computed based on known methods (Damasceno et al., 2013; Finarelli, 2011; Van Valkenburgh, 1990). Bite force will be estimated firstly with the dry method, based solely on cranial measurements, as suggested by Thomasson (1991), and subsequently modified by Christiansen and Wroe, 2007, Sakamoto et al., 2010, and Damasceno et al., 2013. Moreover, bite force will be also estimated with the gross method, based on the physiological cross – sectional area (PCSA) from original dissections (Hartstone-Rose et al., 2019, 2012; Ito and Endo, 2019, 2016; Penrose et al., 2020, 2016). The quotients already proposed by Damasceno et al., 2013 and Sakamoto et al., 2010, will also be applied in order to compare taxa of different sizes in relation to brain volume and bite forces (dry method).

Based on these approaches, this study will test the following predictions: different species of the Eurasian badgers show certain ecomorphological adaptations attributed to different ecologies. Specifically, it is hypothesized that insular badgers discriminate from the mainland ones with respect to ecomorphological characteristics, due to the unique ecosystems of the islands. The fossil *Meles dimitrius* is also expected not to differ greatly from the extant representatives of the genus *Meles*. Moreover, it is tested whether *Meles dimitrius* shares traits with the mainland or the insular extant representatives of *Meles*, or it is discriminated completely. *Meles dimitrius* is expected to be closer to the mainland badgers as no indicator of differences is previously stated.

MATERIAL

The present bone and gross anatomy of the *Meles* skull includes the extant species *Meles meles* (Europe), *Meles canescens* (SW Asia & SE Europe), *Meles leucurus* (mainland Asia) and *Meles anakuma* (Japan), and the fossil species *Meles dimitrius* (Europe).

The fossil material of *M. dimitrius* from Apollonia and Gerakarou sites is part of the collection of the Museum of Geology Palaeontology and Paleoanthropology, Aristotle University of Thessaloniki (LGPOT). The Apollonia material consists of a unique cranium (APL – 544), a partial premaxilla (APL – 545) and three hemi-mandibles (APL – 546, APL – 15, APL – 772) already described by Koufos (1992, 2018) and Koufos and Kostopoulos (1997). The skull has been subjected to postmortem lateral deformation which mainly affects the front area, but it should be taken into consideration. The partial premaxilla is in poor condition while the hemi – mandibles are well preserved with the occasional absence of certain teeth. The material from Gerakarou consists of six specimens: two partial hemi – mandibles (GER – 161, GER – 162), a partial cranium (GER – 164), two partial upper premaxillae (GER – 160, GER – 159) and an individual upper canine (GER – 163) described by Koufos (1992). The GER material is in poor condition and measurements were taken where possible however the samples were mainly used for descriptive observation.

The extant specimens of *M. meles* were acquired from several localities (mainland Greece, Bulgaria) and the specimens of *M. canescens* from the island of Crete. Moreover, the sample was enriched by photographs of the Asian (*M. leucurus*) and Japanese (*M. anakuma*) badger. Photographs of *M. leucurus* are from specimens of Mongolia, Chitinskaya (Russia) (photographs provided by Dr. Aleksandra Panyutina Russian Academy of Sciences, Severtsov Institute of Ecology and Evolution, Moscow, Russia), and China (photographs provided by Song Li Ph.D., Professor Senior Engineer, Kunming Natural History Museum of Zoology, Kunming Institute of Zoology, Chinese Academy of Sciences, No.32 Jiachang Donglu, Kunming, Yunnan, China). Photographs of *M. anakuma* are from Japanese specimens (photographs provided by Yamato Tsuji, Associate Professor, Ishinomaki Senshu University, Ishinomaki, Miyagi, Japan and by Associate Professor Eishi Hirasaki Kyoto University, Primate Research Institute, Inuyama, Japan). Finally, photographs of *M. canescens* (Iran), *M. leucurus*, *M. anakuma* and the fossils *M. m. atavus* and *M. thoralis* from bibliographic sources supplemented the sample (Abramov and Puzachenko, 2013; Argant, 2004; Baryshnikov et al., 2003; Madurell-Malapeira et al., 2011). Digital measurements were taken from the photographs. The sample of the extant *M. meles* includes eight complete skulls. Three of them are part of the LGPUT collection, four part of the National Museum of Natural History of Sofia (NMNHS) and one belongs to a personal collection (from continental Greece). The samples of the extant *M. canescens* (Crete) includes nine skulls. Eight of them are part of the Natural History Museum of Crete (NMHC) and one belongs to a personal collection. A complete list of all the specimens is presented in Table 1.

All measurements and analyses were taken from the sides of the specimens that seem to be more complete, less deformed and less damaged. Not all the specimens were used in the quantitative analyses (PCA), excluding those for which a complete set of

measurements was impossible because of damage. However, all of them were used for the qualitative descriptive comparison.

Table 1. Specimens used in the current analyses.

	Specimen	Source	Location	Preservation
<i>Meles dimitrius</i>	APL 544	LGP	Apollonia	Cranium
<i>Meles dimitrius</i>	APL 545	LGP	Apollonia	Partial premaxilla
<i>Meles dimitrius</i>	APL 546	LGP	Apollonia	Right hemimandible
<i>Meles dimitrius</i>	APL 15	LGP	Apollonia	Left hemimandible
<i>Meles dimitrius</i>	APL 772	LGP	Apollonia	Left hemimandible
<i>Meles dimitrius</i>	GER 164	LGP	Gerakarou	Partial cranium
<i>Meles dimitrius</i>	GER 160	LGP	Gerakarou	Partial premaxilla
<i>Meles dimitrius</i>	GER 159	LGP	Gerakarou	Partial premaxilla
<i>Meles dimitrius</i>	GER 163	LGP	Gerakarou	Upper canine
<i>Meles dimitrius</i>	GER 161	LGP	Gerakarou	Partial hemimandible
<i>Meles dimitrius</i>	GER 162	LGP	Gerakarou	Partial hemimandible
<i>Meles meles</i>	1007	NMNH	Bulgaria	Complete cranium and mandible
<i>Meles meles</i>	1009	NMNH	Bulgaria	Complete cranium and mandible
<i>Meles meles</i>	1010	NMNH	Bulgaria	Complete cranium and mandible
<i>Meles meles</i>	1011	NMNH	Bulgaria	Complete cranium and mandible
<i>Meles meles</i>	K1	LGP	Mainland Greece	Skull
<i>Meles meles</i>	B2	LGP	Mainland Greece	Complete cranium and mandible
<i>Meles meles</i>	H3	LGP	Mainland Greece	Complete cranium and mandible
<i>Meles meles</i>	G4	LGP	Mygdonia, personal collection	Complete cranium and mandible
<i>Meles canescens</i> (Crete)	T5	Personal collection	Crete, Samaria Gorge	Cranium
<i>Meles canescens</i> (Crete)	Fc3802 NHMC 80.5.63.26	NMHC	Crete, Herakleion Galatiana	Complete cranium and mandible
<i>Meles canescens</i> (Crete)	Fc7722 NHMC 80.5.63.47	NMHC	Crete, Vrises Kydonias, Kera Spiliotisa	Cranium
<i>Meles canescens</i> (Crete)	Fc22898 NHMC 80.5.63.92	NMHC	Crete, Antiskari	Complete cranium and mandible



<i>Meles canescens</i> (Crete)	Fc2702 NHMC 80.5.63.15	NMHC	Crete, Herakleion Agiofarago	Complete cranium and mandible
<i>Meles canescens</i> (Crete)	Fc2561 NHMC 80.5.63.17	NMHC	Crete, Rethimnon Psiloritis	Complete cranium and mandible
<i>Meles canescens</i> (Crete)	Fc4685 NHMC 80.5.63.34	NMHC	Crete, Gouvernetou Gorge, Chania	Complete cranium and mandible
<i>Meles canescens</i> (Crete)	Fc3797 NHMC 80.5.63.25	NMHC	Crete, Stalos Chania	Cranium and partial hemi mandible
<i>Meles canescens</i> (Crete)	Fc1364 NHMC 80.5.63.14	NMHC	Crete, Agies Paraskies	Complete cranium and mandible

For the purpose of the myological analysis and the computation of physiological cross – sectional area (PCSA) with the gross method, two complete skulls [1(s), 2(l)] of the species *Meles meles* were dissected. The samples were obtained from road kills, from the area of Northern Greece (Mygdonia) and frozen after death. One of the two skulls was extremely damaged and only the intact parts of it were analyzed.

METHODS

Photos of the physical samples were captured with a Nikon D5200 in order to measure the needed surfaces for the computation of bite force and brain volume with the dry skull method (Damasceno et al., 2013; Sakamoto et al., 2010), as well as compute certain angles and areas for the PCA analyses. All the digital measurements were taken with the software ImageJ (Schneider et al. 2012). Physical measurements were taken with a digital caliper with 0.01 mm precision. The statistical software PAST 4.03 (Hammer et al. 2001) was used for the data analyses (PCA, boxplots, ANOVA, Kruskal – Wallis).

The osteological nomenclature is based on de Lahunta and Evans (2010). The muscle nomenclature is based on Bryden and Halnan (2017) and Penrose et al. (2016).

Morphometric measurements and indices

The measurements and indices computed below are all related to functional aspects and have an ecomorphological interpretation. Each measurement was taken five times and the average score was used in the final analysis.

The Principal Component Analysis (PCA) was used with the purpose of highlighting certain measurements of important ecomorphological effect on the grouping of the different species. In order to control biases from incomplete data and missing values, four PCA analyses were carried out concerning the cranium, mandible, upper and lower dentition, each one restricted on the most complete specimens.

An attempt to standardize the data with the method of geomean of each sample was not successful as the missing data caused an increased error and misplaced the samples where measurements were incomplete. Consequently, the method followed was the use of a proxy measurement that had a good correlation with the mean body size of each extant species, indicating a good predictor of the body mass. The measurements concerning the cranium and upper dentition were standardized using the total condylobasal length (CBL) which could be measured in the majority of the samples. Measurements concerning the mandible and lower dentition were standardized using the length of the lower first molar (m1L). Skull length measurements as well as length of the lower m1 have been previously used in body mass prediction, showing reliable results (Van Valkenburgh 1990, Legendre and Roth, 1988, Meiri et al., 2004 and references therein) so this method was deemed preferable to the method of geomean.

A regression analysis was performed in order to check whether body mass and CBL as well as body mass and m1L have a good correlation relationship. The regression analysis (ordinary least squares regression) was conducted with relation to the mean body mass of the extant specimens (*M. meles*, *M. leucurus*, *M. anakuma*) where data were available from the literature. The regression of body mass and condylobasal length (CBL), showed an intermediate to high correlation ($r=0.54391$, $r^2=0.29584$, $p=0.0209$). The correlation between body mass and length of lower first premolar (m1L) was also found intermediate to high ($r=0.67292$, $r^2=0.45281$, $p=0.0031$).

Furthermore, samples with many missing data (more than half of the measurements) were excluded from further analyses. It should be taken into consideration that measurements of the Asian species (*M. anakuma* and *M. leucurus*) as well as of the

fossil specimens (*M. thoralis* and *M. m. atavus*) were taken digitally so a certain amount of error is to be expected. Moreover, measurements of m2 which was missing from the majority of the samples, were taken from the alveolus of the tooth, as m2 is extremely important for deductions of the feeding preferences and could not be excluded.

In order to better examine the importance of some measurements in distinguishing the species, boxplots of the most influential parameters (inferred from the PCA analysis) were created. These measurements were also examined, so as to evaluate whether they are statistically important. For this purpose, the univariate methods of ANOVA (normal distribution) and Kruskal – Wallis (non-normal distribution) were used.

Cranial measurements and indices

Skull measurements (Figs 2 – 4) and indices were calculated using methods applied in several ecomorphological studies (Christiansen and Adolfsson, 2005; Cox, 2008; Ellis et al., 2009; Law et al., 2018; Meachen-Samuels and van Valkenburgh, 2009; Sacco and Van Valkenburgh, 2004; Sicuro and Oliveira, 2011, 2002; Timm-Davis et al., 2015) and are presented in Tables 2 and 3.

Table 2. Skull measurements (measurements are depicted in Figs. 2 – 4).

Abbreviation	Measurement	Definition
SKL	Total skull length	Distance from prosthion to inion
BCL	Braincase length	Maximum braincase length from the apex of the nuchal crest to the postorbital constriction
BCW	Braincase width	Maximum braincase width perpendicular to BCL
CBL	Condylbasal length	Distance from the apex of the occipital condyle to the anterior of the premaxilla
RL	Rostrum length	Distance between the anterior of the infraorbital foramina to the edge of the premaxilla
IOD	Interorbital distance	Distance between the exterior borders of the postorbital processes
PL	Palatal length	Maximum length of the palatal from tip of alveol to choane
PW	Palatal width	Maximum width of the palate across the lingual borders of the M1
RWC	Rostral width at canine	Maximum width of rostrum at the buccal margin of the canines
RWM	Rostral width at molars	Maximum width of the rostrum at the buccal margin of the first molars
PP	Paroccipital process width	Maximum distance across the paroccipital processes
OSA	Occlusal surface area	Maximum occlusal surface of the postcanine toothrow
MSW	Maximum squamosal width	Maximum zygomatic width (from the exterior border)
ZW	Zygoma width	Maximum width of the zygomatic arch at the jugal squamosal suture
ZFW	Zygomatic fossa width	Maximum width of zygomatic fossa
ZFL	Zygomatic fossa length	Maximum length of zygomatic fossa perpendicular to ZFW

CB	Occipital width	Distance between the exterior border of occipital condyles
OD	Orbital diameter	Maximum orbital diameter from the upper border to the lower
FD	Frontal depth	Maximum distance/depth between the apex of the orbit to the tooth row
VRA	Ventral rostral angle	Angle between center of choane and middle of M1
LRA	Lateral rostral angle	Angle between internasal suture and M1
SKH	Skull Height	Maximum height between the sagittal crest and basion
TRL	Tooth row length	Distance between the I1 to the end of M1
TFL	Temporal fossa length	Distance from the posterior-most point of the temporal fossa to the supraorbital process
POC	Postorbital constriction	Minimum distance across the top of the skull posterior to the postorbital process
MW	Mastoid width	Maximum distance across the mastoid processes

Table 3. Skull indices.

Abbreviation	Index	Definition
MI	Miller's index	$MSW \cdot 100 / SKL$
MI'	Miller's index	$MSW \cdot 100 / CBL$
FR	Facial ratio	RL / SKL

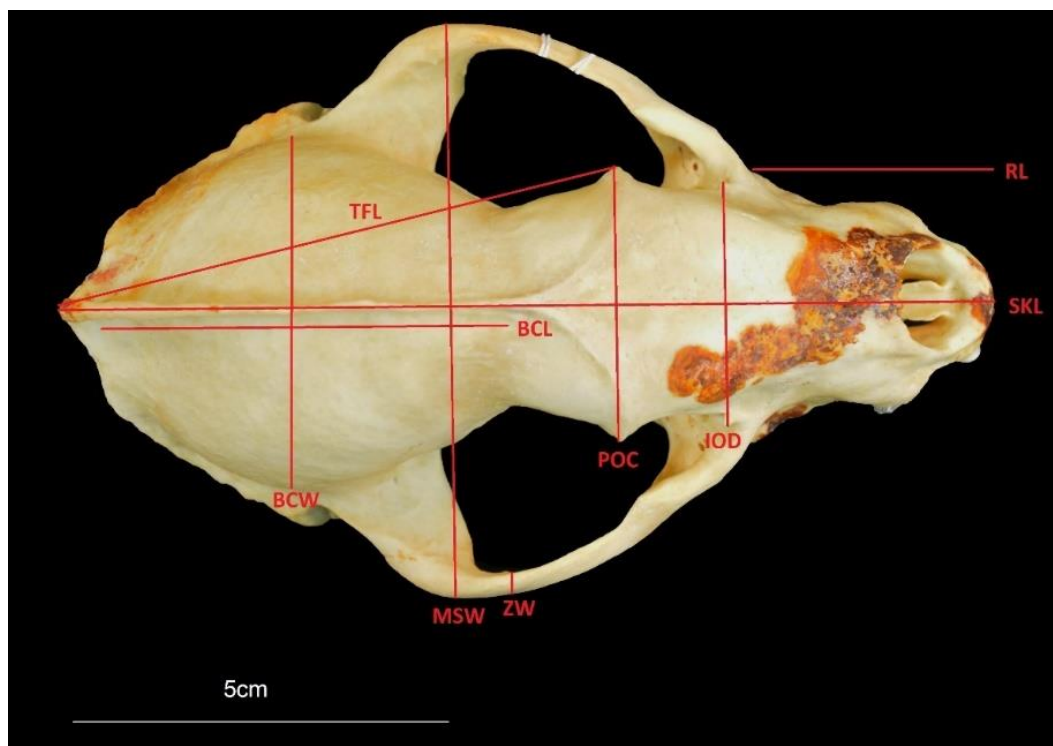


Figure 2. Dorsal view of the Meles cranium. Red lines indicate the skull measurements from the dorsal plane.

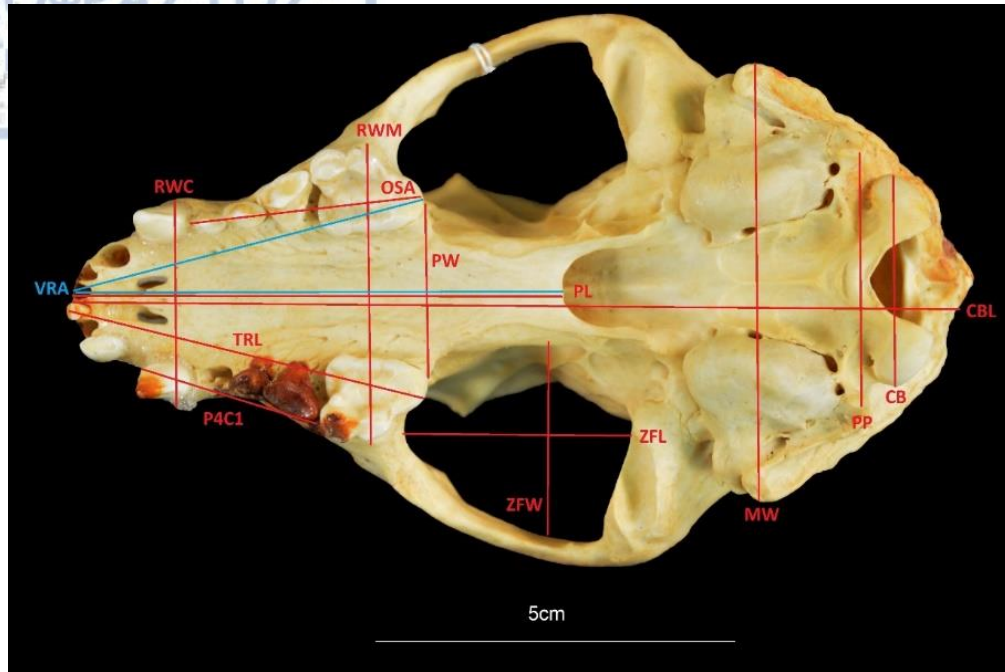


Figure 3. Ventral view of the *Meles* cranium. Red lines indicate the skull measurements from the ventral plane while blue highlights the angles measured.

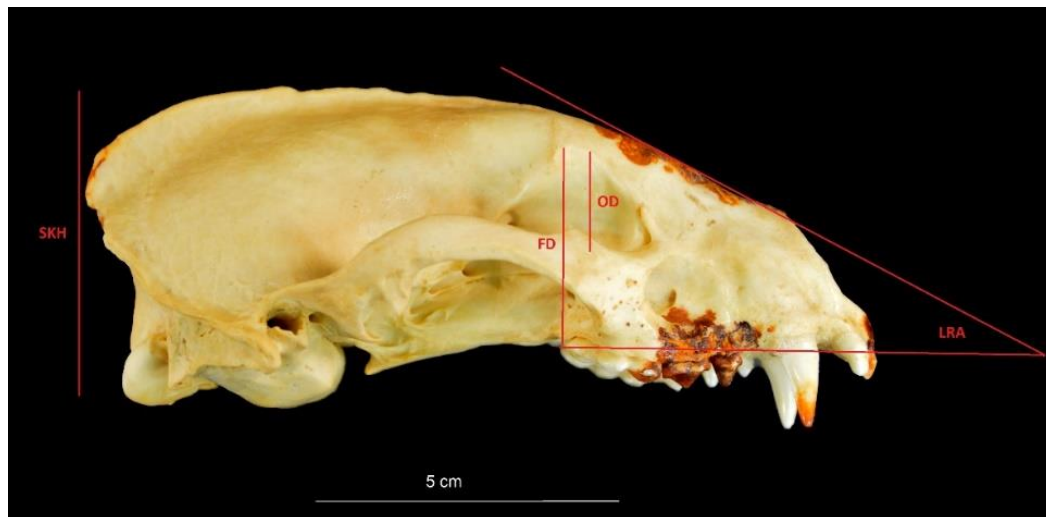


Figure 4. Lateral view of the *Meles* cranium. Red lines indicate the measurements from the lateral plane.

Mandibular measurements and indices

Mandibular measurements (Figs 5 – 6) and indices indicative of functional behavior were computed using methods applied in several of studies (Christiansen and Adolfssen, 2005; Friscia et al., 2007; Kieser, 1995; Meachen-Samuels and van Valkenburgh, 2009; Meloro, 2011; Radinsky, 1981; Sacco and Van Valkenburgh, 2004; Sicuro and Oliveira, 2011, 2002; Timm-Davis et al., 2015; Zhang et al., 2007). The measurements and calculated indices, as well as their definition, are presented in Tables 4 and 5.

Table 4. Mandibular measurements and indices (measurements are depicted in Figs 5-6).

Abbreviation	Measurement	Definition
Dyp3p4	Dentary depth at the p3/p4 junction	Maximum dentary height at the p3/p4 interdental gap
Dym1m2	Dentary depth at the m1/m2 junction	Maximum dentary height at the m1/m2 interdental gap
MAT	Moment of arm of the temporalis	Distance between the apex of the coronoid process and the exterior dorsal border of the mandibular process
MAM/JAPr anterior	Moment of arm of the masseter	Distance between the anterior border of the angular process and the exterior part of the mandibular process
OLCm1	Outer lever moment arm at m1	Distance between the posterior most border of the mandibular process to the most posterior point of m1
OLCc1	Outer lever moment arm at c1	Distance between the posterior most border of the mandibular process to the most posterior point of c1
DL	Dentary length	Distance from the anterior tip of mandibular symphysis to posterior edge of mandibular condyle
MRH	Mandibular ramus height	Maximum height of ramus from apex of coronoid process to deepest point of masseteric fossa
MRW	Mandibular ramus width	Maximum width of ramus from interior condyle process to edge of coronoid process
MFL	Maximum masseteric fossa length	Maximum length of masseteric fossa
JDC1	Jaw depth under the c1	Maximum jaw depth under c1
JDM1	Jaw depth at p4/m1 junction	Maximum jaw depth under the p4/m1 junction
SYML	Symphysis length	Maximum symphysis length at anteroventral margin
WSLA	Working side lever arm	Distance between edge of angular process to anterior border of m1
BSLA	Balancing side lever arm	Distance between apex of coronoid process and jaw line
CPr elevation	Coronoid process elevation	Distance between apex of coronoid process and jaw line
JAPr angle		Angle created by ventral border of angular process, point at corpus below the junction of p4/m1 and condylar process

Table 5. Mandibular indices.

Abbreviation	Index	Definition
MBI	Mandibular bluntness index	Ratio of JW/JL
MATg	Estimator of mechanical advantage of temporalis (general)	MAT/DL
MAMg	Estimator of mechanical advantage of masseter (general)	MAM/DL
MAmasseterm1	Mechanical advantage of masseter at m1	MAM/OLCm1
MAtemporalism1	Mechanical advantage of temporalis at m1	MAT/OLCm1
MAmasseterc1	Mechanical advantage of masseter at c1	MAM/OLCc1
MAtemporalisc1	Mechanical advantage of temporalis at c1	MAT/OLCc1
IXP4	Bending strength at p3/p4 junction, second moment area of the dentary at the interdental gap between p3 and p4 relative to dentary length (DL)	$\sqrt[4]{Ix}/DL$, where $Ix=(\pi Dxp3p4*Dyp3p4^3)/64$
IXM2	Resistance of dentary to bending as measured by the second moment of area at the interdental gap between m1 and m2	$\sqrt[4]{Ix}/DL$, where $Ix=(\pi Dxm1m2*Dym1m2^3)/64$

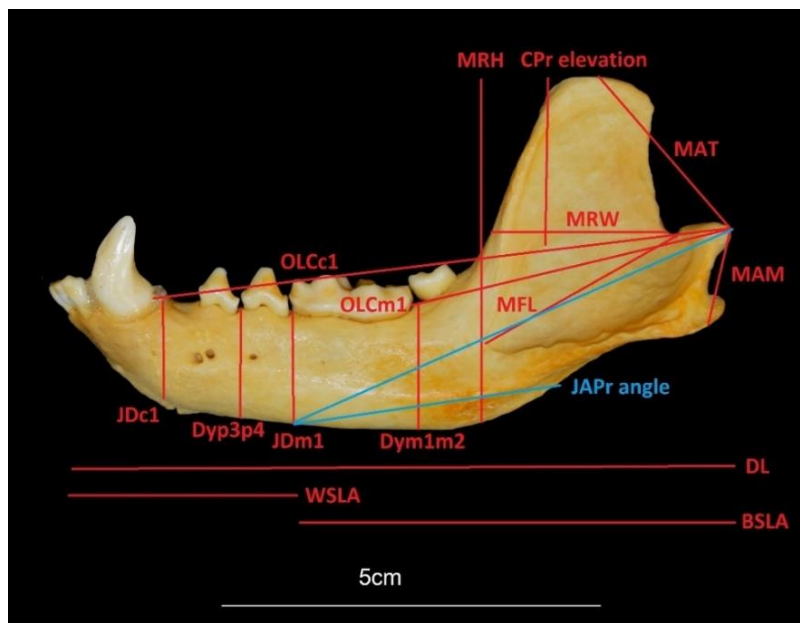


Figure 5. Lateral view of the Meles mandible. Red lines indicate the mandibular measurements of the lateral plane and blue the angles measured.



Figure 6. Dorsal view of the Meles mandible. Red lines indicate the mandibular measurements on the dorsal plane.

Dental measurements and indices

Dental measurements (Figs 7 – 8) and calculated indices, indicative of functional behavior, were based on those from a number of ecomorphological studies (Ely, 2019; Friscia et al., 2007; Friscia and Van Valkenburgh, 2010; Gittleman, 1986; Meachen-Samuels and van Valkenburgh, 2009; Meloro, 2011; Popowics, 2003; Romaniuk, 2018; Sacco and Van Valkenburgh, 2004). The dental measurements and the indices are presented in Tables 6 and 7, respectively. Measured length refers to the anteroposterior diameter of the tooth and width to the mediolateral diameter.

Table 6. Dental measurements (measurements are depicted in Figs 7 – 8).

		Measurement	Definition
Upper dentition	Canine	C1L	Length of C1
		C1W	Width of C1
	Premolars	P3L	Length of P3
		P3W	Width of P3
		P4L	Length of P4
		P4W	Width of P4 (across the protocone)
		P4C1	Distance from P4 to C1
	Molars	M1L	Length of M1
		M1W	Width of M1
		M1a	M1 area
Lower dentition	Canine	c1L	Length of c1
		c1W	Width of c1
	Premolars	p2L	Length of p2
		p3L	Length of p3
		p3W	Width of p3
		p4L	Length of p4

Molars	p4W	Width of p4
	m1L	Length of m1
	m1W	Width of m1
	m2L	Length of m2
	m2W	Width of m2
	m1Ltal	Talonid length of m1
	m1Ltrig	Trigonid length of m1
	pr	Length of lower premolar row
	mr	Length of lower molar row
	m2a	m2 area
	m1a	m1 area

Table 7. Dental indices.

Abbreviation	Index	Definition
CS	Upper canine shape	Ratio of mediolateral width to anteroposterior length, C1W/C1L
P4P	Upper carnassial shape	Ratio of P4 width to P4 length, P4W/P4L
UGR	Relative upper molar grinding area	Ratio of the squared root of the sum of M1 and M2 areas to the dentary length, $\sqrt{(M1a+M2a)}/DL$
M1BS	Carnassial (m1) blade size	Ratio of the length of the trigonid of m1 to the total dentary length, m1Ltrig/DL
M2S	Relative size of m2	Ratio of the squared root of m2 area to the dentary length, $\sqrt{m2a}/DL$
P4S	Lower premolar shape	Ratio of p4 width to p4 length, p4L/p4W
PMZ	Relative total length of premolars	Ratio of the sum of lengths of p2, p3, p4 to the m1 area, $(p2L+p3L+p4L)/m1a$
P4Z	Relative length of p4	Ratio of p4 length to the m1 area, p4L/m1a
LGR	Relative lower molar grinding area	Ratio of squared root of the sum of m1 and m2 areas to the dentary length, $\sqrt{(m1a+m2a)}/DL$

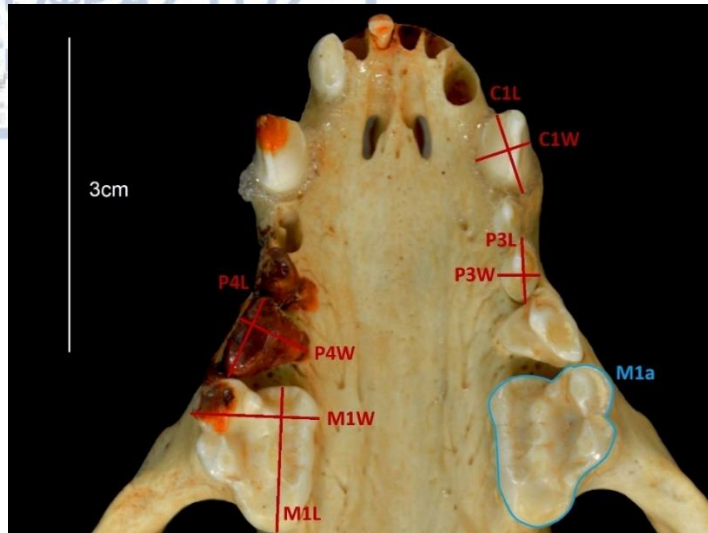


Figure 7. Occlusal view of the Meles upper dentition. Width and length of the teeth are highlighted with red. Blue area indicates the occlusal surface of M1.

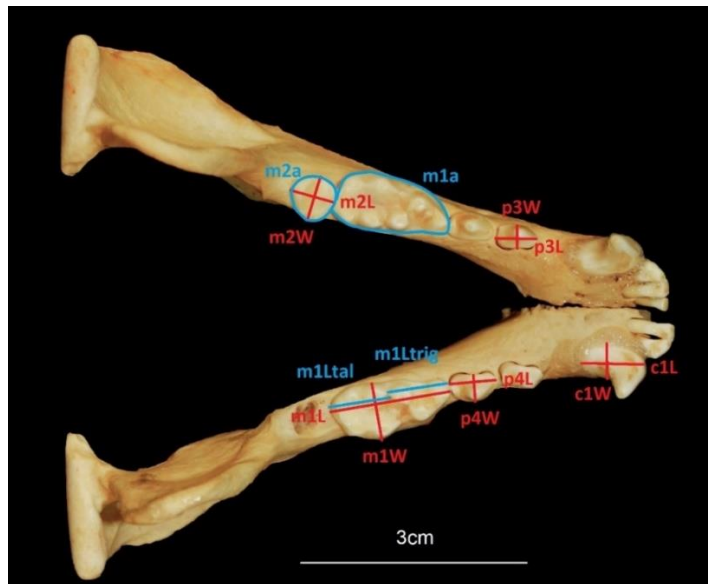


Figure 8. Occlusal view of the Meles lower dentition. Width and length of the teeth are highlighted with red. Blue areas indicates the occlusal surfaces of m1 and m2 while blue lines indicate the length of the talonid and trigonid.

HSB structures

Hunter – Schreger Bands (HSB) were examined under a stereoscope (KONUS Crystal-45) with a digital camera (KONUS#5830, software SCMOS). HSB are formations of the enamel existing in the teeth of living organisms and are presented as alternations of light and dark bands on the teeth, under laterally placed light (Ferretti, 2007). This method is nondestructive, as the teeth can be examined without undergoing any damage. A total amount of 10 measurements was taken from each specimen and the average score was computed.

The HSB structures are considered as an adaptation to withstanding loads, forces and wear induced on the teeth usually during mastication and processing of food (Ferretti, 2007, 1999). There are three different types of HSB structures (Fig. 9) depending on

how folded the bands appear to be. First there is the undulating HSB, with angles exceeding 140° . Second is the acute angled HSB, where the angles are between $70-140^\circ$. Lastly there is the zigzag HSB, where angles are between $50-70^\circ$.

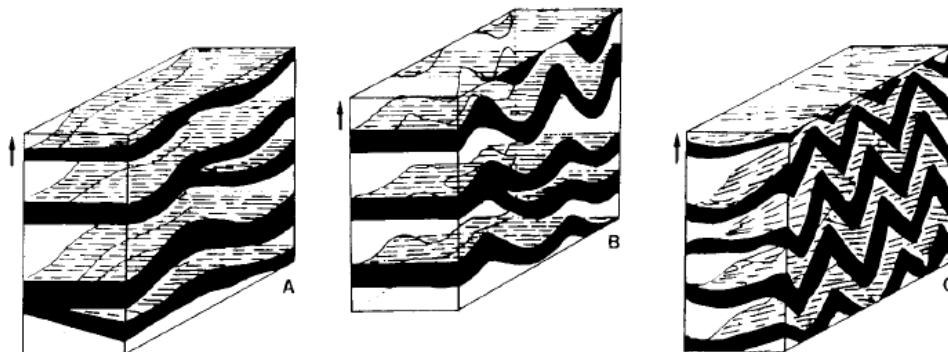


Figure 9. HSB structures. A. undulating HSB, B. acute angled HSB, C. zigzag HSB (adapted from Stefen 1999).

The more acute the angles created, the harder the food processed and consumed by the different taxa. The first category includes a wider variety of dietary groups (insectivorous, frugivorous, carnivorous, piscivorous) while the third is mainly comprised of taxa consuming bones (hyaenas). The second category is intermediate between the two, showing possibly a transitional stage from softer to harder food material (Stefen, 1997).

Dry skull method, computation of bite force and endocranial volume

Bite force is an important component that can be estimated in samples without the application of gross/wet methods (dissection of deceased individuals and measuring of the muscles for the computation of PCSA). This is quite useful as bite force can therefore be estimated even in fossil specimens and compared to extant taxa. Thomason, (1991) was the first one to apply the dry skull method with which he estimated the bite force of an animal solely from skull measurements, computing the physiological cross – sectional area of temporalis and masseter.

Since then, an abundance of studies has been conducted (e.g., Christiansen and Adolfssen, 2005; Christiansen and Wroe, 2007; Damasceno et al., 2013; Sakamoto et al., 2010) and many additions or corrections have been proposed. Moreover, Thomason's initial method seems to result in slightly lower values, so he created a corrective formula that many researchers currently apply. Additionally, for the sole study of bite force unaffected by body mass, a quotient was introduced (BFQ). There are two methods with which it can be computed so that comparisons between taxa of different size be valid. Christiansen and Wroe (2007) introduced the first method which considers the actual body mass (g) of the animals. Such data can only be acquired with certainty from extant specimens while in fossil specimens, body mass has to be computed with other methods which often under- or overestimate the actual values resulting in a greater amount of error. Damasceno et al. (2013) as well as Sakamoto et al. (2010) computed the bite force quotient with a different method that could possibly give better results when fossil samples, or samples whose body mass is unknown, are examined, as it does not include the variable of body mass. These are the methods which will be followed in this analysis, as specimens with unknown initial

body masses are used. The skull measurements involved in these methods are illustrated in Fig. 10.

Damasceno's and Sakamoto's methods are based on Thomason's; however specific alterations have been made. The initial formula used for the calculation of the bite force is:

$$F = \frac{2 * [dm * (M * 300KPa) + dt * (T * 300Kpa)]}{c}$$

where, M and T are the muscle areas computed in ImageJ by digital photos as seen in Fig. 10. These areas are multiplied by the estimated mammalian muscle force (Weijjs & Hillen, 1985) of 300KPa; dm and dt corresponds to the distance between the centroids of each area and the temporomandibular joint and c corresponds to the moment's arm measured as shown in Fig. 10. The estimated mammalian muscle force is a controversial part of the analysis as Christiansen and Wroe (2007) suggest that it led to slightly lower forces and was altered to 370KPa.

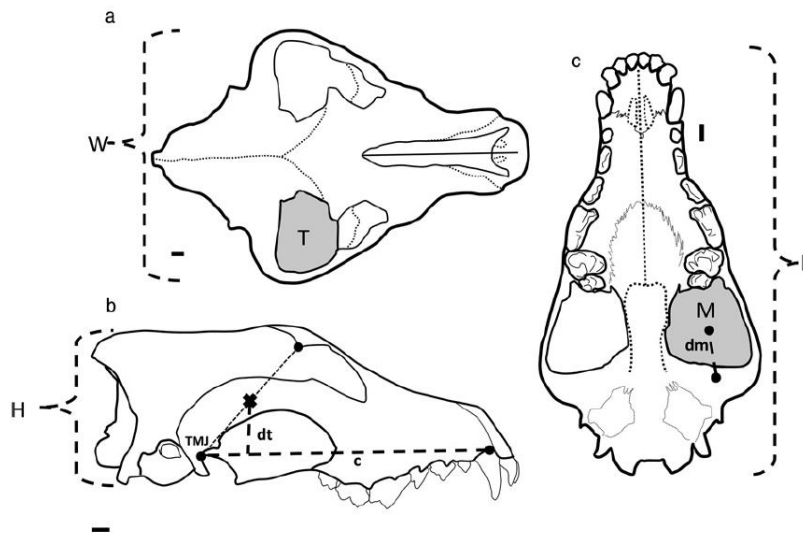


Figure 10. Skull measurements taken for the computation of bite force by the dry skull method, source (adapted from Damasceno et al., 2013)

Thomason's correction method was also applied:

$$F_{corr} = 10^{(0.859 * \log F + 0.559)}$$

Damasceno applied this method in the Canidae while Sakamoto in the Felidae. Both methods were applied here as there is no similar research concerning the Mustelidae. Furthermore, a regression analysis (created by Damasceno and Sakamoto based on their data for the computation of bite force) in order to find a new function better adapted to the Mustelidae could not be accomplished as the matrix does not contain an adequate number of specimens. The two methods differ in the part where BFQ is computed, as Damasceno uses the length of the skull while Sakamoto uses the width. That is to say that the actual numbers of bite force are the same for each method and only the computation of the quotient changes. Nonetheless, BFQ is only used as a comparison variable and not as an actual value of bite force, where body size influence

is nonexistent (Sakamoto et al. 2010). Both of these methods were applied, as Mustelidae are phylogenetically closer to the Canidae (Caniformia), but their killing method is closer to that of the Felidae.

In Damasceno's method, bite force was calculated based on skull length in order to correct the results due to the influence from body size as it was deemed a better proxy for body mass:

$$F_L = 10^{(1.95 \cdot \log L - 1.12)}$$

The bite force quotient was calculated in order to compare the results of bite force of the different species:

$$BFQ = \frac{F_{corr}}{F_L} * 100$$

In Sakamoto's method, skull width is used as an indicator of size.

$$F_{Wsk} = 10^{(1.86 \cdot \log Wsk - 1.06)}$$

Consequently, the BFQ is computed as:

$$BFQ = \frac{F_{corr}}{F_{Wsk}} * 100$$

Brain volume was also computed using the method in Damasceno et al. (2013) and Finarelli (2011). The components of skull height (H), length (L) and width (W) are included (Fig. 10) as well as the natural logarithm:

$$Ln_{(brainvol.)} = -6.23 + 1.06 * \ln(H) + 0.28 * \ln(L) + 1.27 * \ln(W)$$

In order for this number to be corrected without body size influence so as to compare the specimens of different size with each other, a brain volume quotient (BVQ) was computed:

$$BVQ = \frac{brain\ vol.}{bv_{length}}$$

Where bv_{length} is computed by:

$$Log_{(brainvol.)} = 1.7501 * log_{(length)} - 2.0889$$

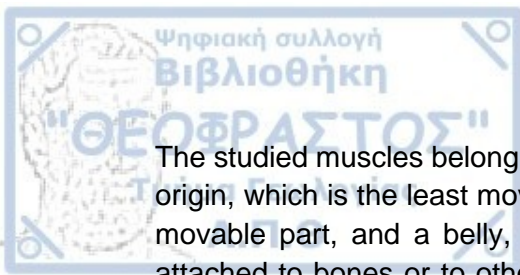
Body mass

Body mass was computed according to Van Valkenburgh (1990), based on skull length by the following formula:

$$B_M = 3.13 * \log_{10}(SKL) - 5.59$$

Myological analysis

For the myological study two completely preserved skulls were dissected. One of the purposes of this analysis was to create a 'muscle map' of the skull of the badger, of the main muscles participating in mastication and to estimate the maximum force production of each muscle by the computation of the PCSA (Physiological Cross – Sectional Area).



The studied muscles belong to the group of skeletal muscles. Each one consists of an origin, which is the least moveable part of the muscle, an insertion, which is the more movable part, and a belly, which is the fleshy portion of the muscle. Muscles are attached to bones or to other muscles by either a rod like tendon or a flattened like aponeurosis. However, several muscles are attached directly to the bone (Evans and DeLahunta, 2013). The studied skulls were dissected in order to observe the origins and insertions of specific muscles as well as the area that each muscle occupies.

Muscles involved in mastication include the mm. temporalis, masseter, pterygoideus and digastricus. These muscles are separated to an adductor and an abductor group. The adductor group includes mm. temporalis, masseter, and pterygoideus and their function is mainly that of closing the mouth. M. digastricus belongs to the abductor group and its function is mainly to open the jaws. The cooperation of these muscles results to the function of mastication, essential to food processing.

Many different suggestions have been made by various authors concerning the division in more superficial and deeper parts of each muscle. No standard nomenclature exists, and each researcher follows their preferable division of the muscle parts. Temporalis and masseter are the muscles with the most complex morphology, while medial, lateral pterygoid and digastricus are more simple. Druzinsky et al. (2011) suggests that in the more primitive taxa, the temporalis is identified with more subdivisions (suprazygomatic, superficial, deep) while many are lost in the more derived forms and their anatomy is presented more simply. The masseter, an extremely complex muscle, is a muscle with multiple layers which is most often separated into three parts (superficial, middle and deep). Nonetheless, deep masseter can usually be referred to as a different muscle called zygomaticomandibularis, further separated into a superficial and a deep layer (Hartstone-Rose et al., 2019; Penrose, 2018 and references therein).

The temporalis is one of the main masticatory muscles and covers a significant part of the skull. It arises laterally from the cranium and inserts on the coronoid process of the mandible. It passes through the temporal fossa up to the sagittal crest and the interior part of the mandible (Evans and DeLahunta, 2013; Hartstone-Rose et al., 2019; Turnbull, 1970).

The masseter arises from the zygomatic arch and inserts onto the masseteric fossa as well as on the lower margins of the mandible and angular process (Hartstone-Rose et al., 2019; Penrose, 2018 and references therein). The temporalis intermingles with masseter between the zygomatic arcs and the coronoid process (Evans and DeLahunta, 2013).

The pterygoids are relatively smaller muscles related to the lateral movements of the mandible when functioning along with the masseter (Penrose, 2018). Pterygoids are usually considered a group consisting of the lateral pterygoid and the medial pterygoid. Their origin is from the pterygoid structure of the skull (pterygopalatine fossa) and their insertion is on the caudomedial part of the mandible. The lateral pterygoid is usually extremely small and often considered insignificant, while sometimes it is regarded along with the medial pterygoid.

The digastricus, which opens the jaws, arises from the paroccipital process and part of the mastoid process (Curtis and Santana, 2018; Hall, 1926) and its insertion is on the caudal part of the mandible (Evans and DeLahunta, 2013). The digastricus also plays a major role in the gape angle. Longer digastricus muscles inserted in a more anterior position of the mandible (as in felids) allow for a wider gape in order to deliver a single lethal bite (Curtis and Santana, 2018). Wider gape is also connected to consumption of larger prey or plant material fitted in the carnassials for processing. Carnivores need a powerful and rapid opening of the jaws in order to capture prey, as well as to disengage the teeth when biting on flesh (Scapino, 1976). Another example is that of the aquatic species, where digastricus is more enhanced in order to open the mandible more easily when underwater which is considered an adaptation to the resistance from water (Scapino, 1976). Nonetheless, the placement and development of digastricus varies among the different families (Curtis and Santana, 2018).

Dissection

Prior to dissection the samples were frozen after death and then preserved in formaldehyde for a few weeks before the final dissection. The decision to work with fixed specimens highly depended on the fact that the samples were mainly road kills, so preservation of the tissues and minimization of the damage was necessary (Martin et al., 2019). Fixation with formaldehyde however has certain drawbacks. According to Martin et al. (2020 and references therein) the fixed material is subjected to certain morphological changes such as a decrease in the mass and shrinkage of the fascicles. Kikuchi and Kuraoka (2014) propose that a correction of 14% for muscle mass and 9 – 13% for fascicle length should be considered to correct the estimated numbers. The first skull was dissected from both sides (right/left) and an average score was computed. The second skull was too damaged from the hit that was deemed to be fatal, that only the right side could be dissected which however was not preserved intact and certain parts (lateral pterygoid) could not be observed.

PCSA (muscle volume, fascicle length, pennation angle)

PCSA requires three components to be estimated according to Gans and Bock (1965) and Gans and de Vree (1987): muscle volume, fascicle length and pennation angle.

$$PCSA(cm^2) = \frac{Muscle\ mass\ (g) * Pennation\ angle\ (cos\theta)}{Muscle\ density\ (gcm^{-3}) * fascicle\ length\ (cm)}$$

Muscle volume

Muscle volume was estimated from muscle mass / muscle density, where muscle density is the muscle density constant of 1.06 gcm⁻³ (simplified), determined by Mendez and Keys (1960) and Murphy and Beardsley (1974).

Muscle mass was estimated using the dry muscle method (over the wet one) meaning that muscles were dried after removal from the cranium and weighted afterwards. This method aims to the least variation of hydration which would affect the muscle mass otherwise (Martin et al., 2020). Consequently, by drying them, all muscles are set to the same amount of hydration. The samples were left to dehydrate for two weeks and then weighted.

Fascicle length

Fascicle length was measured with the method of muscle belly length due to lack of equipment for the application of other more accurate ones (Martin et al., 2020). The length was considered as the length of the fascicles observed along the muscle belly. Several fascicles were measured, and an average score was finally computed.

Pennation angle

The pennation angle of a muscle refers to the arrangement of each muscle fascicle attaching to the muscle tendon. Greater angles indicate greater forces due to the increase on the muscle fascicles accommodated in the area of a muscle (Martin et al., 2020 and references therein).

The masticatory muscles however are particularly complex and similar analyses tend to exclude the pennation angle from the equation for several reasons. Firstly, small angles (usually below 30°) appear to be of little importance and have little effect on the calculation of the force. Moreover, the pennation angle changes rapidly during movements, thus the use of an estimated angle would not be indicative of the actual used during the bite. Additionally, the majority of analyses concerning masticatory muscles, seem to completely exclude the angle due to the fact that these specific muscles are extremely complex and increase the error in the results (Martin et al., 2020).

In order to estimate the actual produced force, PCSA was multiplied by the maximum isometric stress of the mammalian muscles. There are two main suggestions as to what this value is. The first and older one suggested a value of 300KPa. However, this value was said to result in lower computed forces and was corrected to 370KPa (Christiansen and Wroe, 2007).

RESULTS

Myological analysis

The dissection process of the two skulls of the taxon *Meles meles* resulted in the creation of a 'muscle map' for the species, which is presented below (Figs 20 – 27).

All muscles were removed from the most superficial layer to the deepest. The order of detachment was from the digastricus to masseter (superficial, middle, deep), to temporalis (superficial, suprazygomatic, deep) to medial and, finally, lateral pterygoid.

Digastricus

The digastricus (Fig. 11) is the main abductor muscle. It is a quite lengthened muscle and originates from the caudoventral part of the cranium, at the curved surface created between the paroccipital and mastoid process. It has a tendinous origin (Fig. 12). Its insertion is at the caudoventral part of the mandible extending from the angular process to approximately 1/3 of the dentary bone just below the end of the masseteric fossa (prior to the beginning of the tooth row), laterally inserting at the interior part of the mandible. The insertion is deemed fleshy. After removal of the digastricus, the muscle scars where it was attached on the mandible were obvious. This trait was extremely useful for the reconstruction of the position of the muscle on fossil specimens. Digastricus is a single muscle which does not appear to be divided in multiple layers. An anterior and posterior part can be recognized. The anterior part is more extended and develops from the insertion to the end of the mandible. The posterior part continues from the end of mandible (angular process) to the area of the origin (paroccipital – mastoid process area). During opening of the mandible, part of the anterior digastricus moves and contracts as it pulls the mandible to an open position (Fig. 13). The overall shape of the digastricus is elliptical and elongated, with the fibers stretched in parallel to the direction of the mandible.

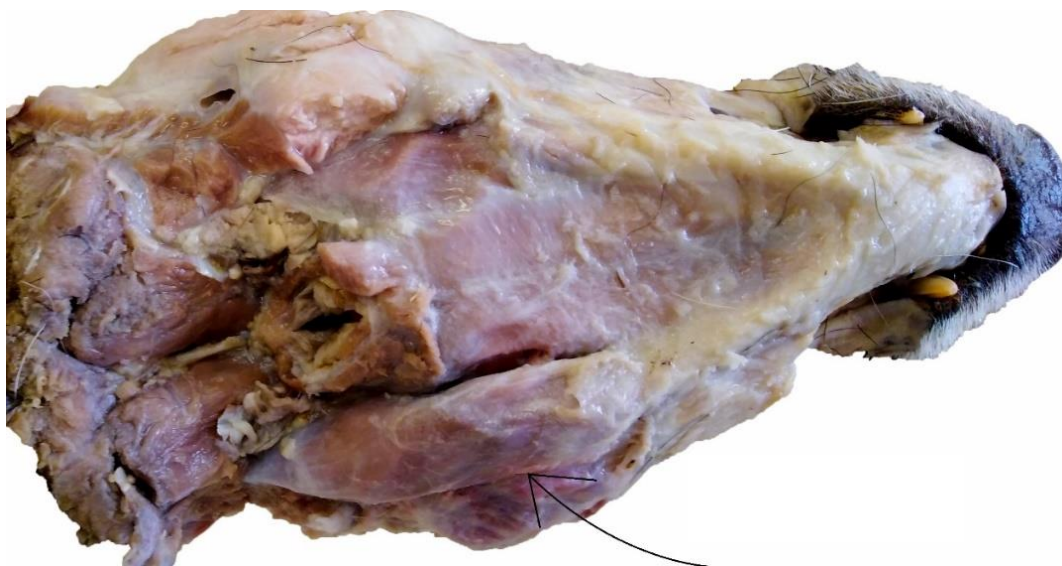


Figure 11. Digastricus muscle of *Meles meles* indicated by the black arrow.

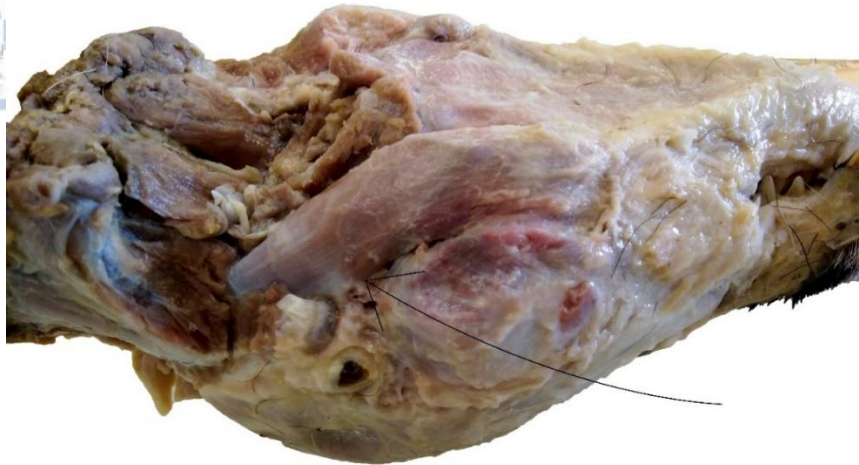


Figure 12. Tendinous origin of the digastricus of *Meles meles* indicated by the black arrow.

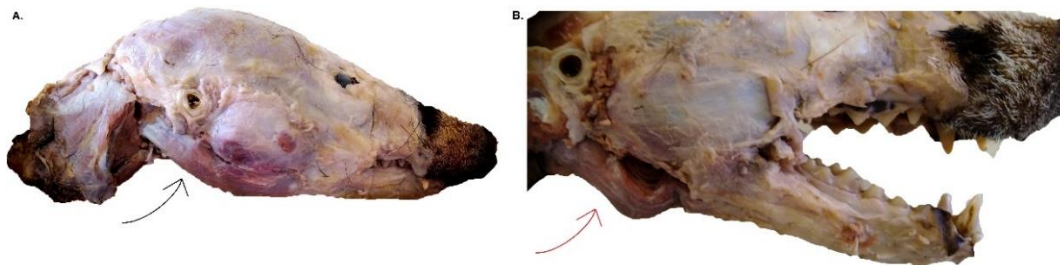


Figure 13. Digastricus of *Meles meles* when mandible is closed (A) and when mandible is open (B) indicated by the arrows.

Masseter

Masseter is one of the main adductor muscles used during mastication. It is quite a complex muscle when compared to digastricus, including three layers which are not always clearly distinguishable. The three layers are the superficial, middle, and deep masseter (or zygomaticomandibularis). The muscle fibers have different directions in each layer (Figs 14 – 15, 26 – 27). Moreover, the superficial and middle parts are hardly separated from each other (mainly at the edges), while the deep masseter is the most distinguishable. Superficial masseter is the larger of the layers followed by the middle and lastly by deep masseter. The superficial layer originates at the rostroventral part of the zygoma covering up to half of the zygomatic area. It has a tendinous origin, while its insertion is partly tendinous and partly fleshy. It inserts on the lower part of the mandible below the masseteric fossa (just after the beginning of the fossa) with the fleshy part, and up to the angular process stopping at the area of the mandibular condyle where a tendinous area exists. The part of the tendinous insertion of the superficial masseter is in contact with the insertion of the medial pterygoid which extends from the internal part of the mandible (Fig. 16). The muscle fibers of the superficial masseter are diagonally placed. Middle masseter is the intermediate layer, and it is not always differentiated from the superficial. It originates at the caudoventral part of the zygoma with a fleshy origin and covers an extended part on the posterior zygoma (approximately half). The insertion of the middle masseter is tendinous and fleshy and is located on the trenchlike morphology of the external caudolateral part of the mandible and continues around the outline of the masseteric

fossa. The muscle fibers are directed almost perpendicular to the development of the dentary bone. Deep masseter is the more internal part of the masseter muscle and originates via a mainly tendinous origin at the posterior part of the zygomatic arch just in front of the temporomandibular joint. The origin turns to fleshy as it proceeds more anteriorly at the zygoma. The insertion is fleshy at its entirety and extends to the area of the mandibular fossa below the tip of the coronoid process. Its fibers are directed almost perpendicular to the fibers of the superficial masseter.



Figure 14. Superficial masseter of *Meles meles* indicated by the arrow.

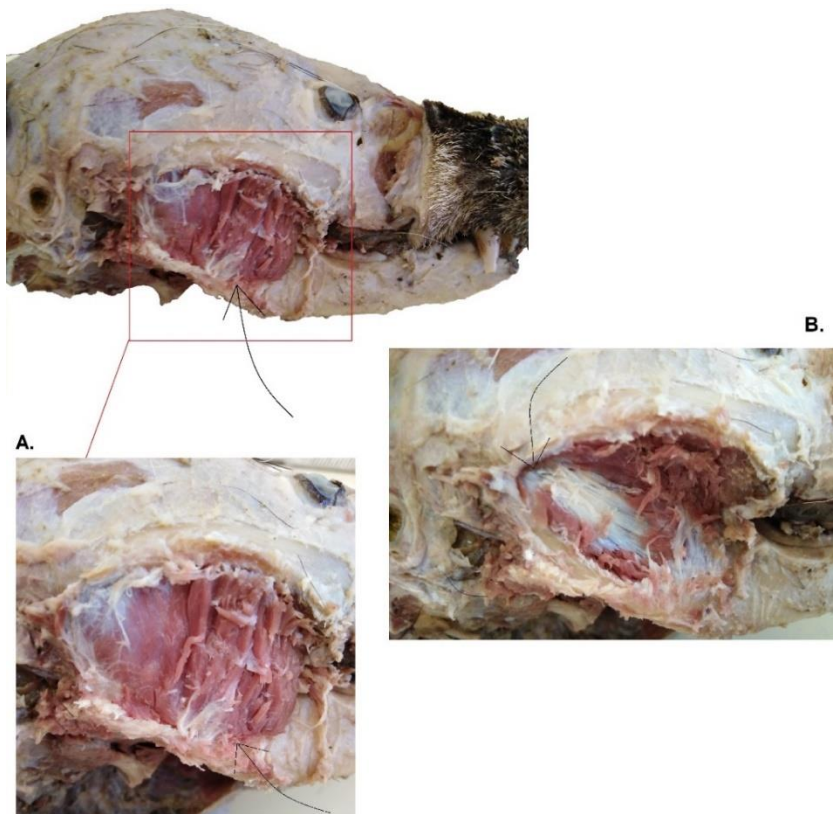


Figure 15. Middle (A) and deep masseter (B) of *Meles meles*. Change of the direction of the muscle fibers in each layer is apparent. B. black arrow indicates the origin of the deep masseter.

Pterygoids

The pterygoids are a group of adductor muscles consisting of the medial and lateral pterygoid. Their function is to move the mandible laterally. The lateral pterygoid is the

smaller of the two and is usually not taken into consideration due to its negligible size. The medial pterygoid is the one to be noticed after extracting the digastricus (Figs 16 – 17). It has a tendinous (partly fleshy) origin which extends from the process of the pterygoid bone to the lateral side of the ventral part of the palate. The medial pterygoid inserts on the lingual caudal part of the mandible just above the angular process via a mainly tendinous and partly fleshy insertion. The muscle fibers have a lateral direction following the development of the muscle. The lateral pterygoid develops accordingly with the medial and originates right above the pterygoid process at a fossa that exists, with a fleshy origin. Its tendinous insertion is located on the lingual side of the mandible just in front of the mandibular condyle. The muscle fibers are directed mediolaterally.

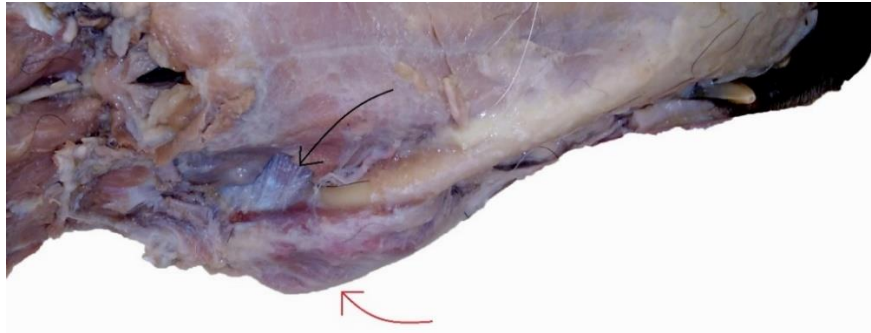


Figure 16. Medial pterygoid of *Meles meles* after extracting digastricus. Black arrow indicates the medial pterygoid which develops lingually and the red arrow indicates the masseter which develops buccally.

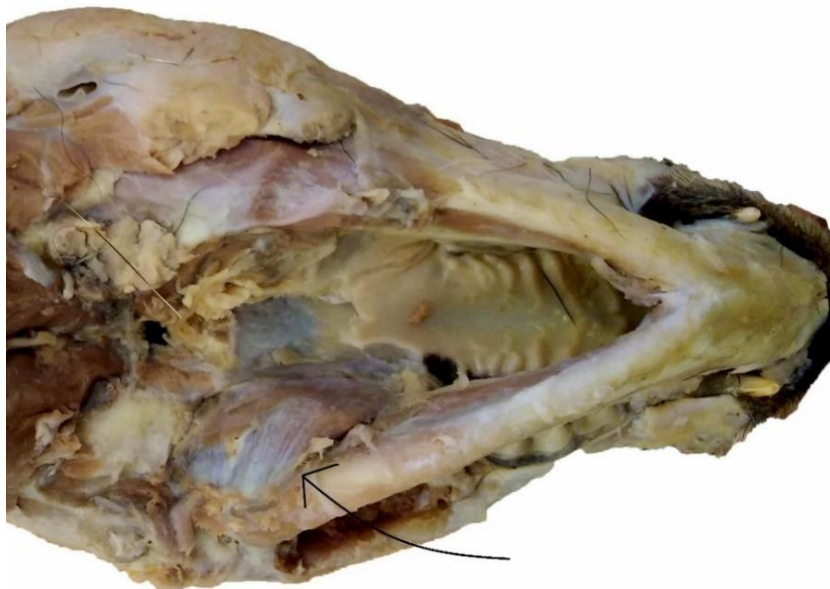


Figure 17. Medial pterygoid of *Meles meles* indicated by the black arrow.

Temporalis

Temporalis is the largest of the main adductor muscles and it is separated into various layers. There is no standard division of the multiple layers and many different separations have been proposed. In this analysis, three main layers were observed (superficial, suprazygomatic and deep) (Fig. 18). The superficial is the largest layer followed in size by the deep and lastly by the suprazygomatic temporalis. The

superficial temporalis originates at the sagittal crest via fleshy parts and inserts onto the internal part of the upper half of the zygomatic arch via tendinous parts, as well as on the anterior and posterior part of the mandibular ramus, dorsal and ventral to the tip of the coronoid process. The muscle fibers are directed diagonally but shift to a more vertical position at the anterior part near the postorbital constriction. The middle layer, referred to as suprazygomatic, originates at the end of the sagittal crest with a fleshy origin and inserts with a tendinous part to the tip of the coronoid process (Fig. 19), extending to the height of the zygomatics, as well as to the internal part of the zygomatic (upper half) contacting the layers of the masseter. The muscle fibers are more caudolaterally directed. Lastly, the deep temporalis is quite developed as a large part of the muscle mass is concentrated there. It originates with a fleshy origin, at the part of the braincase where width is maximum, extending to the front part of the braincase below the postorbital constriction. Its insertion begins on the tendon of the suprazygomatic temporalis and extends deep into the medial part of the mandible covering all of the ramus, down to approximately the height of the mandibular condyle (a few mm below), connecting to the tendon insertion of the lateral pterygoid. The muscle fibers are directed perpendicularly.



Figure 18. Layers of temporalis of *Meles meles*, differentiation shown in black lines.



Figure 19. Insertion of the zygomatic temporalis on the coronoid process of *Meles meles*.

Muscle Map (*Meles meles*, *Meles dimitrius*)

Meles meles

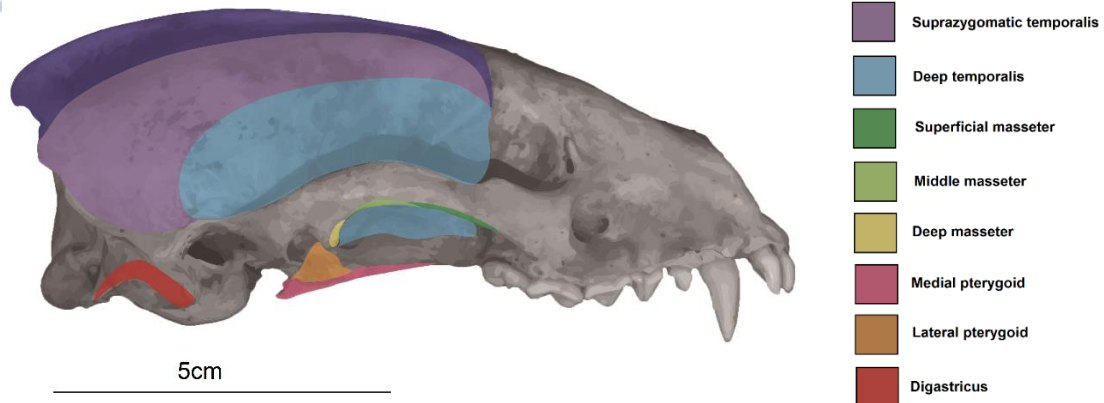


Figure 20. Muscle map, lateral view of the cranium of *Meles meles*, muscle area indicated at the colored areas.

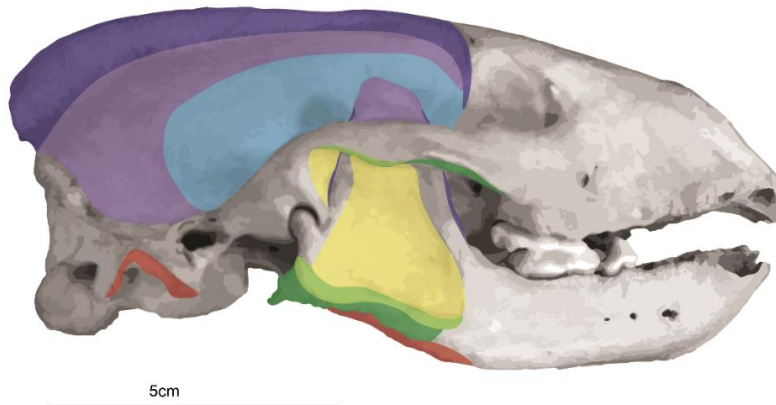


Figure 21. Muscle map, lateral view of the cranium and mandible of *Meles meles*, muscle area indicated at the colored areas.

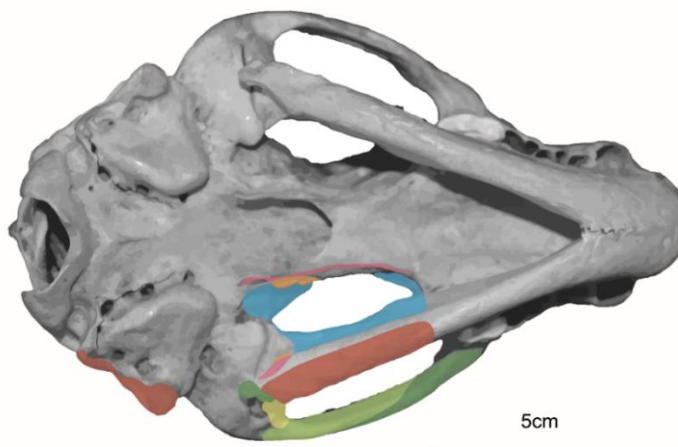


Figure 22. Muscle map, ventral view of cranium and mandible of *Meles meles*, muscle area indicated at the colored areas.

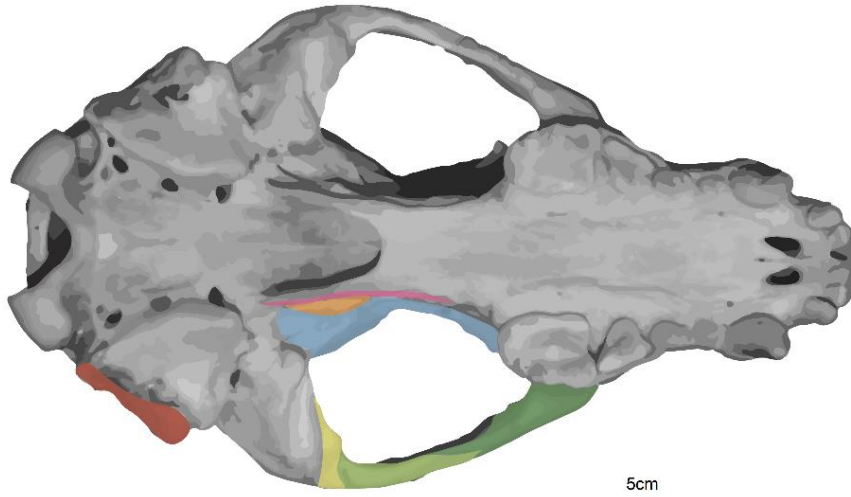


Figure 23. Muscle map, ventral view of cranium of *Meles meles*, muscle area indicated at the colored areas.

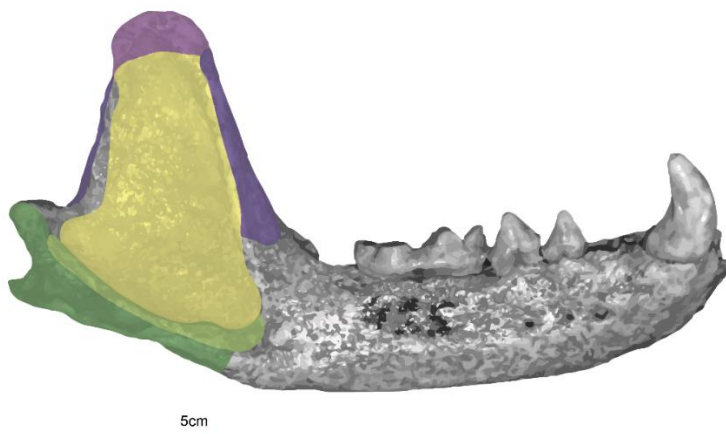


Figure 24. Muscle map, buccal side of the mandible of *Meles meles*, muscle area indicated at the colored areas.

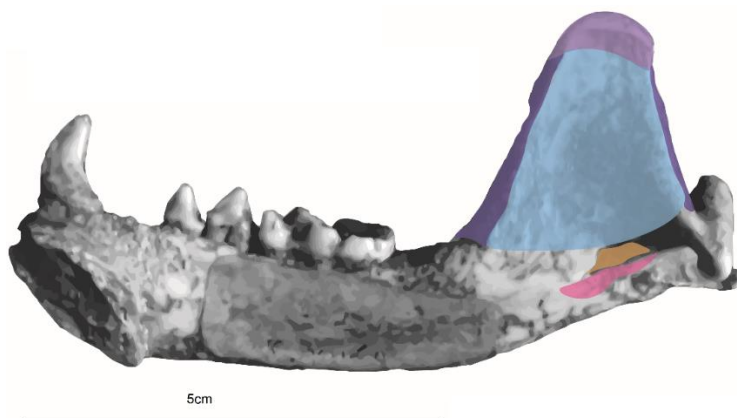


Figure 25. Muscle map, lingual side of the mandible of *Meles meles*, muscle area indicated at the colored areas.

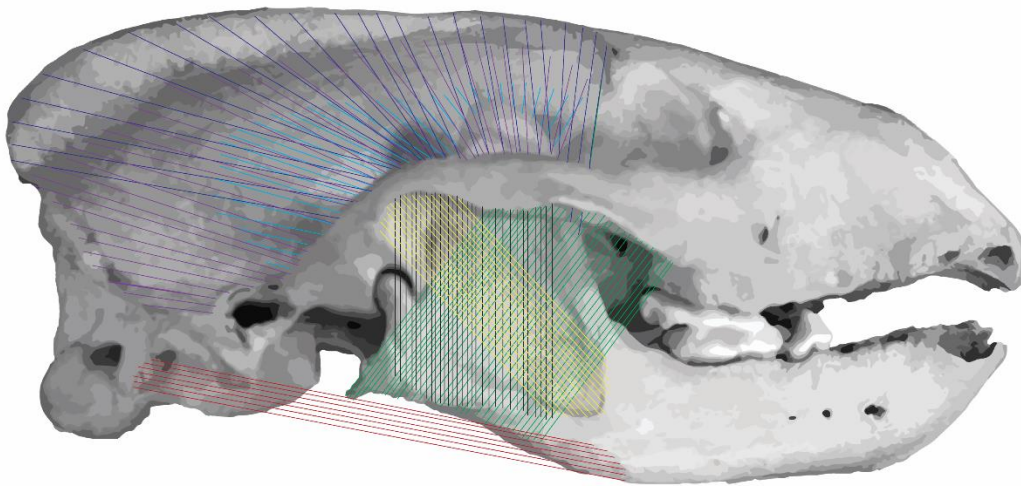


Figure 26. Direction of the muscle fibers (lateral view) on the skull of *Meles meles*.

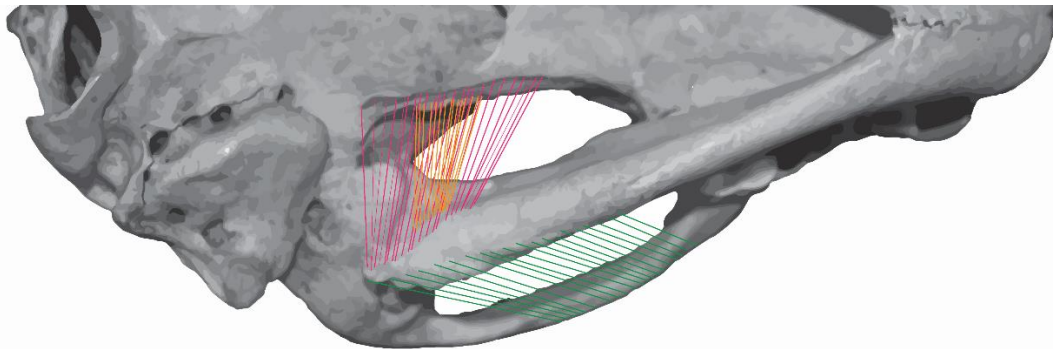


Figure 27. Direction of the muscle fibers (ventral view) on the skull of *Meles meles*.

Fossil species *Meles dimitrius*

After observing the muscle arrangement on the extant *M. meles*, a myological reconstruction map (Figs 28 – 32) of the fossil species *M. dimitrius*, was created. It was based on the muscle scars of the origins and insertions imprinted on the skull left by the muscles which were also observed from the process of dissection.

In general, the muscle arrangement does not seem to differ significantly. Some specific observations which stand out concern the development of certain muscle layers. In detail, superficial temporalis seems to have a larger area of origin as an extra structure related to the sagittal crest exists (Figs 28 – 29). Furthermore, the sagittal crest itself appears extremely high and developed, starting just after the postorbital constriction. The lingual side of the mandibular fossa is straighter in *M. dimitrius* than in *M. meles*, where it is more concave. Thus, superficial temporalis could be more developed in *M. dimitrius* than in the extant species (Figs 28 – 29) and deep temporalis could have a different arrangement of the muscle mass in the extinct and extant taxa (Figs 28 – 30). The angular process is more constricted in the fossils suggesting a more limited attachment area for the superficial masseter (Fig. 31). The insertion area of the middle masseter is more developed in the mainland group (*M. meles*, *M. leucurus*) than in the insular and in *M. dimitrius*, indicating a more developed middle masseter of the first

group (Fig. 31). The rest of the structures do not present any differences affecting the relative placement of the muscles.

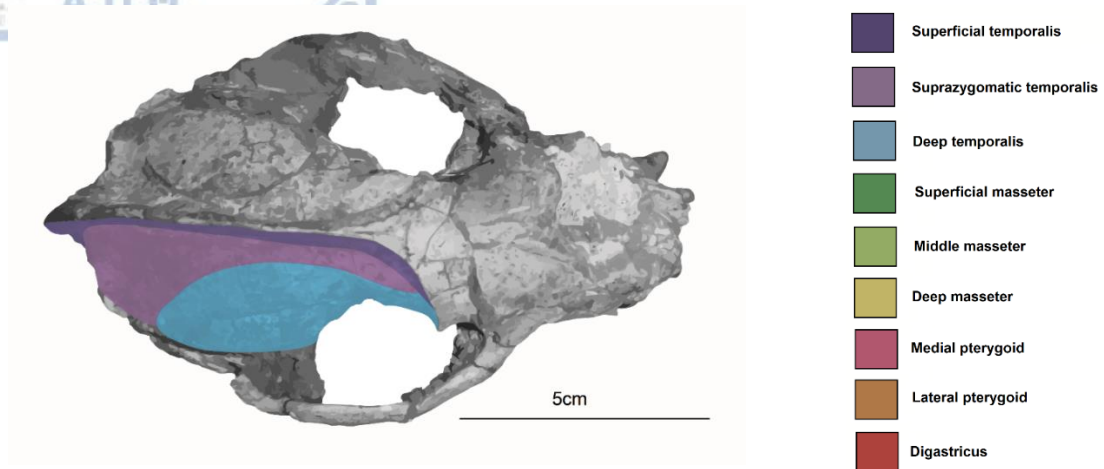


Figure 28. Dorsal view of the cranium of *Meles dimitrius*, colored area indicates muscle area.

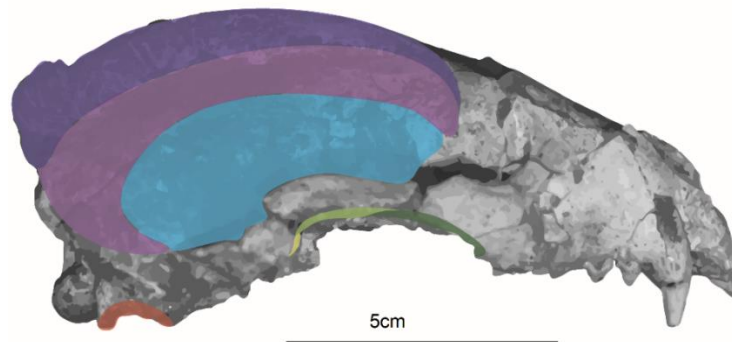


Figure 29. Lateral view of the cranium of *Meles dimitrius*, colored area indicates muscle area.

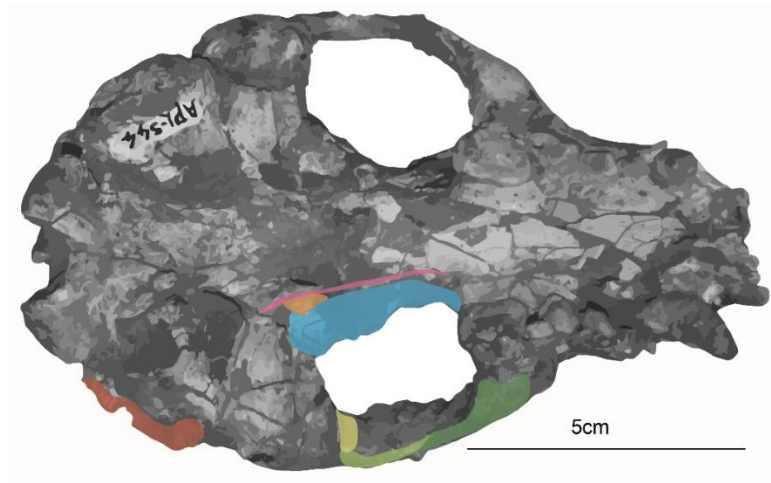


Figure 30. Ventral view of the cranium of *Meles dimitrius*, colored area indicates muscle area.

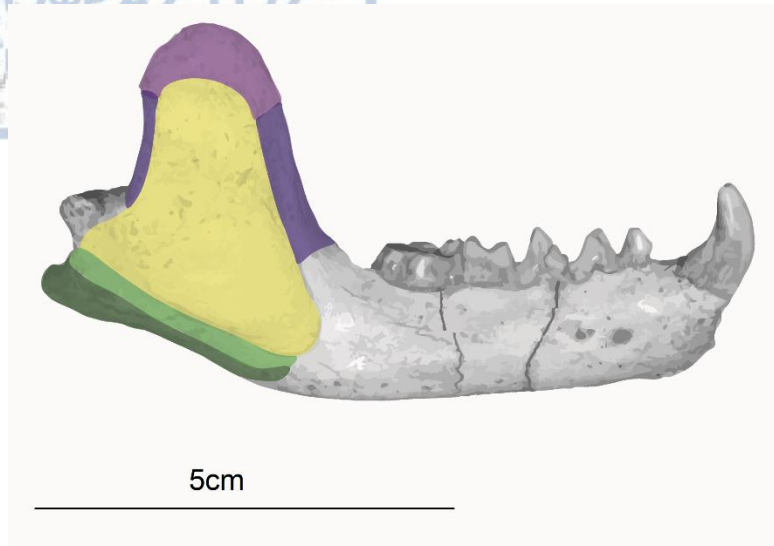


Figure 31. Buccal side of the mandible of *Meles dimitrius*, colored area indicates muscle area.

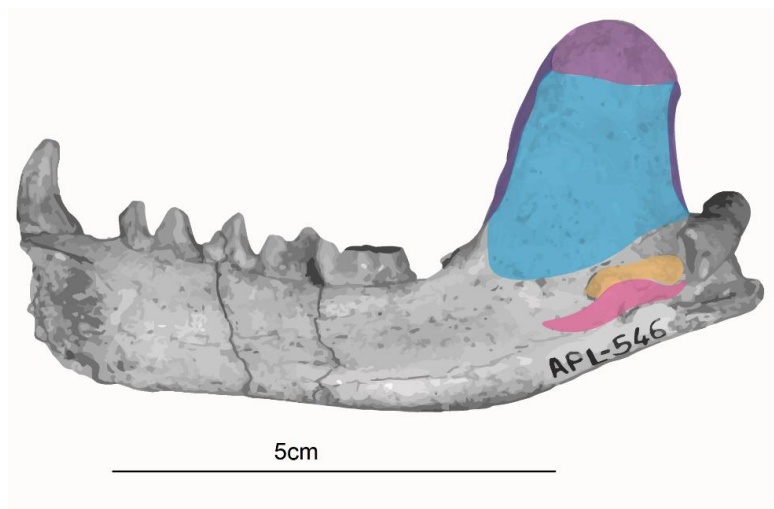


Figure 32. Lingual side of the mandible of *Meles dimitrius*, colored area indicates muscle area.

Non-metric descriptive comparison of the fossil *Meles dimitrius* and the extant *Meles* [*Meles meles*, *Meles canescens* (Crete), *Meles anakuma*, *Meles leucurus*]

Cranium

When examining the specimens in more detail, a notable trait that is observed in *M. dimitrius*, is the over – developed sagittal crest (Fig. 33), indicative of the insertion area of the superficial temporalis muscle (Dumont et al., 2016). In *M. dimitrius* it is developed as a whole structure (height and length) while in *M. meles* and *M. leucurus*, it is less intense, and its beginning is more apparent a few mm after the postorbital constriction. *Meles anakuma* as well as skulls of *M. canescens* (Crete) do not seem to have such developed structures in their majority.



Figure 33. Sagittal crest of the species, red boxes highlight the area. A. *Meles dimitrius*, B. *Meles canescens* (Crete) (robust specimen Fc 1364), C. *Meles leucurus*, D. *Meles meles*, E. *Meles canescens* (Crete), F. *Meles anakuma*. Not in scale.

An additional structure that differentiates the extant and extinct species is located on the front part of the sagittal crest (Fig. 34) which also corresponds to the insertion of the temporalis and specifically of the superficial layer, as observed during dissection. In *M. dimitrius*, there is an extra extended part connected to the sagittal crest which is absent from the rest of the species. The area on both sides of the postorbital constriction appears more triangular in *M. dimitrius* referring to deeper muscle scars than in the group of the extant *Meles* where the area is smoother and more spherical.

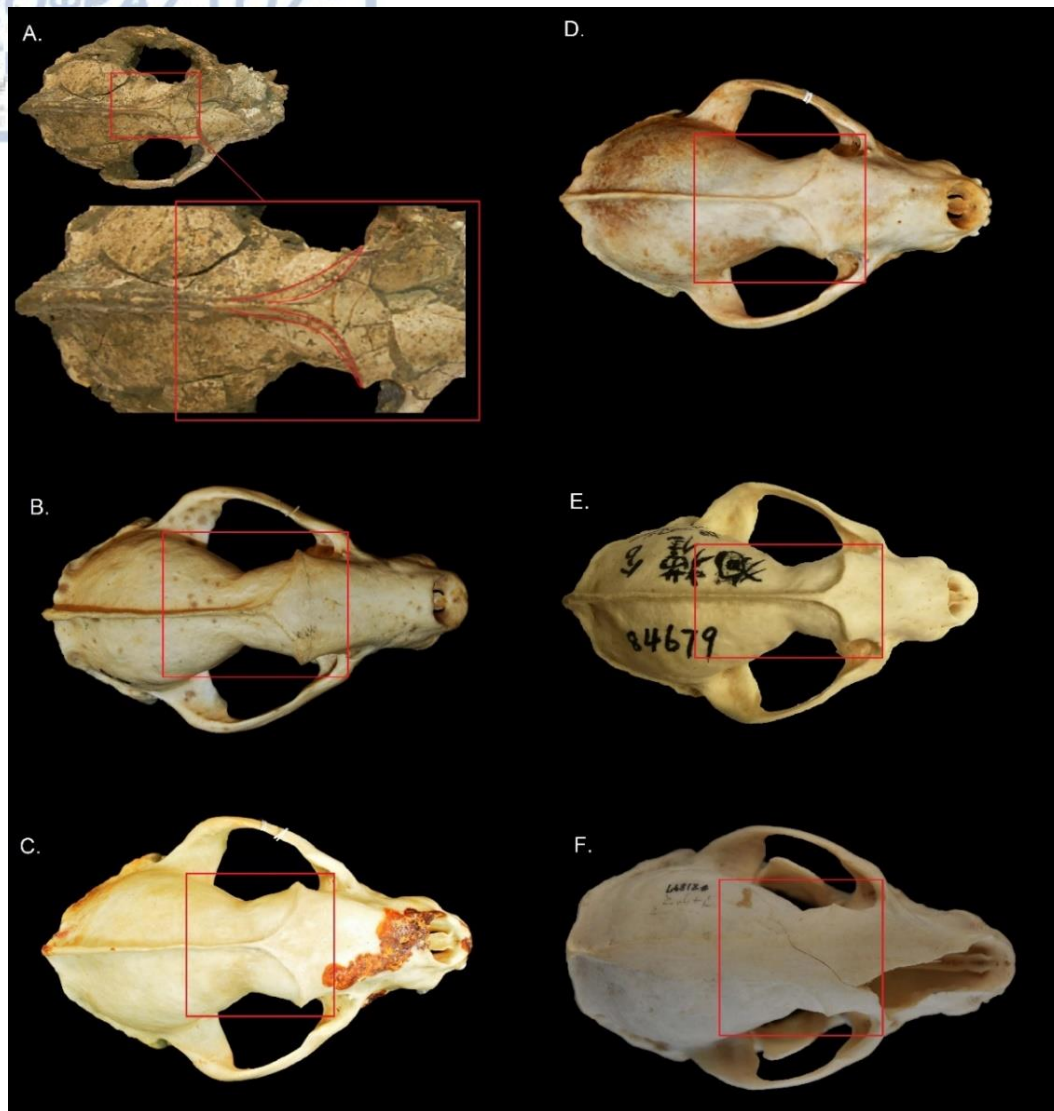


Figure 34. Front area of the sagittal crest. A. *Meles dimitrius*, B. *Meles meles*, C. *Meles canescens* (Crete) (robust specimen Fc 1364), D. *Meles canescens* (Crete), E. *Meles leucurus*, F. *Meles anakuma*. Not in scale.

The nuchal crest of *M. dimitrius* also constitutes a more robust structure than that of *M. meles* and *M. leucurus*, in which it seems to be more delicate but more protruding (constituting a thin outward projection). This area corresponds to the attachment site of muscles concerning neck movement. *Meles anakuma* and *M. canescens* (Crete) have a restricted development of this trait.

The brain case of *M. dimitrius* appears to be wider than in *M. meles* and *M. leucurus*, indicating a larger area for the insertion of the temporalis (Timm-Davis et al., 2015). However, *M. anakuma* as well as the specimens of *M. canescens* (Crete) possess a morphology of the brain case closer to that of *M. dimitrius* by having a wider than longer structure especially in the caudal part and a more circular shape. The braincase is where some layers of the temporalis (suprazygomatic, deep) attach.

The pterygoid bone, specifically the area where the medial pterygoid originates, is well – developed in *M. canescens* (Crete) when compared to *M. meles*. The area was damaged in *M. dimitrius* and could not be examined.

The caudoventral morphology of the skull also appears to differentiate the two groups (fossil and extant). Firstly, the mastoid process of *M. dimitrius* is more circular at its tip and larger as a structure than that of the group of extant *Meles*. Also, *M. canescens* (Crete) has a more elongated mastoid process than *M. meles*. The mastoid process was observed to be the origin area for the digastricus muscle as well as of certain neck – related muscles. The paroccipital process of *M. dimitrius* is developed with a wider angle in relation to the occipital condyle and the area correlates with the insertion of the digastricus muscle as well. The occipital condyles of *M. dimitrius* are larger and more spherical in contrast to extant *Meles*, which have a more triangular shape and are more constricted, a trait related to attachment sites of the neck muscles.

The foramen magnum presents differences among the species correlated to differentiation of head mobility (Fig. 35). *Meles dimitrius*, *M. canescens* (Crete) and *M. anakuma* have quite a narrow opening which is more vertically placed when compared to *M. meles* and *M. leucurus*.

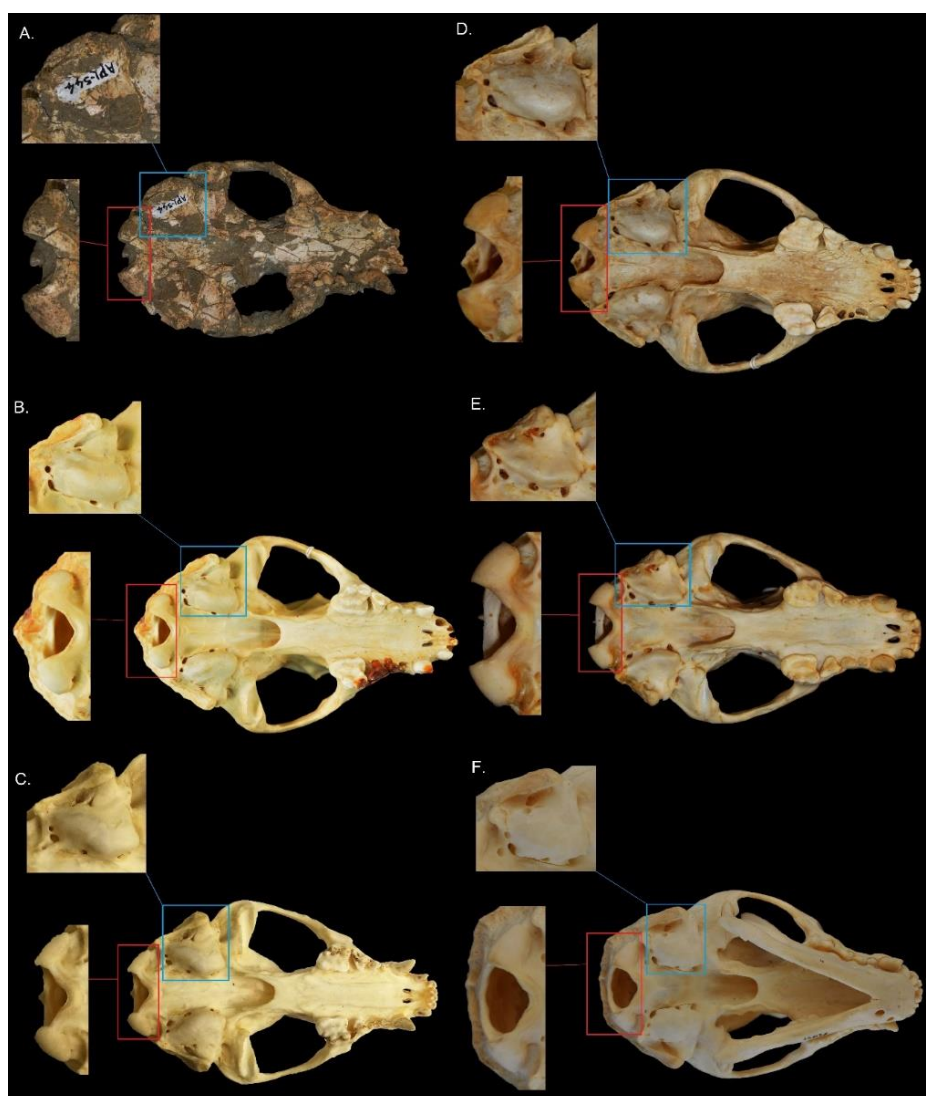


Figure 35. Magnum foramen and auditory bulla of the species, red boxes indicate the magnum foramen/occipital condyles and blue boxes the auditory bullae. A. *Meles dimitrius*, B. *Meles canescens* (Crete) (robust specimen Fc 1364), C. *Meles leucurus*, D. *Meles canescens* (Crete), E. *Meles meles*, F. *Meles anakuma*. Not in scale.

The rostrum of *M. dimitrius* is wider than the rostrum of the extant *Meles*, referring to overall induced forces and resistance. Observations in the rest of the extant group species could not be detected with the naked eye and will be examined with quantitative methods.

An additional distinguishing character is the morphology of the auditory bullae (Fig. 35). The main discrimination is between the group of mainland *Meles* (*M. meles* and *M. leucurus*), and the insular group [*M. canescens* (Crete), *M. anakuma*]. The mainland population possesses a flattened auditory bulla while the insular group has a more spherical and inflated one. *Meles dimitrius* has a damaged auditory bulla and no certain conclusions can be drawn concerning its shape. It could be closer to the *M. canescens* (Crete) group, without any certainty. The morphology of the auditory bullae is quite important as it is related to hearing.

Mandible

The mandible was examined with respect to structures related to certain muscular attachments as well as to functional behavior. It is noted that the structures do not appear to vary extremely, a fact which is confirmed by the subsequent PCAs. Insular specimens appear somewhat smaller than the mainland group, however, a few other observations can be noticed.

In the insular group [*M. canescens* (Crete), *M. anakuma*] and *M. dimitrius* the masseteric fossa appears to be quite extended. This structure covers a larger area than in the mainland group. However, the masseteric fossa of *M. meles* and *M. leucurus* appears deeper, accomodating a large quantity of the muscle mass. This structure constitutes the insertion area of the deep masseter. The lingual side of the masseteric fossa in *M. meles* and *M. canescens* (Crete) appears more concave whereas it has a straighter shape in *M. dimitrius*. This area corresponds to the insertion of the deep temporalis indicating increased muscle mass in the former two species.

Buccally and beneath the masseteric fossa a concave trench can be noticed developing in parallel to the lower border of the masseteric fossa (Fig. 36). It corresponds to the insertion of the middle masseter. This structure appears more pronounced in the extant *M. meles* and even more in *M. leucurus* than in the fossil *M. dimitrius* and the insular *M. canescens* (Crete) and *M. anakuma*.

The coronoid process does not appear to be developed differently among the species (Fig. 36). *Meles leucurus* and *M. meles* could possibly have a slightly less circular shape than the rest of the species but this trait is not always apparent. In *M. dimitrius*, *M. canescens* (Crete) and *M. anakuma* it appears more circular. The morphology of the coronoid process is of great importance as the temporalis muscle (and specifically the suprazygomatic temporalis) attaches to it. The angular process (Fig. 36) in *M. dimitrius* is more confined and consists of an almost pointy tip that lacks the lateral development as in the rest of the extant group of *Meles*. *Meles meles*, *M. canescens* (Crete), *M. leucurus* and *M. anakuma* have much more developed caudal areas of the angular process which is where the superficial masseter inserts.

The general construction of the mandible and specifically of the dentary bone, is indicative of the forces induced while biting. No notable differences are observed between the specimens.

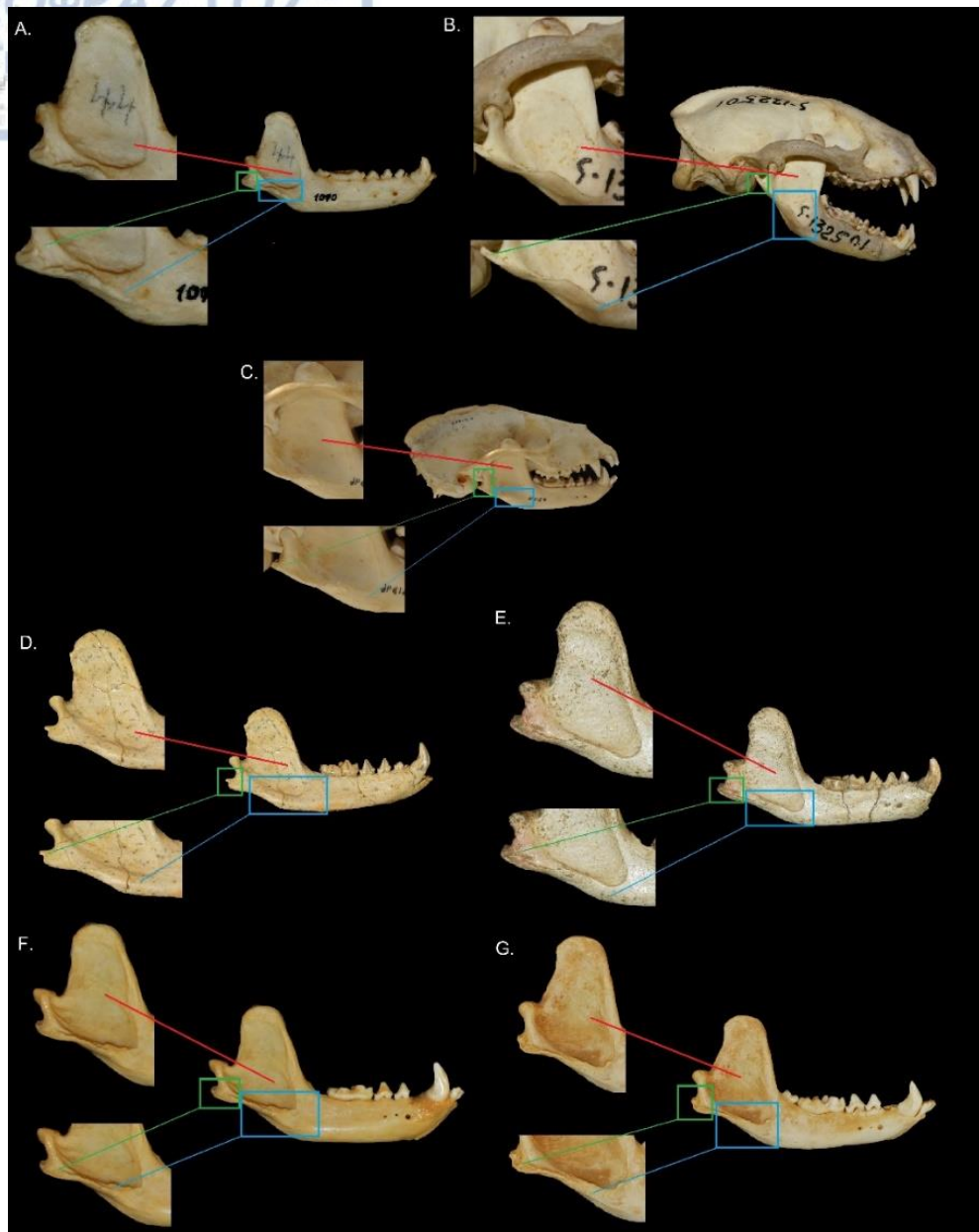


Figure 36. Insertion areas of the masseter, red lines indicate the masseteric fossa (deep masseter), green the angular process (superficial masseter) and blue the concave trench (middle masseter). A. *Meles meles*, B. *Meles leucurus*, C. *Meles anakuma*, D. *Meles dimitrius*, E. *Meles dimitrius*, F. *Meles canescens* (Crete) (robust specimen Fc 1364), G. *Meles canescens* (Crete). Not in scale.

Dentition

Upper dentition

The precarnassial dentition is reduced in size with smaller teeth, while extreme emphasis is given in the fourth premolar but mostly in the first molar which presents a rather peculiar morphology (Fig. 37). The canine shape of all the specimens seems rather circular.

P4 is obviously smaller than M1 changing the allocation of the applied force and consequently the overall produced forces. M1 is extremely developed with three characteristic rows of cusps enhancing both the ability to crush and slice (Fig. 37). The

area of M1 seems to slightly differentiate among the species. M1 appears to be wider and more rectangular in *M. meles*, *M. leucurus* and *M. dimitrius* while it has a more elongated talonid in *M. anakuma* and *M. canescens* (Crete). *Meles leucurus* is also differentiated from the rest by having an extra cusp at the protocone of M1 and by a more subquadrate shape.

P4 blade of *M. dimitrius*, *M. anakuma* and *M. canescens* (Crete) is more developed while the protocone is more triangular than subquadrate as in the rest of the group of extant *Meles*. *Meles leucurus* also has a more pronounced P4 protocone with larger surfaces than *M. meles*.

It is also of importance to note the generally more blade-like and sharper tooth morphology that seems to dominate in *M. canescens* (Crete).

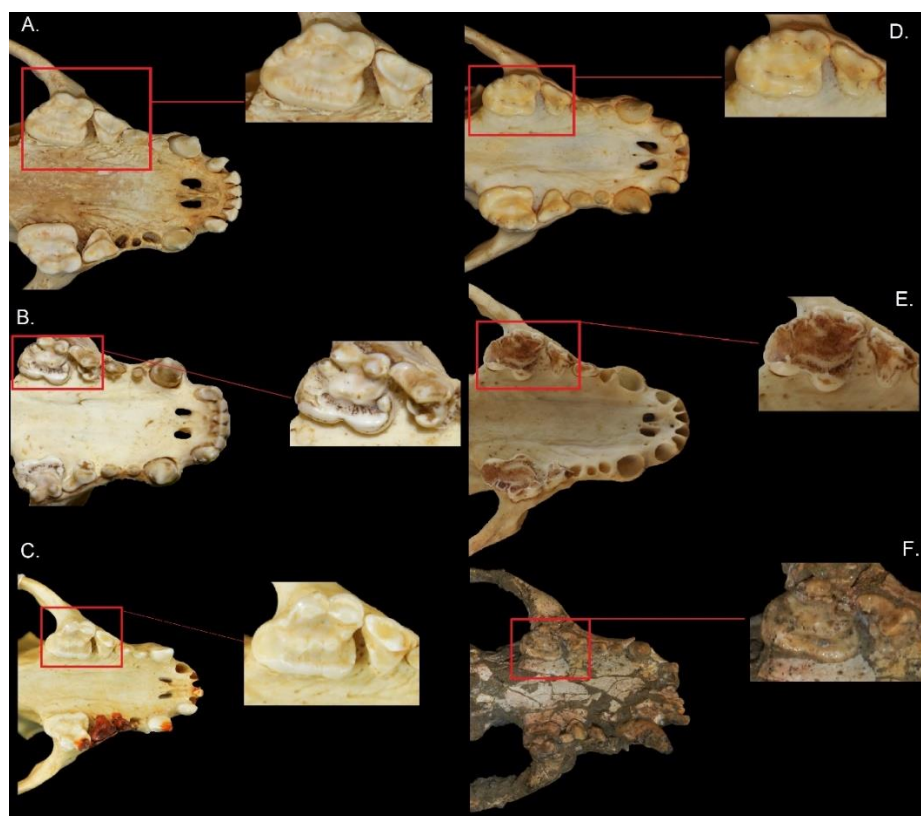


Figure 37. Upper dentition of the species. Red boxes indicate M1. A. *Meles canescens* (Crete), B. *Meles leucurus*, C. *Meles canescens* (Crete) (robust specimen Fc 1364), D. *Meles meles*, E. *Meles anakuma*, F. *Meles dimitrius*. Not in scale.

Lower dentition

No specific remarks were noted concerning the lower dentition, except for the absence of p1 and p2 in the Asian and Japanese badgers which is also one of their diagnostic characters (Baryshnikov et al., 2003). The European badgers present a residual p1. The relative placement of the lower canines appears to be in an outward direction in all species in question, creating a hook like canine shape. Morphology of the lower dentition (Fig. 38) is quite confusing when comparing the species between them, as no obvious differentiation is observed in contrast to the upper dentition. The size of the second molar (m2) is extremely reduced when compared to the first molar (m1), which seems to be the main tooth for food processing. Moreover, the first lower molar (m1)

of *M. dimitrius* is more elongated when compared to the rest of the species. *Meles anakuma* appears to have a similar shape, while *M. canescens* (Crete) has a broader, more robust m1, even from the mainland populations of *M. meles* and *M. leucurus*.

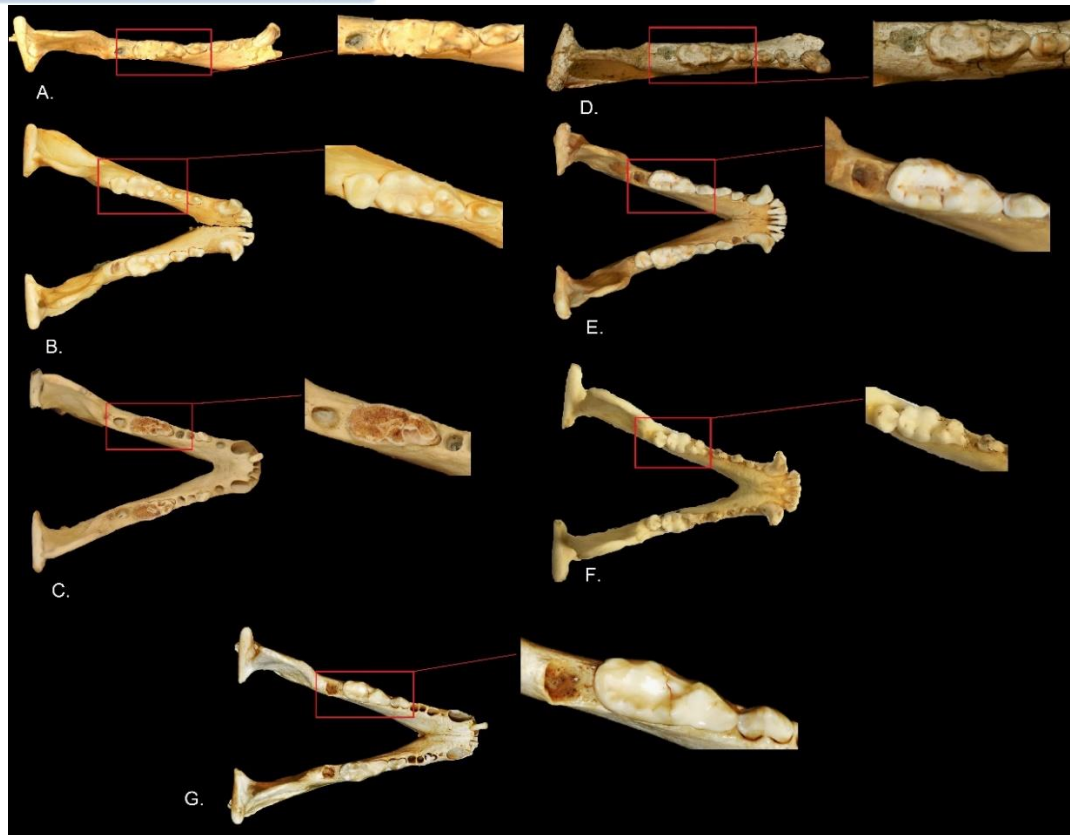


Figure 38. Lower dentition of the species. Red boxes show the m1. A. *Meles dimitrius*, B. *Meles canescens* (Crete) (robust specimen Fc1364), C. *Meles anakuma*, D. *Meles dimitrius*, E. *Meles canescens* (Crete), F. *Meles leucurus*, G. *Meles meles*. Not in scale.

HSB structures

The teeth of *M. meles*, *M. canescens* (Crete) and the fossil *M. dimitrius* were analyzed. HSB structures were traced on the majority of the teeth (c1, p2, p3, p4) however they were not always easily observed. They were most often noticed near the parts of the teeth which have been damaged or broken. Canines were the teeth where HSB were most often and clearly observed. Results of measurements from the canine are given in Table 8 and HSB structures are shown in Fig. 39.

Table 8. HSB angles of *Meles canescens* (Crete), *Meles meles* and *Meles dimitrius*.

Genus	Species	Angle (°)
<i>Meles</i>	<i>canescens</i> (Crete)	143°
<i>Meles</i>	<i>meles</i>	144°
<i>Meles</i>	<i>dimitrius</i>	138°

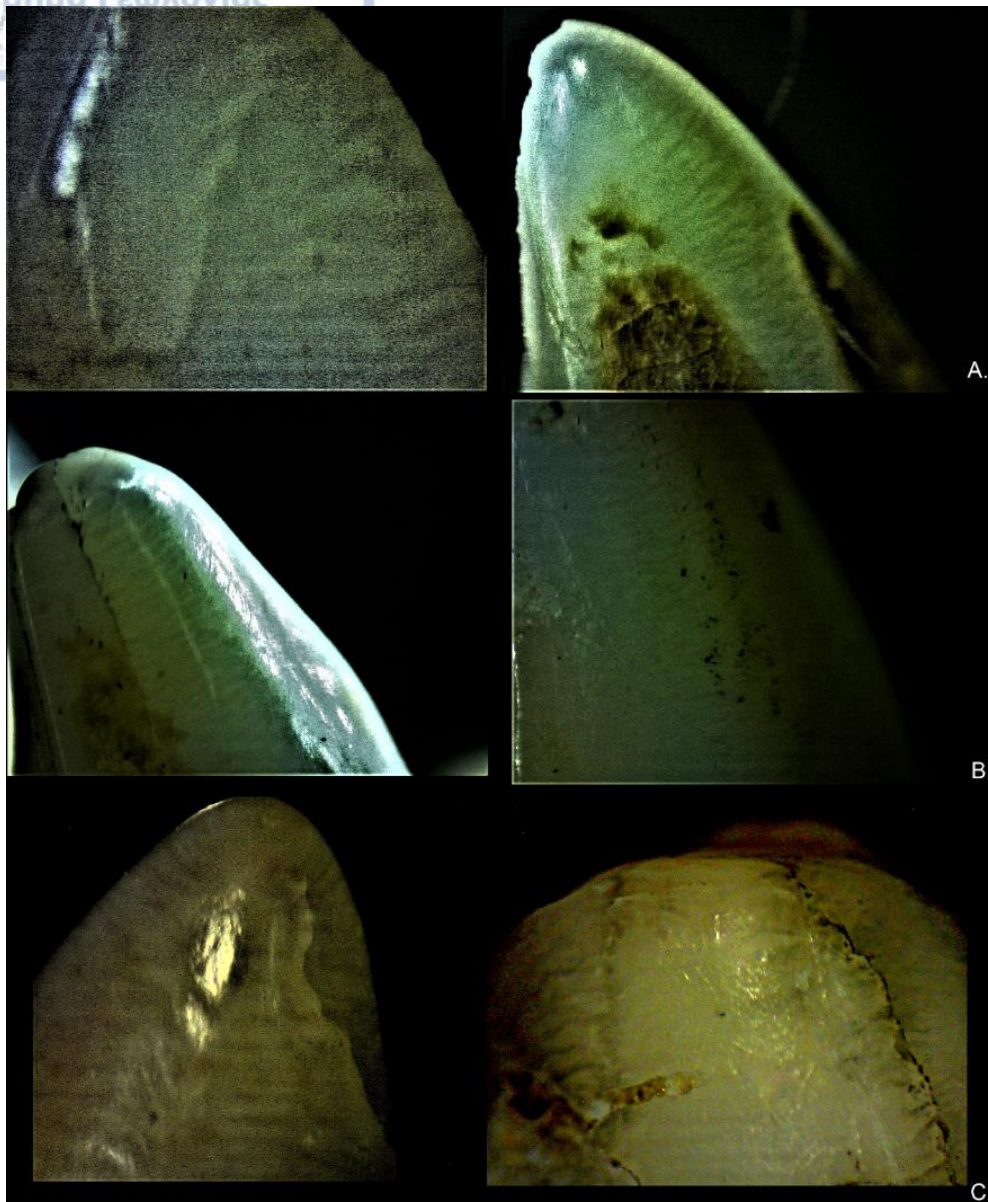


Figure 39. HSB of *Meles canescens* (Crete) (A), *Meles meles* (B) and *Meles dimitrius* (C).

The HSB seem to create wide angles for the genus *Meles* with a narrow range between the species (138° – 144°). No particular differentiation can be noticed between the different species, and all would be categorized as having undulating HSB with a tendency to the acute angled category. The extant species *M. canescens* (Crete) and *M. meles* have almost identical HSB with angles exceeding 140° only by a few degrees (143° and 144° accordingly). *Meles dimitrius* creates more acute angles (138°) but still remains very close to 140° .

Metric comparisons

PCAs

Four different PCAs were performed separately concerning the cranium, the mandible, the upper and the lower dentition.

PCA Cranium

The PCA of the cranium was based on twenty-five normalized variables given in Table 9 along with the Eigenvalues and %variances. A plot for PC1 – PC2 (Fig 40) explains 64.55% of the total variance. PC1 explains 41.61% of the total variance, PC2 explains 22.9% and PC3 axis explains only a weak percentage of 7.29%. The badger is an omnivorous animal with no preference in a specific type of food so intense diversification was not expected, however, results of the PCA analysis indicate certain differences among the various species (Fig. 40).

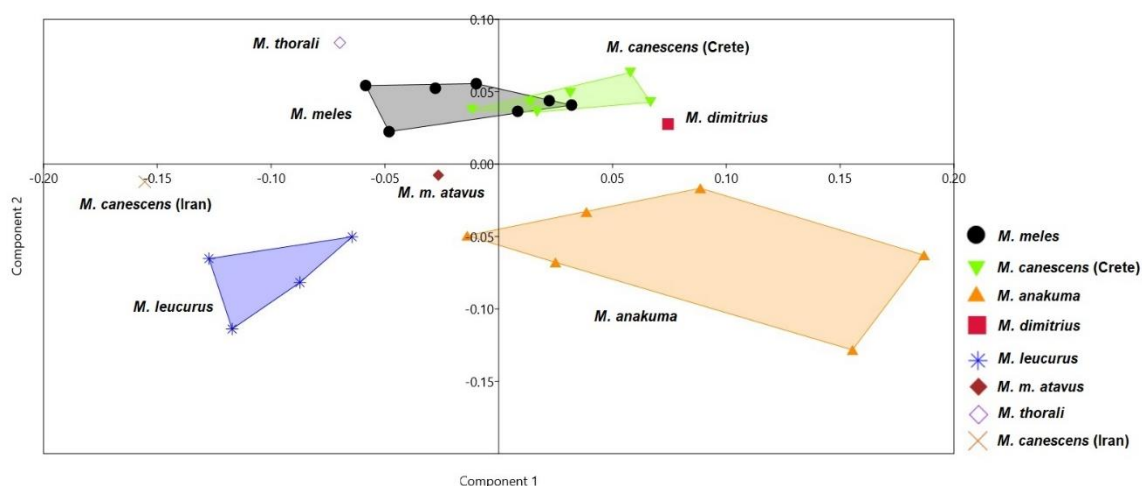
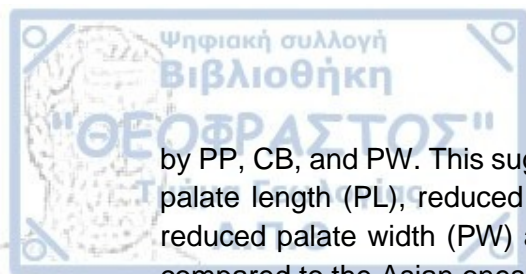


Figure 40. PCA of the cranium of Meles.

PC1 (variance 41.61%) differentiates the mainland [*M. meles*, *M. canescens* (Iran) and *M. leucurus*] as well as the fossils *M. thoralis* and *M. m. atavus* from the insular specimens [*M. canescens* (Crete) and *M. anakuma*] and *M. dimitrius*. The PC1 reflects a clustering based on differences mostly in the TFL, SKH, and SKL and secondarily in TRL, BCW, IOD, MSW and MW (Table 9). This suggests that mainland taxa have shorter temporal fossae (TFL) and skulls (SKL, which could be related to the shortened TFL) compared to the insular ones. Additionally, insular taxa and *M. dimitrius* have a more developed tooth row length (TRL), braincase width (BCW), maximum squamosal width (MSW) and interorbital distance (IOD) compared to the mainland taxa. However, it should be noted that an overlap between *M. meles* and *M. canescens* (Crete) exists. This could be partly explained by the origin of the specimens. Samples of *M. meles* are mainly from mainland Greece and neighboring Bulgaria. Consequently, *M. canescens* (Crete) and the studied samples of *M. meles* could be overlapping due to their close geographical range. European badgers of more Northwestern origin could differ from these. Moreover, specimens which seem to overlap, are either males of *M. canescens* (Crete) (Fc34, Fc26) or females of *M. meles* (1009) so sexual dimorphism could play a role in the arrangement.

Two groups are also distinguished along PC2 (variance 22.94%): one including *M. meles*, *M. canescens* (Crete), *M. thoralis* and *M. dimitrius* and a second one including *M. canescens* (Iran), *M. m. atavus*, *M. leucurus* and *M. anakuma*. Hence, PC2 differentiates taxa of European origin [*M. meles*, *M. canescens* (Crete), *M. canescens* (Iran), *M. m. atavus*, *M. thoralis* and *M. dimitrius*] from those of Asian (*M. leucurus* and *M. anakuma*). PC2 is mainly affected by BCL, TRL, MW, PL (Table 9) and secondarily



by PP, CB, and PW. This suggests that European taxa are characterized by increased palate length (PL), reduced braincase length (BCL), reduced mastoid width (MW), reduced palate width (PW) and reduced distance of the paroccipital processes (PP) compared to the Asian ones.

Table 9. Normalized variables of the PCA of the cranium. Scores of the most influential measurements of the cranium are given in bold.

	PC1 Eigenvalue 0.00630059 % variance 41.61	PC2 Eigenvalue 0.00347368 % variance 22.941
SKL	0.33945	0.041986
BCL	0.29516	-0.40781
BCW	0.17878	-0.0081151
RL	0.047852	0.10096
IOD	0.1873	0.12543
PL	0.033302	0.3293
PW	0.062253	-0.2495
RWC	0.03424	0.1244
RWM	0.053595	-0.0070374
PP	0.052845	-0.30894
OSA	-0.014296	0.17549
MSW	0.22686	0.20242
ZW	0.010768	0.036297
ZFW	0.12278	0.17177
ZFL	-0.022487	0.13802
CB	0.067266	-0.26876
OD	0.072149	0.13039
FD	0.27922	-0.079334
VRA	0.0034332	-0.0017553
LRA	0.0026415	0.0011983
SKH	0.34032	-0.15887
TRL	0.30538	0.36078
TFL	0.55187	0.10587
POC	0.11924	0.12819
MW	0.18322	-0.35223

Univariate analyses concerning the most influential parameters of both PC1 and PC2 are presented below. Skull length (SKL) (Fig. 41) was not found statistically important ($p > 0.05$) in contrast to the rest of the examined measurements ($p < 0.05$). It also shows a great overlap of the species.

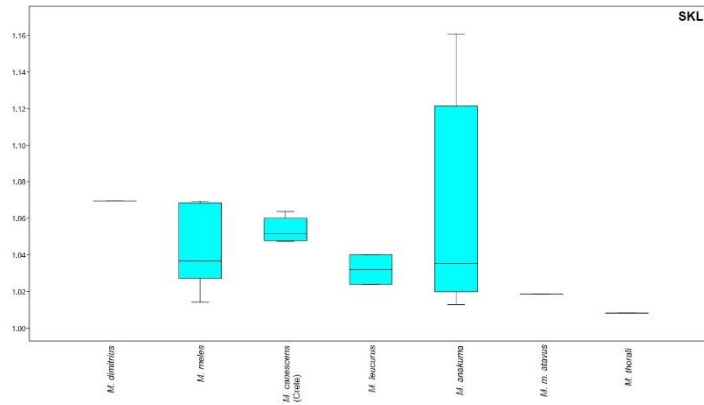


Figure 41. Boxplot of SKL of Meles.

Skull height (SKH) (Fig. 42) shows a great overlap as well, where mainly *M. anakuma* and *M. m. atavus* seem to differentiate with slightly increased values and *M. leucurus* which shows lower values.

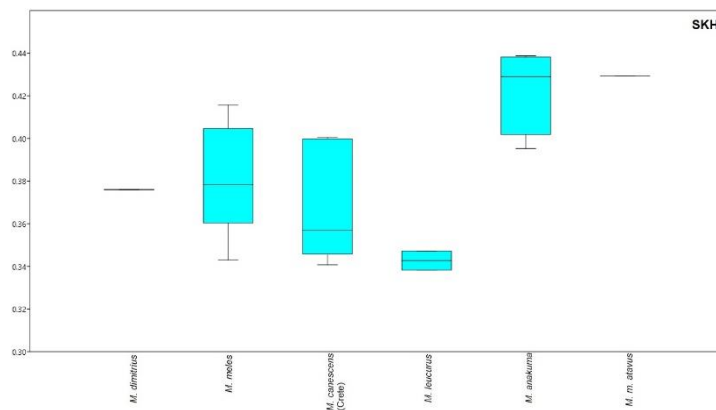


Figure 42. Boxplot of SKH of Meles.

Temporal fossa length (TFL) (Fig. 43) shows increased values for *M. dimitrius*, *M. canescens* (Crete) and *M. anakuma* while the mainland group (*M. meles*, *M. leucurus* and *M. m. atavus*) has lower values. This trait is connected with the development of temporalis. TFL along with POC (distance of postorbital constriction) define the area of this muscle.

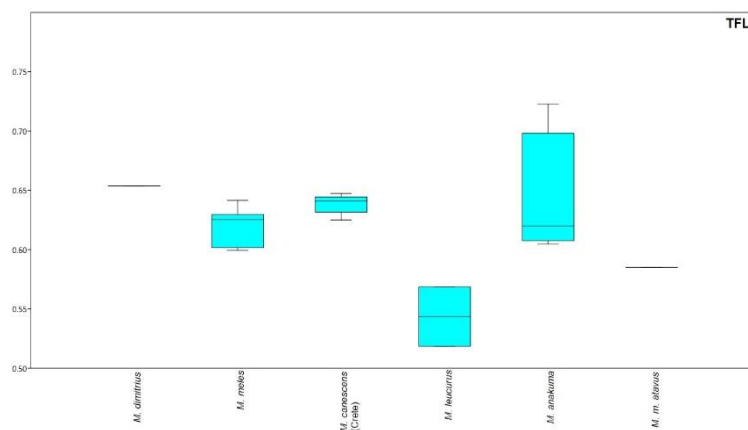


Figure 43. Boxplot of TFL of Meles.

MSW, BCW and IOD, though secondarily most influential variables on PCA, show a grouping of the insular and the mainland species (Figs 44 – 46).

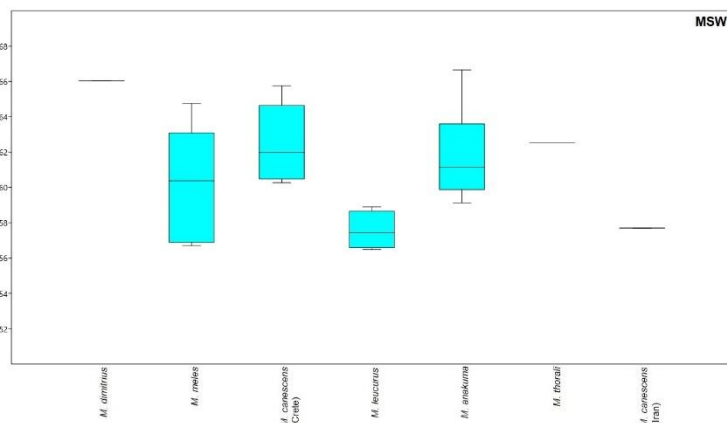


Figure 44. Boxplot of MSW of Meles.

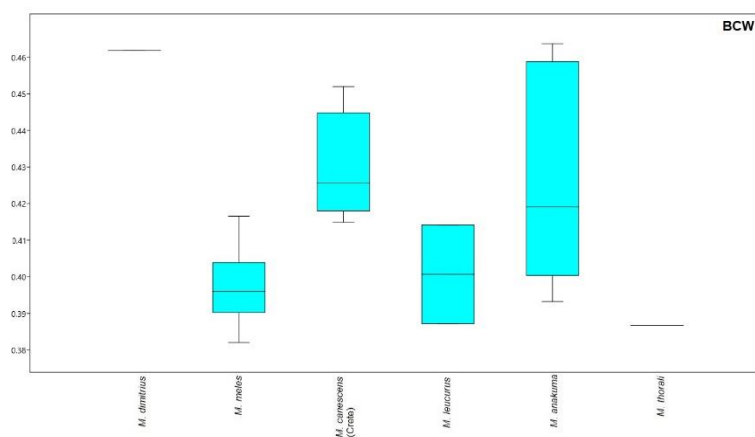


Figure 45. Boxplot of BCW of Meles.

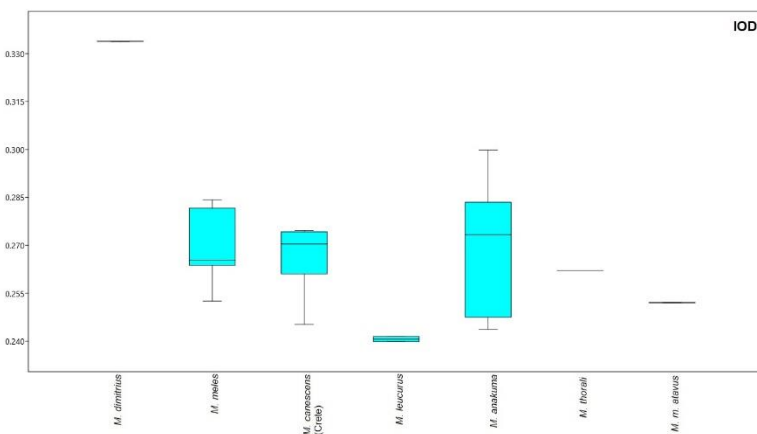


Figure 46. Boxplot of IOD of Meles.

Tooth row length (TRL) (Fig. 47) does not show extreme diversification among the species. *Meles leucurus* is the only taxon which seems to have quite lowered values, something that could be attributed to the limited number of specimens that were

available or even to the digital measurement of the specimens. *Meles m. atavus* also has a tendency for lower values.

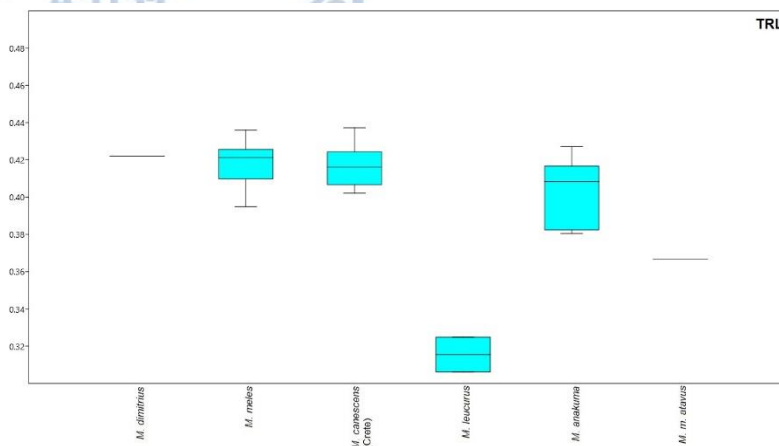


Figure 47. Boxplot of TRL of Meles.

Braincase length (BCL), mastoid width (MW) and palate length (PL) (Figs 48 – 50) separate European from Asian species. Values of the insular specimens were compared with the analogous mainland ones (from the same continent) and a pattern was observed separating mainland from insular. BCL (Fig. 48) was found with increased values in the insular specimens of both continents when compared to their equivalent mainland, while Asian species (as a whole) have increased lengths when compared to the European. Mastoid width (MW) was also increased in insular specimens, however *M. dimitrius* (European) seems to have a widened area of the mastoid corresponding better to the values of *M. anakuma* (Asian) rather than *M. canescens* from Crete. Palate dimensions (length and width) (PL, PW) (Figs 50 – 51) were also increased in insular specimens while, European taxa have generally increased lengths and decreased widths. PL is increased in European species while PW is increased in Asian species. *Meles canescens* (Iran) seems to group with the Asian species in this case. Insular species present increased dimensions of the palate.

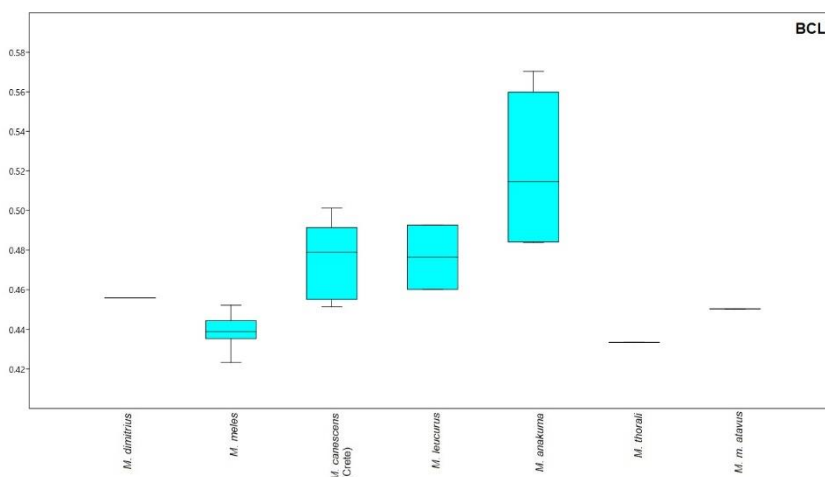


Figure 48. Boxplot of BCL of Meles.

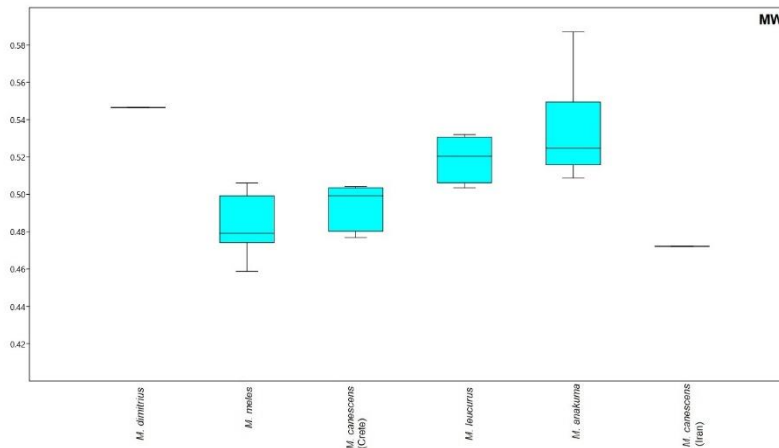


Figure 49. Boxplot of MW of Meles.

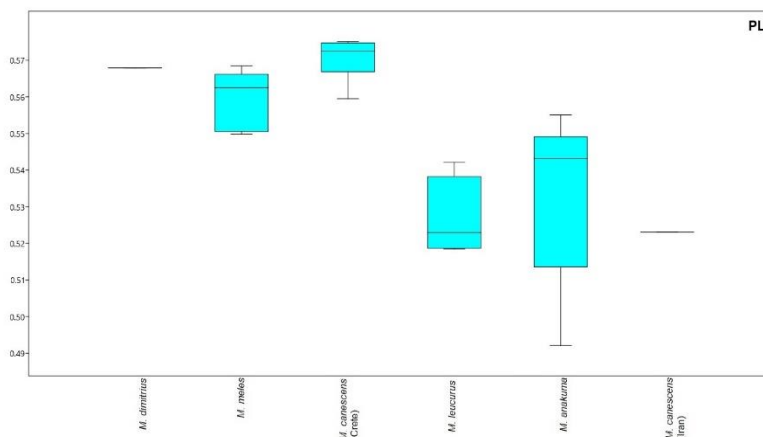


Figure 50. Boxplot of PL of Meles.

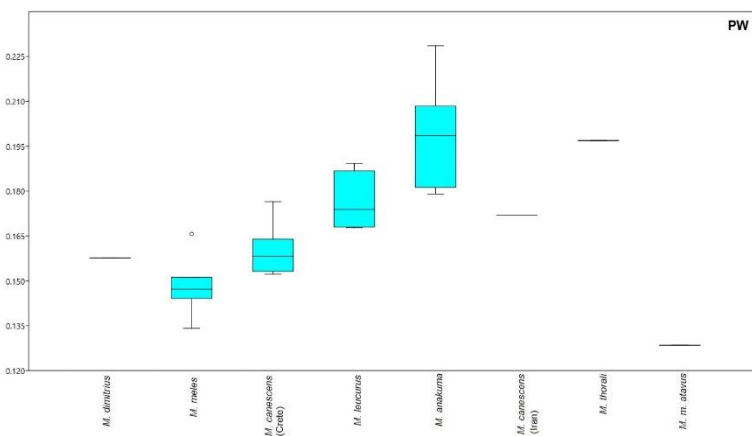


Figure 51. Boxplot of PW of Meles.

INDICES

Indices concerning the skull morphology were also computed, where there was adequate data. Facial ratio (FR) (Fig. 52), which indicates the length of the rostrum to the overall skull length, shows reduced values for *M. leucurus* and *M. thoralis*, while *M. m. atavus* shows the highest. The rest of the species present intermediate values.

Miller's index (MI and MI'), (Figs 53 – 54), which indicates the maximum zygomatic width to the overall skull length (MI) and to the overall condylobasal length (MI'), shows increased values for *M. dimitrius*, *M. canescens* (Crete), *M. anakuma* and *M. thoralis*. *Meles meles*, *M. leucurus* and *M. m. atavus* have lower values. In general, the skulls of the mainland *M. meles* and *M. leucurus* appear somewhat longer than wider when compared to *M. dimitrius*, *M. canescens* (Crete) and *M. anakuma*, a trait which affects the overall forces and velocity of the bite.

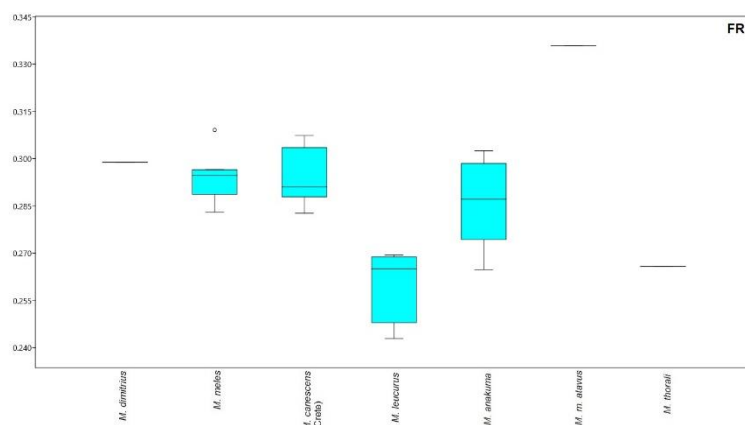


Figure 52. Boxplot of FR of Meles.

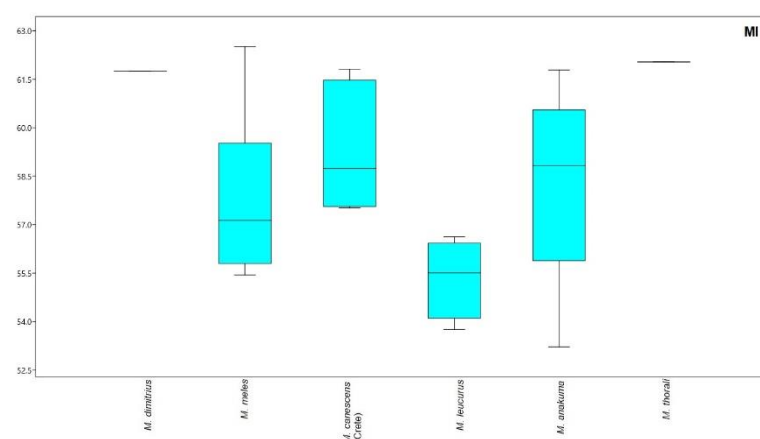


Figure 53. Boxplots of MI of Meles.

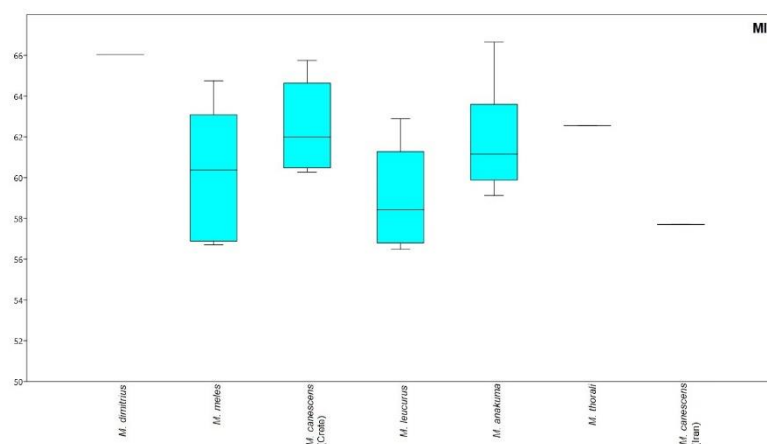


Figure 54. Boxplot of MI' of Meles.

PCA Mandible

The PCA of the mandible was based on seventeen normalized variables given in Table 10 along with the Eigenvalues and %variances. A plot for PC1- PC2 (Fig. 55) explains 81.27% of the total variance. PC1 explains 75.56% of the total variance, PC2 explains a weak percentage of variance 5.71% and PC3 axis explains 4.98%. The analysis of the mandible does not show extreme differences among the species and there is a great overlap (Fig. 55).

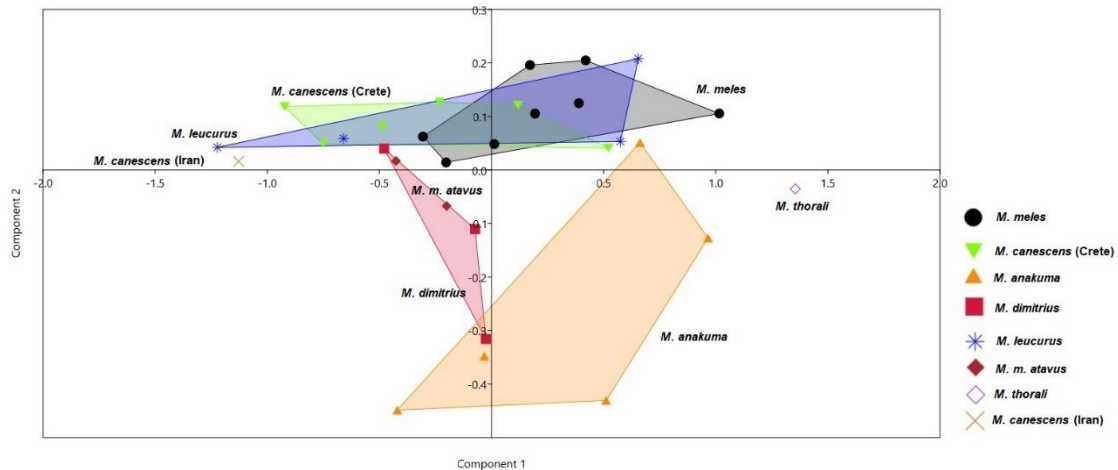


Figure 55. PCA of the mandible of Meles.

The main separation (Fig. 55) is noticed in PC2 (variance 5.71%), while in PC1 (variance 75.56%) there is a great overlap of the taxa.

PC1 shows that *M. canescens* (Crete), *M. dimitrius* and *M. m. atavus* are on average smaller than *M. meles*, *M. thoralis* and *M. anakuma* however there is no clear discrimination. *Meles leucurus* overlaps with all of the taxa. The measurements that are most influential in PC1 are DL, OLCm1, OLCc1 and WSLA. MAT, MRH, MRW and CPr elevation affect the grouping at a lesser extent.

PC2 groups *M. dimitrius*, *M. anakuma* and *M. thoralis* on the one hand and *M. canescens* (Iran), *M. leucurus*, *M. canescens* (Crete) and *M. meles* on the other. *Meles thoralis* has increased values in all of the parameters indicating more developed characteristics. PC2 is mainly affected by MRH, MFL and CPr elevation and secondarily by DL (Table 10). This suggests that the group of *M. dimitrius*, *M. m. atavus*, *M. anakuma* and *M. thoralis* have more developed mandibular fossa and reduced height of mandibular ramus and coronoid process, compared to *M. meles*, *M. leucurus*, and *M. canescens* (Iran). Most of the specimens of *Meles canescens* (Crete) is placed on the upper left part of the diagram differentiating from *M. meles* and is characterized by decreased height of mandibular ramus and coronoid process. *Meles anakuma* and *M. thoralis* also have longer dentary bone (DL).

Certain traits appear to group together *M. dimitrius* and *M. canescens* (Crete). Specifically, DL, OLCm1, OLCc1, WSLA and MAT have lower values compared to *M. meles*, *M. leucurus* and *M. anakuma*. *Meles anakuma* is close to *M. canescens* (Crete) and *M. dimitrius* in small/lower values concerning MRH, CPr elevation, JDc1, JDm1 and Dyp3p4. Lastly, *M. dimitrius* and *M. anakuma* have increased values of MFL.

Table 10. Normalized variables of the PCA of the mandible. Scores of the most influential measurements are given in bold.

	PC1 Eigenvalue 0.400513 % variance 75.566	PC2 Eigenvalue 0.0302683 % variance 5.7108
DL	0.49955	-0.33261
Dyp3p4	0.088357	0.28189
Dym1m2	0.071242	0.23987
JDm1	0.078887	0.273
MAT	0.18977	-0.066418
MAM	0.078312	-0.17521
OLCm1	0.33486	0.096806
OLCc1	0.49002	-0.2158
MRH	0.24087	0.41365
MRW	0.2123	0.074791
MFL	0.16273	-0.34359
JDc1	0.092684	0.24978
SYML	0.15667	0.23828
WSLA	0.3356	0.012538
BSLA	0.16615	0.008376
CPr elevation	0.18436	0.4155
JAPr angle	0.0030045	-0.0023711

Univariate analyses concerning the most influential parameters on both PC1 and PC2 are presented below. When tested statistically (ANOVA and Kruskal – Wallis tests) only MFL was found statistically important ($p > 0.05$). Despite the obvious overlap, *M. dimitrius* and *M. canescens* (Crete) seem to have similar tendencies of increasing or decreasing the values of the variables while *M. anakuma* does not always follow the same allocation.

The dentary length (DL) (Fig. 56) is elongated in *M. meles*, *M. leucurus*, *M. anakuma*, *M. thoralis* and shortened in the rest of the species. DL relates to the overall bite forces and bite velocity.

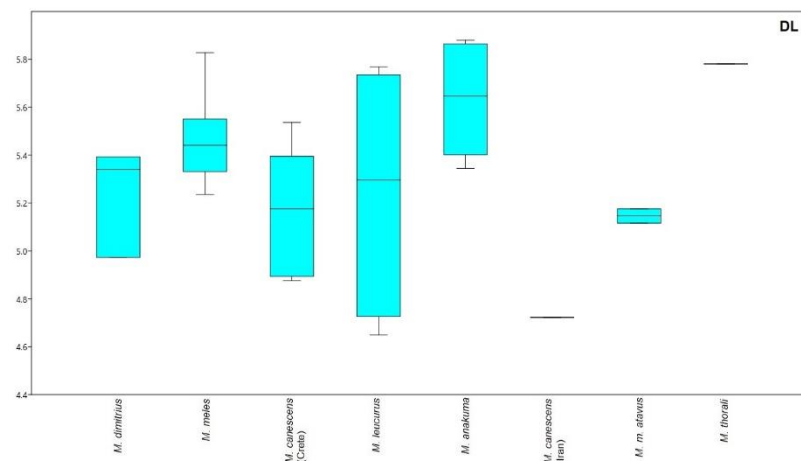


Figure 56. Boxplot of DL of Meles.

Values of the outer lever moment arm at m1 and c1 (OLCm1, OLCc1) (Figs 57 – 58) are similar between all of the species with the exception of *M. thoralis* and *M. canescens* (Iran). *Meles dimitrius* and *M. canescens* (Crete) do appear to have a tendency for lower values, nonetheless, *M. canescens* (Crete) has wide ranges. Increased values are noted in the former and decreased in the latter.

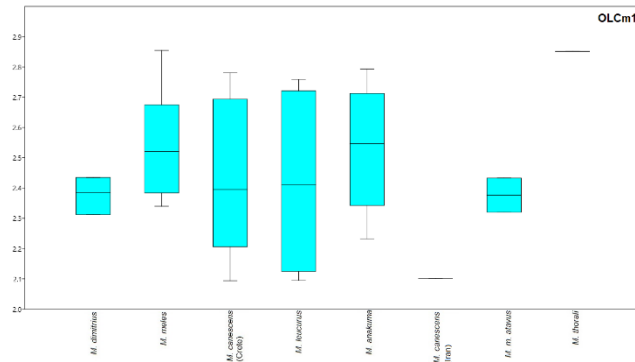


Figure 57. Boxplot of OLCm1 of Meles.

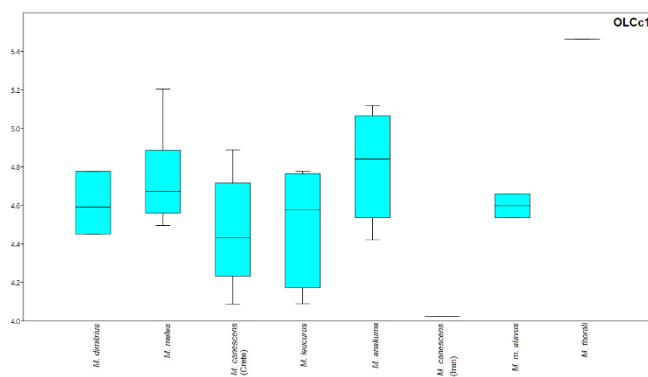


Figure 58. Boxplot of OLCc1 of Meles.

Working side lever arm (WSLA) (Fig. 59) shows no intense diversification. The mean values of each species show a tendency to lower values in *M. dimitrius* and *M. canescens* (Crete) as well as *M. canescens* (Iran) and *M. m. atavus*. Increased values are observed in *M. meles*, *M. leucurus*, *M. anakuma* and *M. thoralis*.

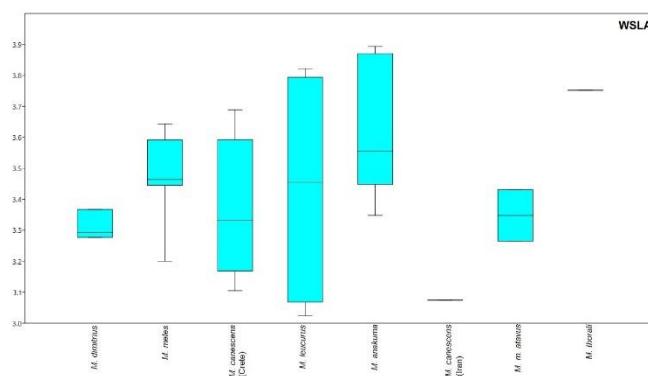


Figure 59. Boxplot of WSLA of Meles.

Mandibular height (MRH) (Fig. 60) and elevation of the coronoid process (CPr elevation) (Fig. 61) appear to have similar allocation for the species of the genus.

Meles meles, *M. leucurus* and *M. anakuma* have increased values contrary to the rest specimens which have lower values the rest lower. *Meles anakuma* appears very close to the group of *M. dimitrius* – *M. canescens* (Crete) as well.

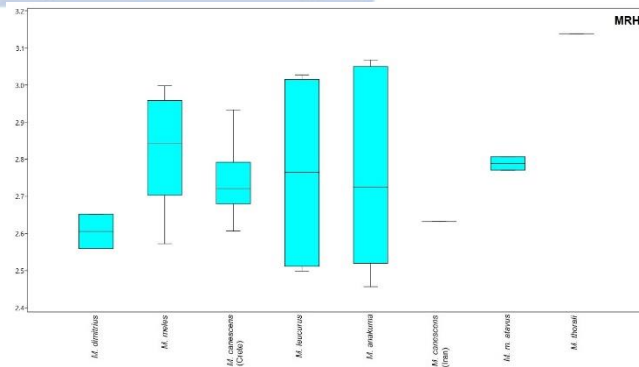


Figure 60. Boxplot of MRH of Meles.

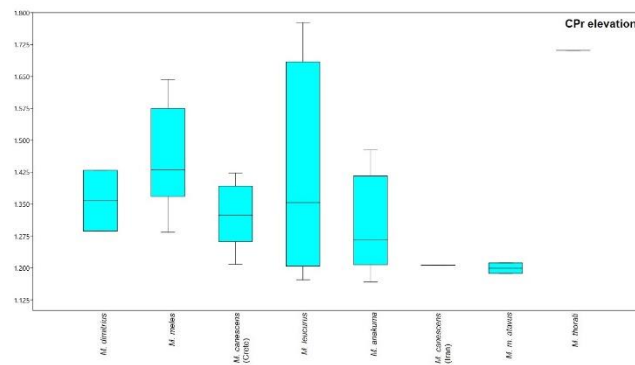


Figure 61. Boxplot of CPr elevation of Meles.

Mandibular fossa length (MFL) (Fig. 62) shows some differentiation among the species. *Meles thoralis* presents the higher values while *M. meles* and surprisingly *M. canescens* (Crete) the lower. The rest of the species have intermediate values. Development of the mandibular fossa correlates with the development of the masseter. However, its length is not the only parameter that should be concerned. Overall size and depth of the mandibular fossa should be examined nonetheless this was not a possible in our case.

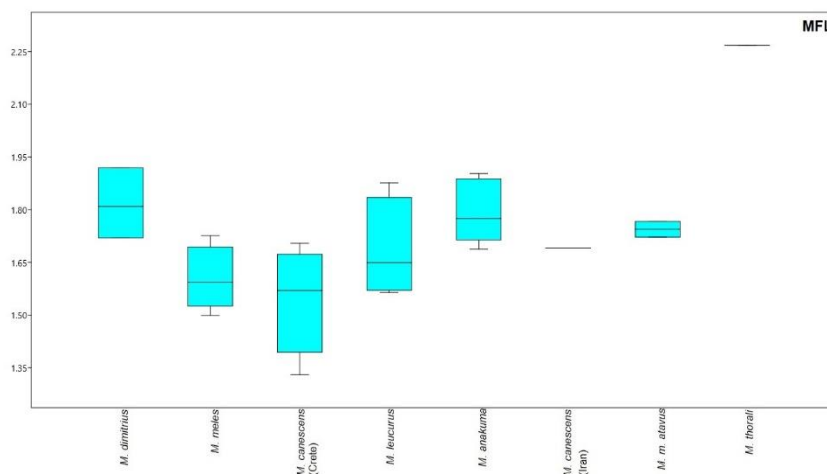


Figure 62. Boxplot of MFL of Meles.

INDICES

The vast majority of mandibular indices concern the mechanical advantage of the masseter and temporalis, while other examine the bending stresses of the mandible.

Mechanical advantage (Figs 63 – 66) is increased in *M. dimitrius*, *M. canescens* (Crete) and *M. anakuma*. *M. canescens* (Iran) and *M. thoralis* also appear to have increased values in both masseter and temporalis. However due to the lack of specimens, their placement was not considered indicative. These results were expected as the moment arm was increased (MATg, MAMg) (Figs 67 – 68) and the area where force was applied reduced (OLC).

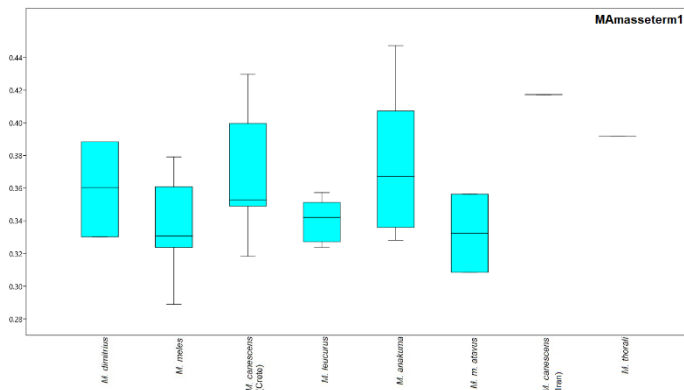


Figure 63. Boxplot of MAmasseterm1 of Meles.

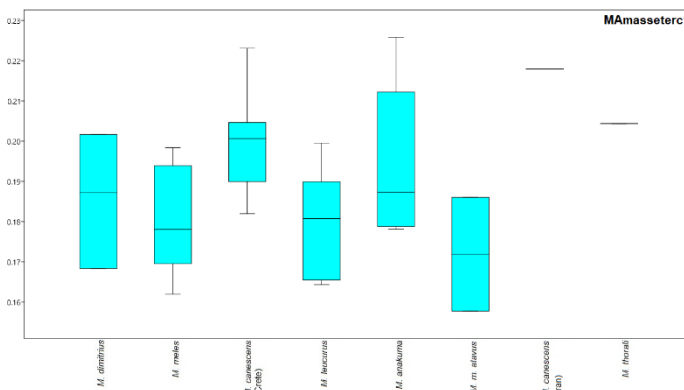


Figure 64. Boxplot of MAmasseterc1 of Meles.

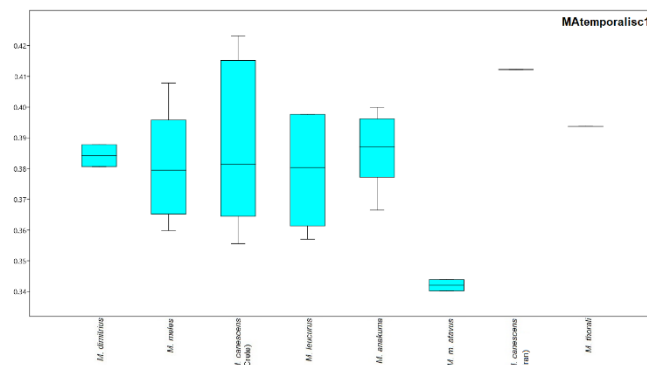


Figure 65. Boxplot of MAtemporalisc1 of Meles.

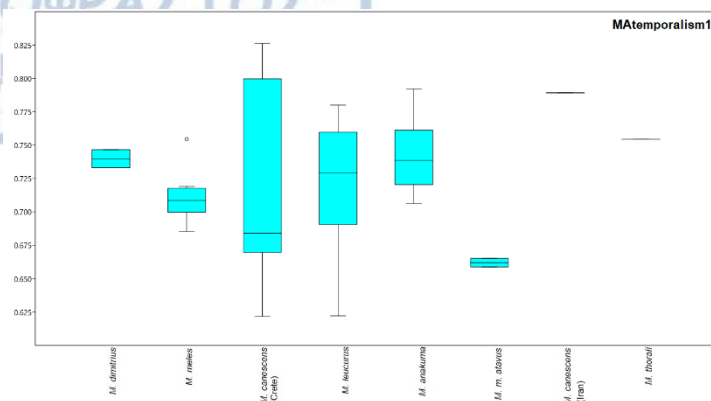


Figure 66. Boxplot of MAtemporalism1 of Meles.

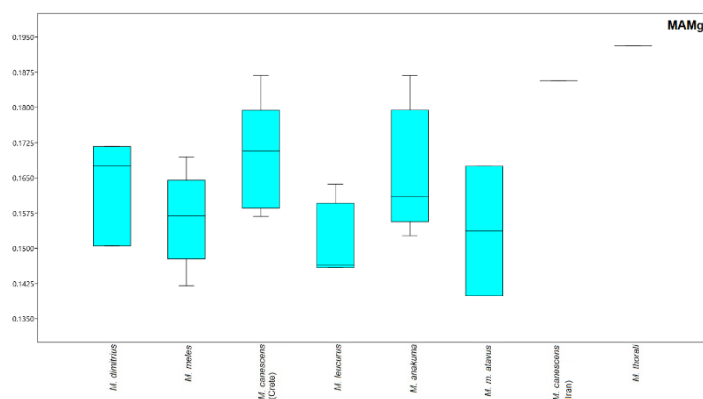


Figure 67. Boxplot of MAMg of Meles.

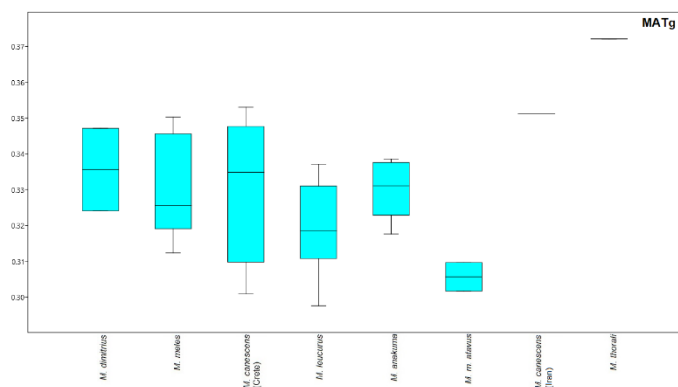


Figure 68. Boxplot of MATg of Meles.

The resistance of dentary to bending shows a wide range of values in *M. dimitrius* and partly in *M. canescens* (Crete), but more constricted range in the rest of the species. Resistance to dentary bending in the junction of m1 and m2 (IXM2) (Fig. 69) is increased in *M. thoralis*, *M. leucurus* and *M. canescens* (Crete). *Meles dimitrius* has an extremely wide range of values while its mean value appears lower than the rest. *Meles meles* has reduced values and *M. anakuma* has even lower. The resistance of dentary bending at p4 (IXP4) (Fig.70) is increased in *M. thoralis* and lower in the rest of the specimens. *Meles leucurus* has low values while *M. dimitrius* preserves its wide range.

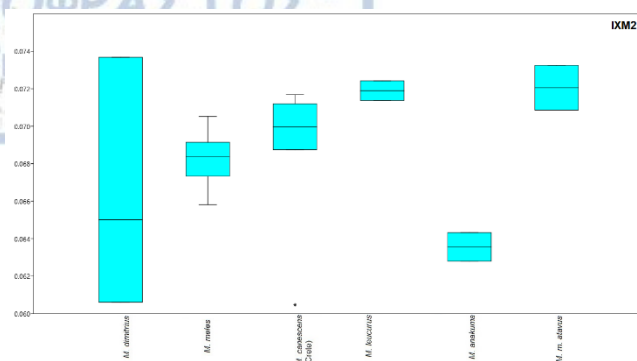


Figure 69. Boxplot of IXM2 of Meles.

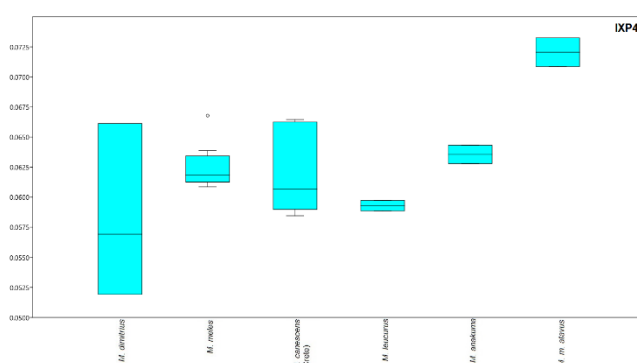


Figure 70. Boxplot of IXP4 of Meles.

PCA dentition

The shape and size, especially of the carnassials, was used to make inferences about the preferable food resources of the examined specimens.

PCA Upper dentition

The PCA of the upper dentition was based on 9 normalized variables given in Table 11 along with the Eigenvalues and %variances. A plot for PC1 – PC2 (Fig. 71) explains 99.3% of the total variance. PC1 explains 98.86% almost all of the total variance and PC2 explains only a weak percentage of 0.44%. The PCA shows a certain grouping of the different species (Fig. 71). Once more, an overlap of the species exists noticed more profoundly in *M. canescens* (Crete) which has an extremely wide range of values.

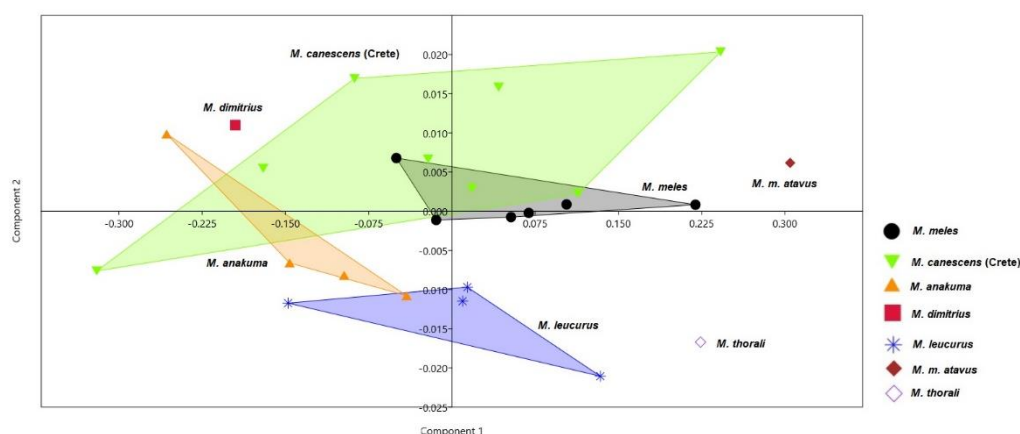


Figure 71. PCA of the upper dentition of Meles.

The area of the first molar (M1a) seems to have the most influential role in PC1 while the rest measurements have a supplementary role (Table 11). PC2 is mainly influenced by M1L and P4W. *Meles dimitrius* shows low values of M1a, a trait which groups it together with *M. anakuma* and some specimens of *M. canescens* (Crete). *Meles meles*, *M. m. atavus*, *M. thoralis*, *M. leucurus* as well as a few specimens of *M. canescens* (Crete) have increased values of M1a. *Meles thoralis* and *M. leucurus* discriminate from the rest of the taxa in PC2 by having lower values of M1L and P4W.

Table 11. Scores of the most influential measurements of the upper dentition (bold).

	PC1 Eigenvalue 0.0250781 % variance 98.862	PC2 Eigenvalue 0.000113239 % variance 0.44641
C1L	0.0096782	0.14573
C1W	0.0037504	0.235547
P3W	0.0039469	0.11533
P3L	-0.005915	0.30911
P4L	0.019376	0.12036
P4W	0.0081233	0.54071
M1L	0.042727	0.61286
M1W	0.019751	0.36096
M1a	0.99859	-0.041018

When examined with univariate methods, M1 area (M1a) (Fig. 72) does not show significant differentiation among the species ($p>0.05$). A tendency for increased M1a is noticed in *M. m. atavus* and *M. thoralis*. The lowest values are noted in *M. dimitrius* and *M. anakuma*, while *M. canescens* (Crete) has a wide range but possibly a tendency to higher mean value. *Meles meles* and *M. leucurus* have increased values.

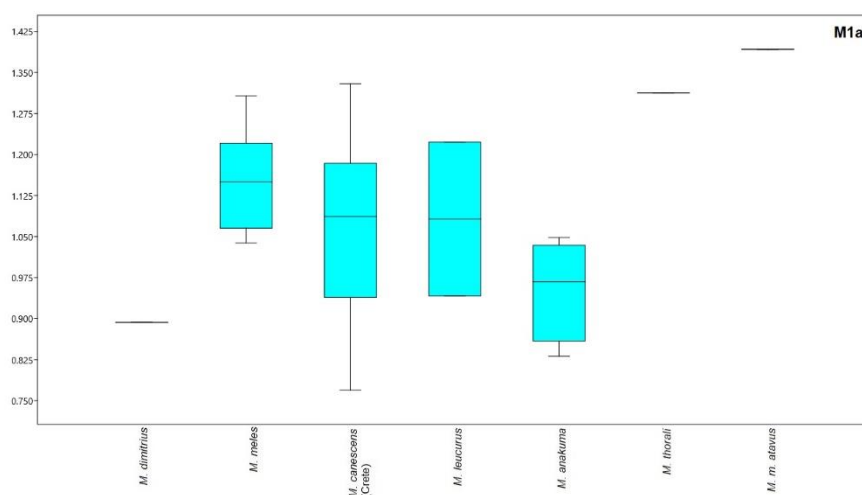


Figure 72. Boxplot of M1a of Meles.

Length of M1 (M1L) (Fig. 73) is found statistically important ($p<0.05$). *Meles dimitrius* and *M. thoralis* show lower values. *Meles anakuma* shows lower mean values but a wide range. *Meles meles*, *M. leucurus* and *M. m. atavus* have increased values and *M. canescens* (Crete) shows an increased mean value but a wide size range.

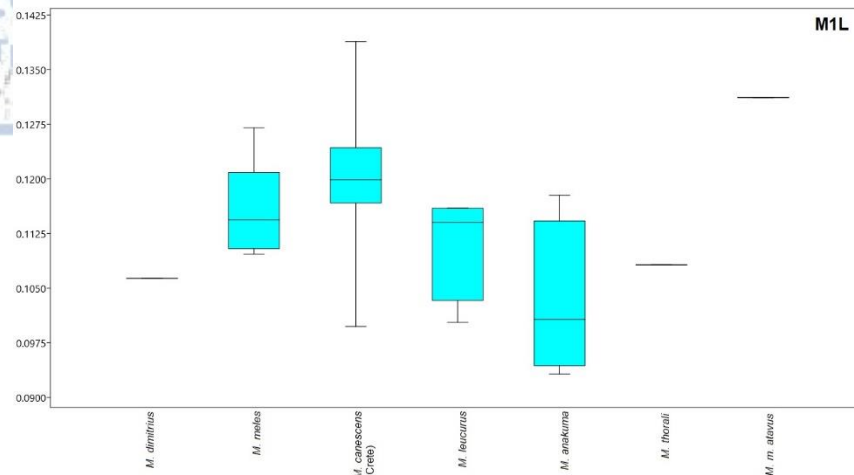


Figure 73. Boxplot of M1L of Meles.

Width of P4 (P4W) (Fig. 74) is also statistically important ($p < 0.05$). Its values are increased in *M. dimitrius*, *M. meles*, *M. canescens* (Crete) and *M. m. atavus*. *Meles anakuma*, *M. thoralis* and *M. leucurus* have decreased values.

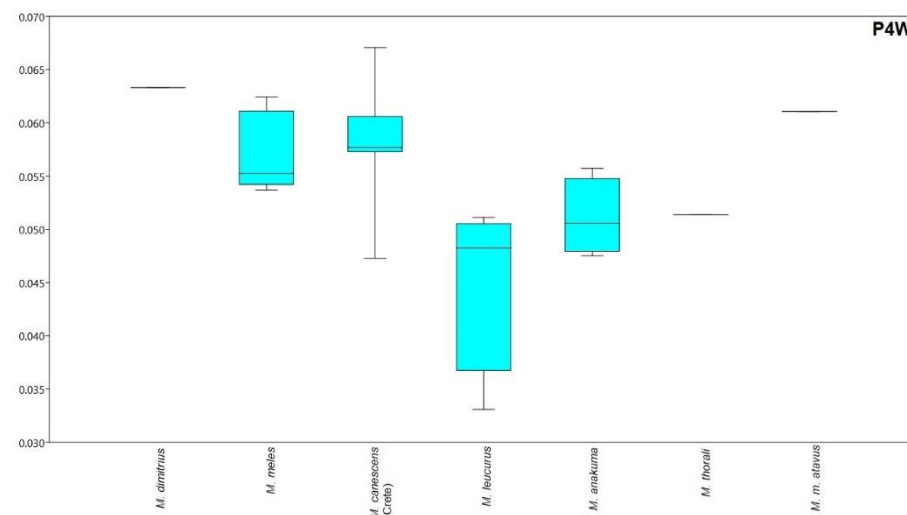


Figure 74. Boxplot of P4W of Meles.

INDICES

The indices computed concerning the upper dentition are presented below. The canine shape (CS) (Fig. 75) shows no obvious differentiation (except for decreased values for *M. dimitrius* and *M. thoralis*, indicating longer than wider canines). The relative upper grinding area (UGR) (Fig. 76) appears decreased in *M. dimitrius*, while the rest of the species seem to have intermediate values. Shape of P4 (P4P) (Fig. 77) appears increased in the insular specimens [*M. canescens* (Crete), *M. anakuma*] as well as in *M. dimitrius* and decreased in the rest. This indicates slightly wider P4 for the former species which could correspond to more developed P4.

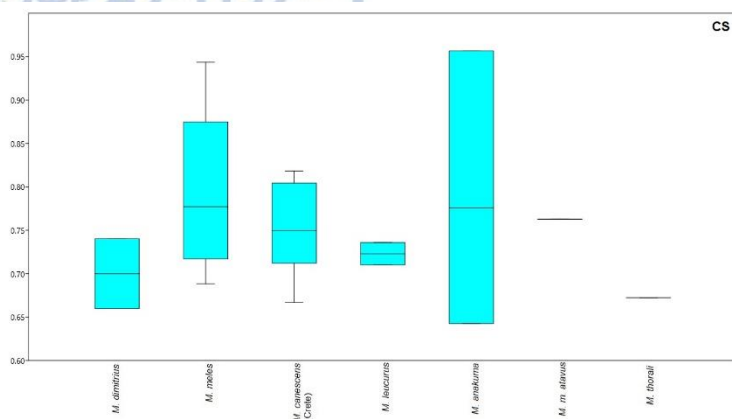


Figure 75. Boxplot of CS of Meles.

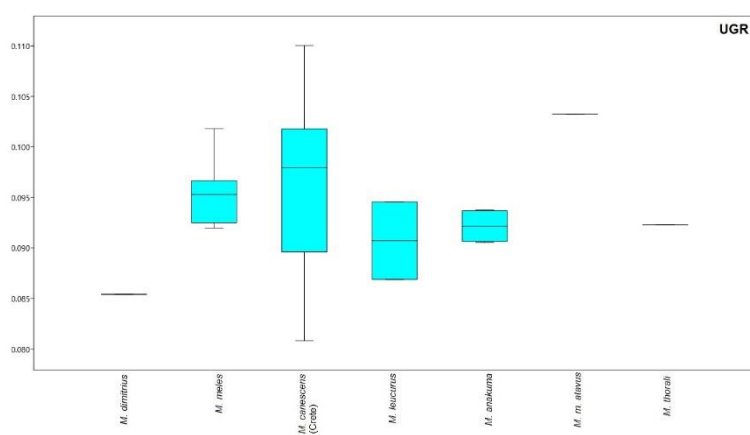


Figure 76. Boxplot of UGR of Meles.

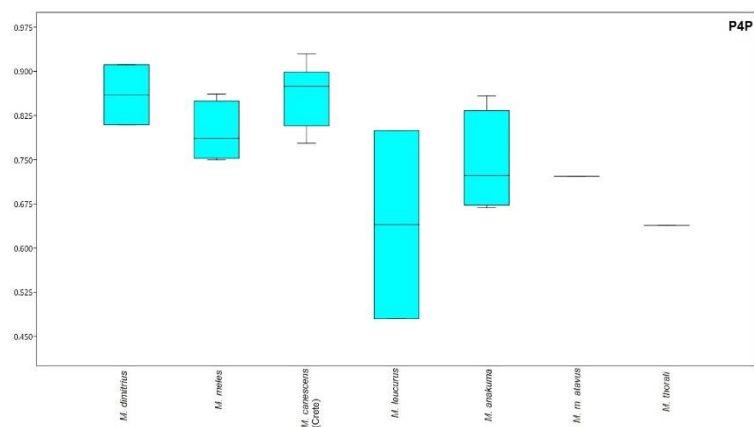


Figure 77. Boxplot of P4P of Meles.

PCA Lower dentition

The PCA of the lower dentition was based on sixteen normalized variables given in Table 12 along with the Eigenvalues and %variances. A plot for PC1 – PC2 (Fig. 78) explains 93.56% of the total variance. PC1 explains 64.32% and PC2 explains 29.24%. PC3 explains only a weak percentage of 2.91%.

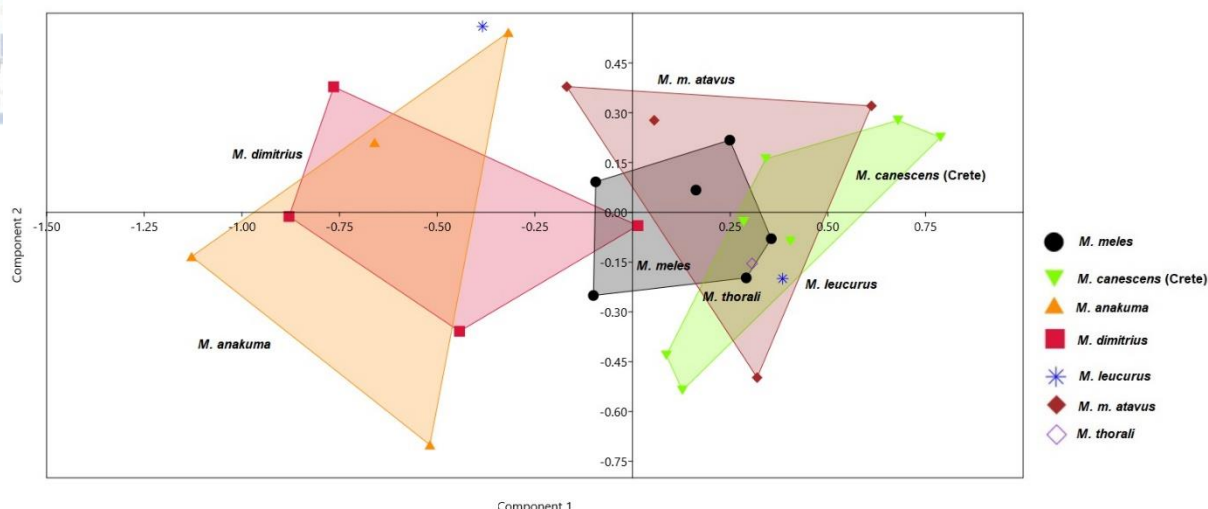


Figure 78. PCA of the lower dentition of Meles.

A discrimination can be noticed along PC1, despite the apparent overlap, while PC2 does not discriminate the taxa (Fig. 78). Based on PC1, a main group appears to be that of *M. anakuma* and *M. dimitrius*, and a second one that of *M. meles*, *M. canescens* (Crete), *M. m. atavus* and *M. thorali*. Once more, areas of m1 and m2 appear to be the most influential measurements (Table 12) for PC1. *Meles dimitrius* and *M. anakuma* have the smaller areas of m1 and m2 when compared to the second group which has increased values.

Table 12. Scores of the most influential measurements of the lower dentition (bold).

	PC1 Eigenvalue 0.233971 % variance 64.324	PC2 Eigenvalue 0.106375 % variance 29.245
c1L	0.017317	-0.05422
c1W	0.01991	0.038604
p2L	0.026545	-0.0098752
p3L	0.015243	-0.012184
p3W	-0.0050368	-0.011612
p4L	-0.0081078	-0.009237
p4W	0.005795	0.0040433
m1W	0.037617	-0.039238
m2L	0.040693	0.041587
m2W	0.04532	0.14711
m1Ltal	-0.015192	-0.026637
m1Ltrig	0.018576	0.018376
pr	-0.090559	-0.11573
mr	0.027053	-0.044083
m2a	0.35676	0.90515
m1a	0.92538	-0.36675

Univariate analyses of the most influential measurements (Figs 79 – 80) show decreased values (for both m1a and m2a) in *M. dimitrius* and *M. anakuma*. Interestingly, *M. canescens* (Crete), an insular representative, presents similar values to mainland representatives with increased areas of m1 and m2.

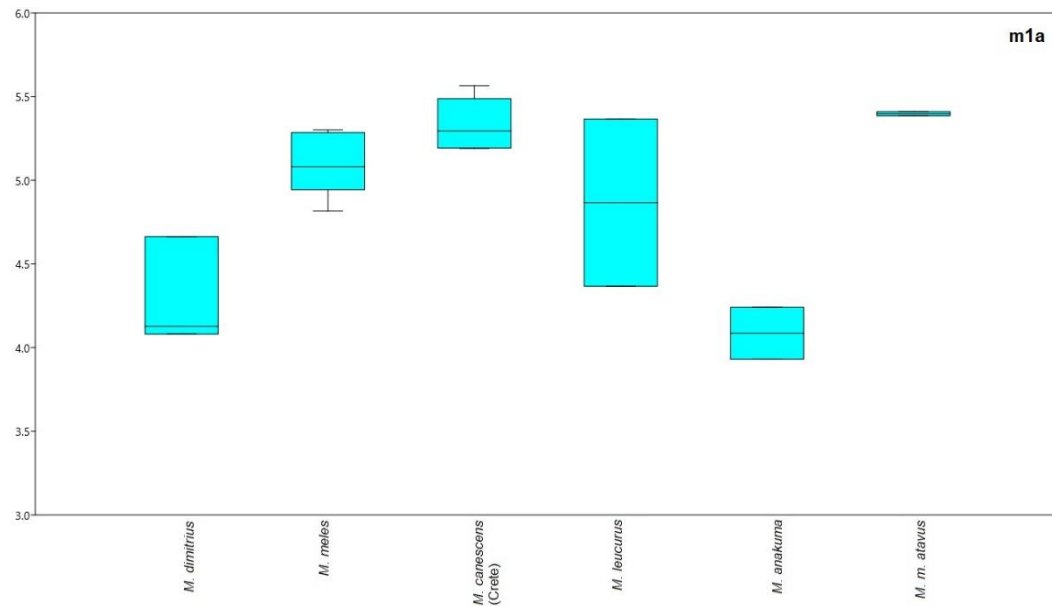


Figure 79. Boxplot of m1a of Meles.

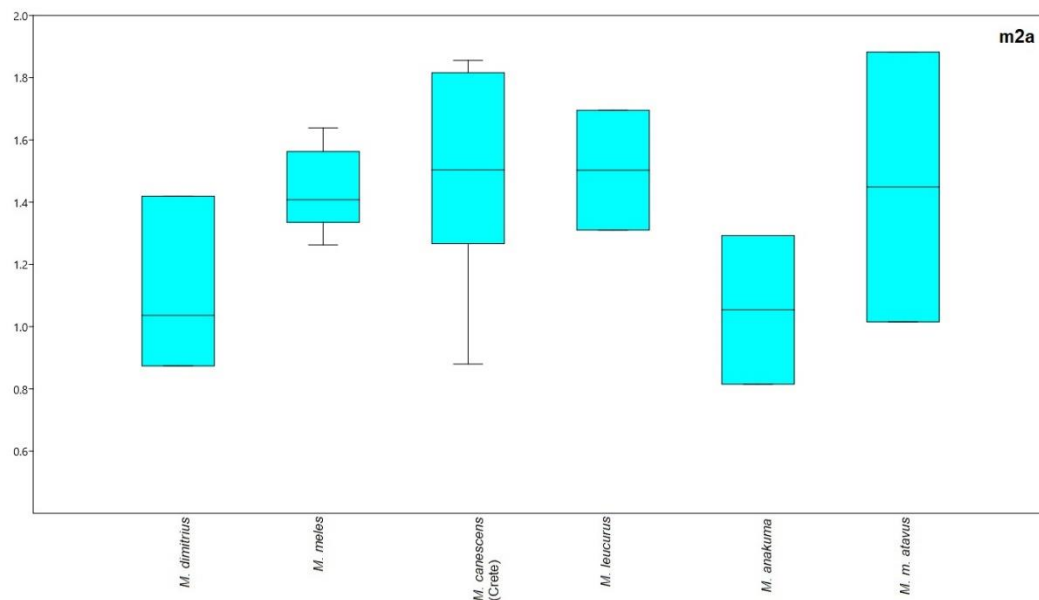


Figure 80. Boxplot of m2a of Meles.

INDICES

The dental indices concerning the lower dentition are presented below. The lower grinding area (LGR) (Fig. 81) is extremely increased in *M. canescens* (Crete) and *M. m. atavus*, while lower in *M. meles*, *M. leucurus* and at a lesser extent *M. dimitrius* and *M. anakuma*.

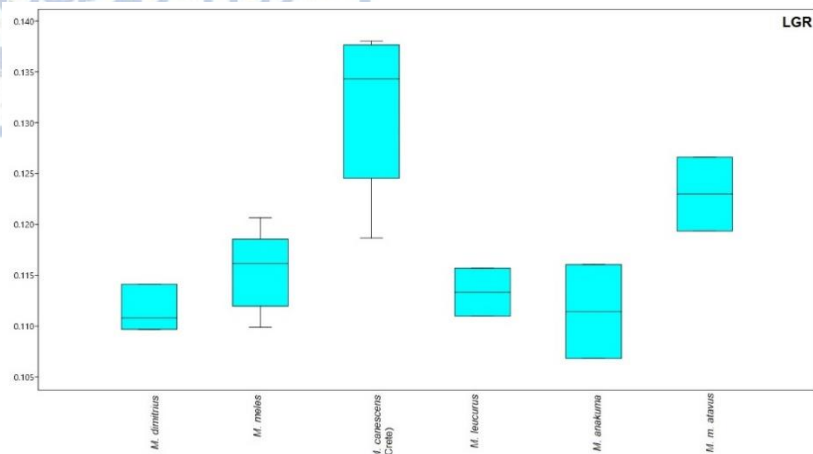


Figure 81. Boxplot of LGR of Meles.

The relative size of m2 (M2S) (Fig. 82) has the same allocation as m2a (Fig. 80) where *M. canescens* (Crete) has the highest values. Carnassial blade size (M1BS) (Fig. 83) is shown increased in *M. canescens* (Crete) and *M. m. atavus*, lower in *M. meles* and *M. leucurus* and slightly higher than the mainland group in *M. dimitrius* and *M. anakuma*.

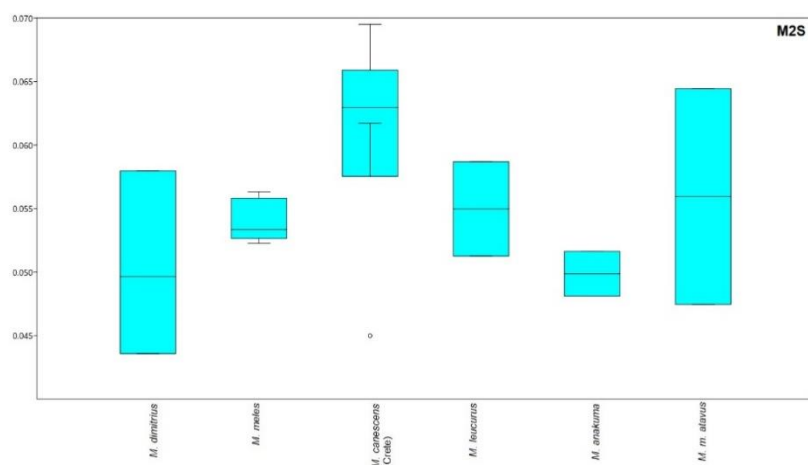


Figure 82. Boxplot of M2S of Meles.

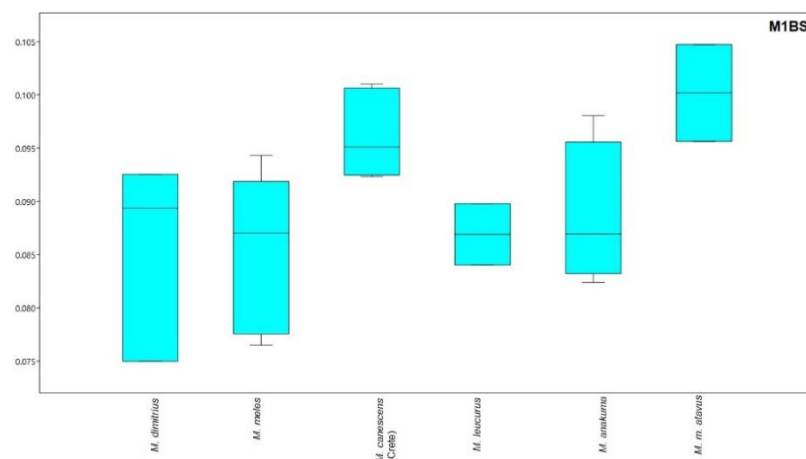


Figure 83. Boxplot of M1BS of Meles.

As far as premolars are concerned, *M. dimitrius* and *M. anakuma* show more developed and elongated teeth than the rest of the species (PMZ) (Fig. 84), the relative length of p4 (P4Z) (Fig. 85) is also increased in these two taxa (however in different extent) while *M. canescens* (Crete) has the lowest values. Shape of p4, which is the ratio of width to length (P4S) (Fig. 86), is increased in *M. canescens* (Crete) and *M. meles* indicating wider than longer p4.

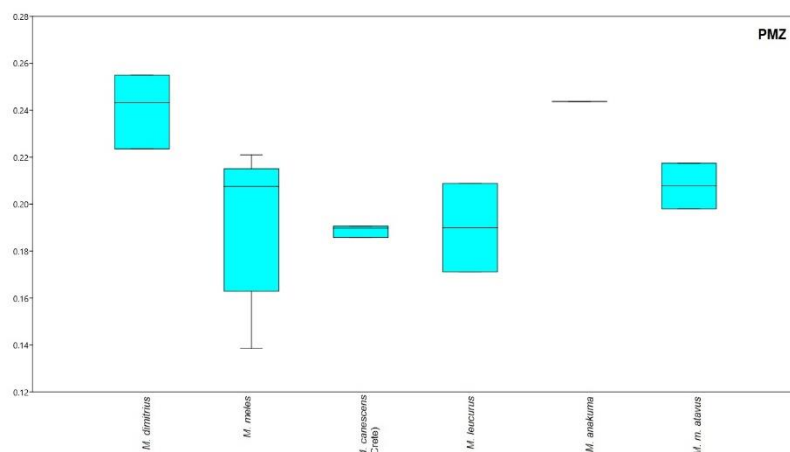


Figure 84. Boxplot of PMZ of Meles.

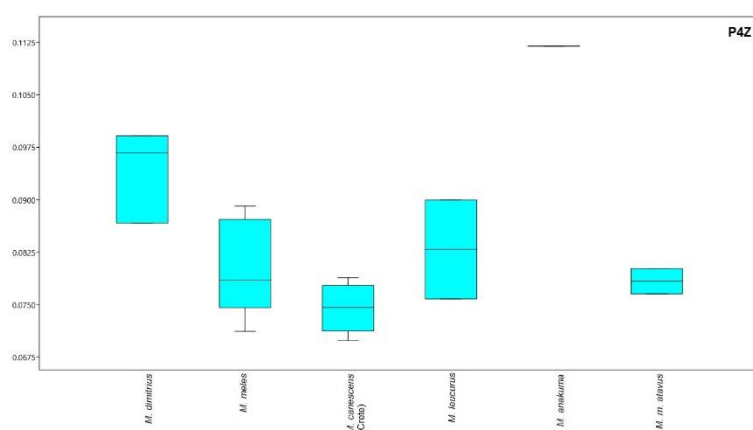


Figure 85. Boxplot of P4Z of Meles.

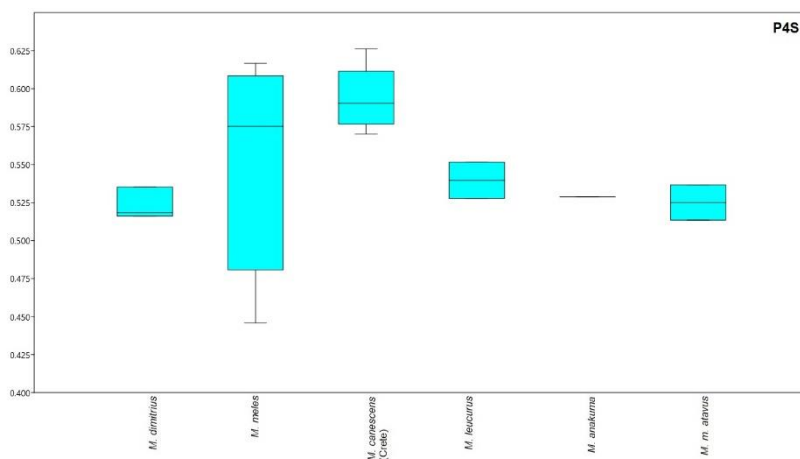


Figure 86. Boxplot of P4S of Meles.

Dry skull method; Bite force and Endocranial volume

The computed bite forces are presented below (Table 13). The two methods resulted in different bite force quotients (BFQ) as different variables were used to normalize the size effect based on the methods of Damasceno et al. (2013) and Sakamoto et al. (2010). Nonetheless, the analogies remained the same as far as to which species have increased bite forces and which lowered.

When examining the raw uncorrected data, the mainland forms of *M. meles* have increased bite forces which could be linked to their bigger size. Thus, the brain volume quotient is necessary to compare the results. When minimizing the effect of size, the smaller species appear to have the relative higher values. The first method (Damasceno et al. 2013) (Fig. 87) shows that the bite forces of the taxa are all in the same range. *Meles anakuma* overlaps with the rest of the taxa. The mean values of *M. meles* are placed lower and the mean values of *M. anakuma* are placed higher. The value of APL – 546 (*M. dimitrius*) is placed within the range of all the species however, it is closer to the mean value of *M. canescens* (Crete). The second method (Sakamoto et al. 2010) (Fig. 87) shows, as before, that all species are in the same wider range of values. *Meles anakuma* overlaps with the values of the rest of the taxa, however, its mean values are placed high. *Meles meles* also has a wide range but its mean values are placed lower than the rest of the taxa. *Meles dimitrius* exceeds the values of the mainland *M. meles* and is clearly within the range of *M. canescens* (Crete) and closer to the mean values of *M. anakuma*. Unfortunately, there were not enough data to compute bite force and brain volume for *M. leucurus*.

Table 13. Computed bite forces, bite force quotients and brain volume quotients, Damasceno's method, Sakamoto's method.

Species	Specimen	Fcorr	BFQ Damasceno	BFQ Sakamoto	BVQ
<i>Meles dimitrius</i>	APL 544	357.248	35.338	129.642	156.377
<i>Meles meles</i>	K1	342.458	31.463	135.141	117.390
<i>Meles meles</i>	B2	341.063	30.042	102.909	163.510
<i>Meles meles</i>	H3	363.608	35.651	-	144.878
<i>Meles meles</i>	G5	421.087	38.818	120.353	160.734
<i>Meles meles</i>	1009	345.802	31.809	121.262	138.608
<i>Meles meles</i>	1010	330.357	29.972	112.308	127.729
<i>Meles meles</i>	1011	251.681	27.360	105.788	143.052
<i>Meles canescens</i> (Crete)	T4	325.914	35.282	130.429	191.665
<i>Meles canescens</i> (Crete)	Fc3802	301.495	34.240	123.731	125.950
<i>Meles canescens</i> (Crete)	Fc22898	277.623	33.487	117.494	125.660
<i>Meles canescens</i> (Crete)	Fc2702	341.786	46.935	147.500	163.286
<i>Meles canescens</i> (Crete)	Fc4685	283.405	34.817	123.684	136.074
<i>Meles canescens</i> (Crete)	Fc1364	334.615	37.813	121.115	156.091
<i>Meles anakuma</i>	PRI 177	271.264	41.794	149.953	136.709
<i>Meles anakuma</i>	PRI 1846	297.062	40.049	126.934	157.348

Meles anakuma	PRI 1847	229.848	37.971	127.523	146.359
Meles anakuma	Y1	239.386	24.520	101.352	163.200

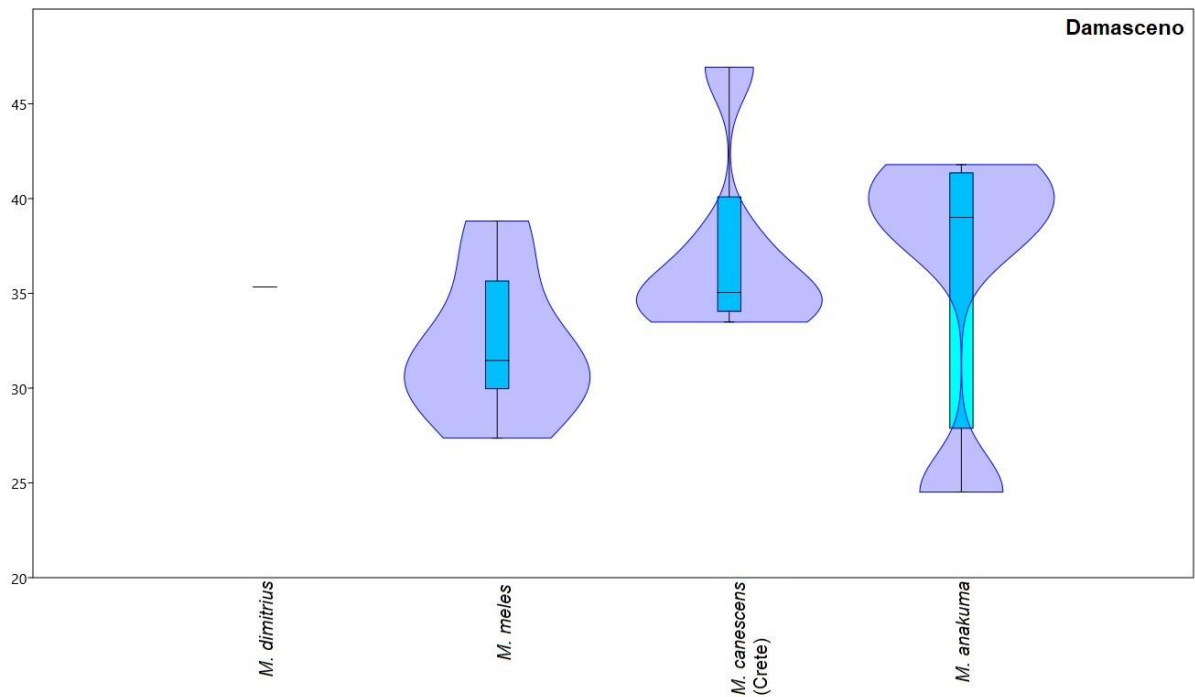


Figure 87. Bite force quotients of Meles (Damasceno's method).

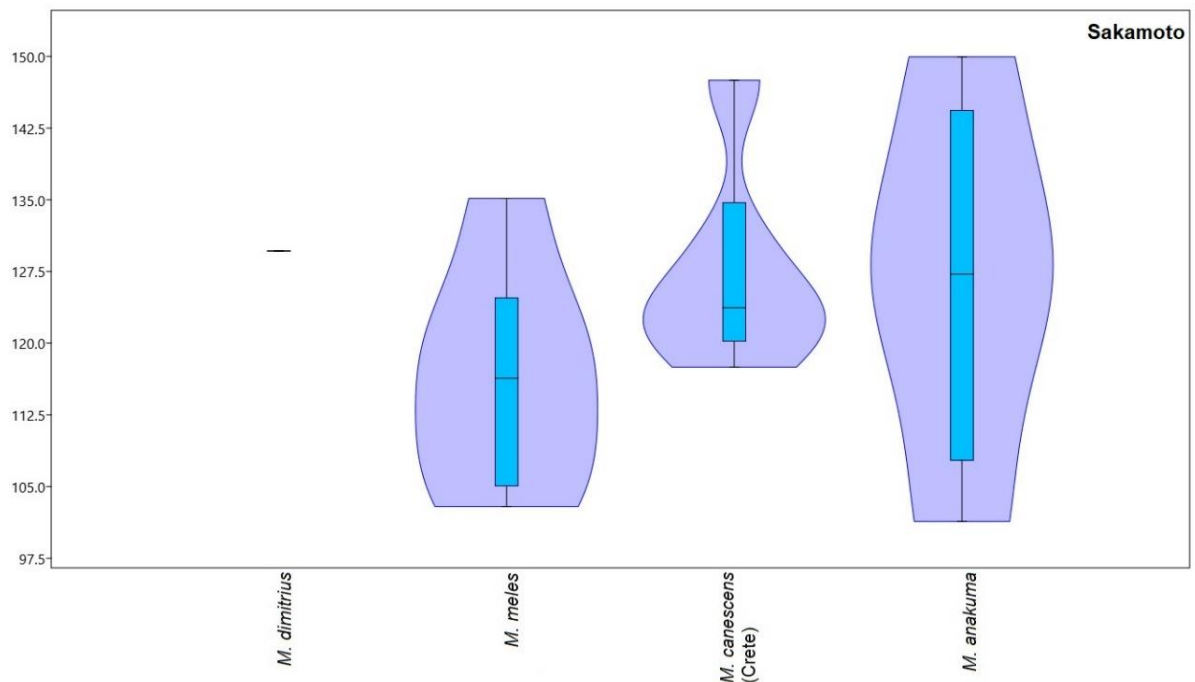


Figure 88. Bite force quotients of Meles (Sakamoto's method).

As far as braincase volume is concerned (Fig. 89), the species are placed in the same range. *Meles canescens* (Crete) overlaps with all of the taxa but with mean values closer to *M. anakuma*. The mean values of *M. meles* are placed lower than the insular species however they are extremely close, and the difference is not extreme. *Meles*

dimitrius is placed within the range of *M. canescens* (Crete) and *M. anakuma* closer to the mean values of *M. anakuma* (Fig. 89). A slight tendency for increased braincase volume based on the mean values, is noticed in the insular species and in *M. dimitrius* just as in the computation of bite force. Kargopoulos (2019) has also computed a bite force and brain volume value for *M. dimitrius* (without however eliminating the size effect). His results differ from those of our study (which are relatively lower when compared with bite force and higher when compared with brain volume), possibly due to the slight differences of the used methodology.

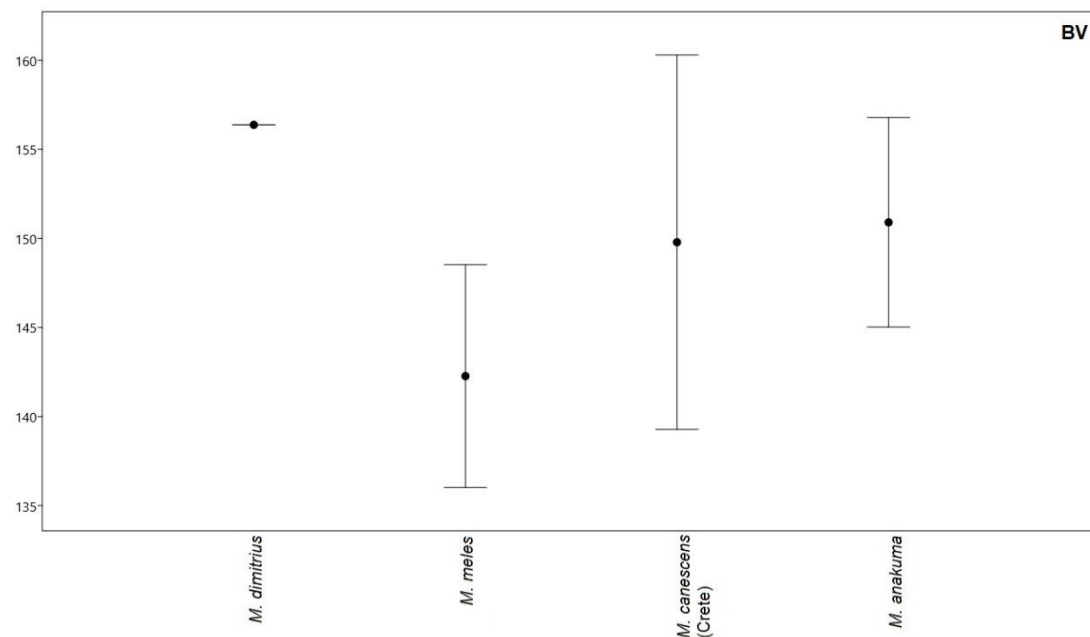


Figure 89. Braincase volume quotients of Meles based on Damasceno et al. (2013) estimation method.

Muscle accommodation

Percentages of mass of the adductor muscles (Table 14) as well as percentages of the Physiological Cross Sectional Area (PCSA) (Table 15) were computed showing the relative accommodation of each muscle. The PCSA percentages were compared with results from Ito and Endo (2016) containing a list of carnivorous species (Table 16) (Figs 90 – 93). The relative variance of each muscle of the different species is presented in Figs 90 – 91, while Mustelidae are isolated in Figs 92 – 93.

What can be inferred from the percentages of mass (Table 14) and PCSA (Table 15) is that the dominant muscle is the temporalis followed by the masseter and lastly by the pterygoids (medial and lateral). Specifically, temporalis is by far the largest muscle, approximately 3/4 of the total muscle mass and 2/3 of total PCSA of adductors. The pterygoids have the smaller percentage while masseter is less than 1/3 of the total mass and PCSA.

Table 14. Percentages of the mass of the adductor muscles of the dissected skulls of Meles meles.

	Masseter (%)				Pterygoids (%)	Temporalis (%)
	Whole	Superficial	Middle	Deep		

Cranium 1 (s)	17.35	9.58	4.45	3.29	4.64	78.05
Cranium 2 (l)	17.06	8.65	5.11	2.91	5.07	77.86
Mean values	17.21	9.12	4.78	3.1	4.86	77.96

Table 15. Percentages of the PCSA of the adductor muscles of the dissected skulls of *Meles meles*.

	Masseter (%)				Pterygoids (%)	Temporalis (%)
	Whole	Superficial	Middle	Deep		
Cranium 1 (s)	25.04	9.41	9.09	6.55	10.58	64.38
Cranium 2 (l)	21.58	8.42	8.11	5.04	10.59	67.82
Mean values	23.31	8.92	8.60	5.80	10.59	66.1

Interestingly, the layers of the masseter in *Meles* differentiate in their development when compared to other taxa (Table 16) (Figs 91, 93). The superficial is the largest layer. The middle masseter is the second largest layer and the deep masseter the smallest, differentiating the genus *Meles* from the majority of the species where the deep layer seems to dominate over the middle (Ito and Endo, 2019; Penrose et al., 2016).

PCSA data computed from the dissection of *M. meles* as well as PCSA data by Ito and Endo (2016) (Table 16) were plotted on ternary diagrams (Figs 90 – 91). *Meles meles* groups with the rest of the Mustelidae clade. The groups that are observed are mainly differentiated based on the diet preferences of each species which therefore affect the overall development of the different muscle groups. Species from the same family also appear to group together, a case most apparent in the Mustelidae. Certain species (*Martes melampus*, *Aonyx cinerea*, *Potos flavus* and *Canis lupus familiaris*) are placed further from the representatives of their clade.

Table 16. Percentages of the PCSA of the adductor muscles. Data from Ito and Endo, 2016. *Meles meles* data (bold) calculated from the dissected skulls.

Family	Species	Temporalis	Pterygoid	Masseter	Layers of masseter (%)			
				Whole	Superficial	Middle	Deep	
Felidae	<i>Puma concolot</i>	38.85	16.48	44.7	48.7	24.88	26.42	
	<i>Felis catus</i>	42.59	10.64	46.76	55.71	20.42	23.12	
	<i>Panthera uncia</i>	45.47	14.26	40.27	56.25	18.25	25.5	
Viverridae	<i>Paguma larvata</i>	48.15	12.27	39.59	54.36	16.7	29.17	
Mustelidae	<i>Aonyx capensis</i>	62.65	9.71	27.64	32.34	24.02	43.63	
	<i>Aonyx cinerea</i>	54.31	14.09	31.6	47.37	25.63	26.99	
	<i>Enhydra lutris</i>	64.89	7.22	27.88	41.75	21.74	36.51	
	<i>Neovison vison</i>	64.82	9.32	25.86	49.46	32.52	18.06	
	<i>Mustela itatsi</i>	70.37	8.24	21.39	35.62	38.1	34.46	
	<i>Martes melampus</i>	45.02	9.85	45.13	23.38	34.66	41.95	
	<i>Meles anakuma</i>	68.05	7.37	24.58	47.72	38.89	13.38	
	<i>Meles meles</i>	66.10	10.59	23.31	38.27	36.89	24.88	
	Procyonidae	<i>Nasua nasua</i>	54.7	13.45	31.85	50.77	12.72	36.51
		<i>Procyon lotor</i>	49.87	13.55	36.58	41.09	23.84	35.07

	<i>Potos flavus</i>	61.66	8.84	29.5	44.95	30.68	24.34
Phocidae	<i>Phoca largha</i>	51.17	13.56	35.27	43.78	35.21	21.01
Canidae	<i>Canis lupus familiaris</i>	52.54	18.98	28.47	42.01	25.15	32.84
	<i>Nyctereutes procyonoides</i>	47.26	14.77	37.97	53.07	21.57	26.02
	<i>Vulpes vulpes japonica</i>	48.98	11.39	39.64	50.45	20.94	28.61

Compared with other carnivores, the relative allocation of the PCSA of the muscles appears to be the same (Fig. 90). The temporalis represents the majority of the adductor muscular system, the masseter is the second largest and the pterygoids are last. In some specific taxa (*Martes melampus*, *Felis catus* and *Puma concolor*), the masseter seems to be equal or even larger than the temporalis. As far as the PCSA of the different layers of the masseter are concerned (Fig. 91), *Meles* has a developed middle layer rather than deep in contrast with most of the representatives of the Felidae and Canidae.

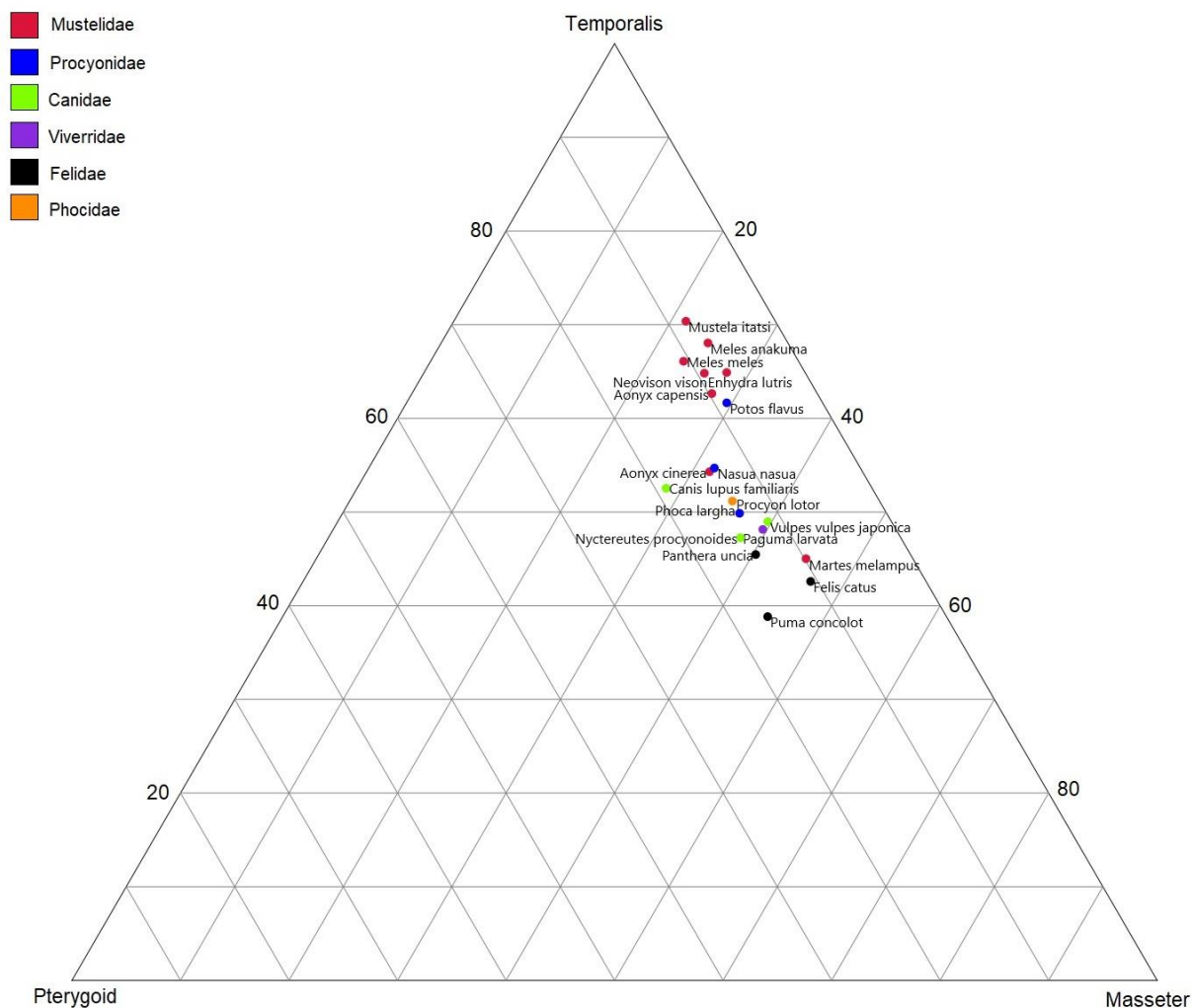


Figure 90. Ternary plot of percentages of PCSA of the adductor muscles of various carnivores (data for *Meles meles* computed from the dissection and data concerning the rest of the taxa adapted from Ito & Endo, 2016).

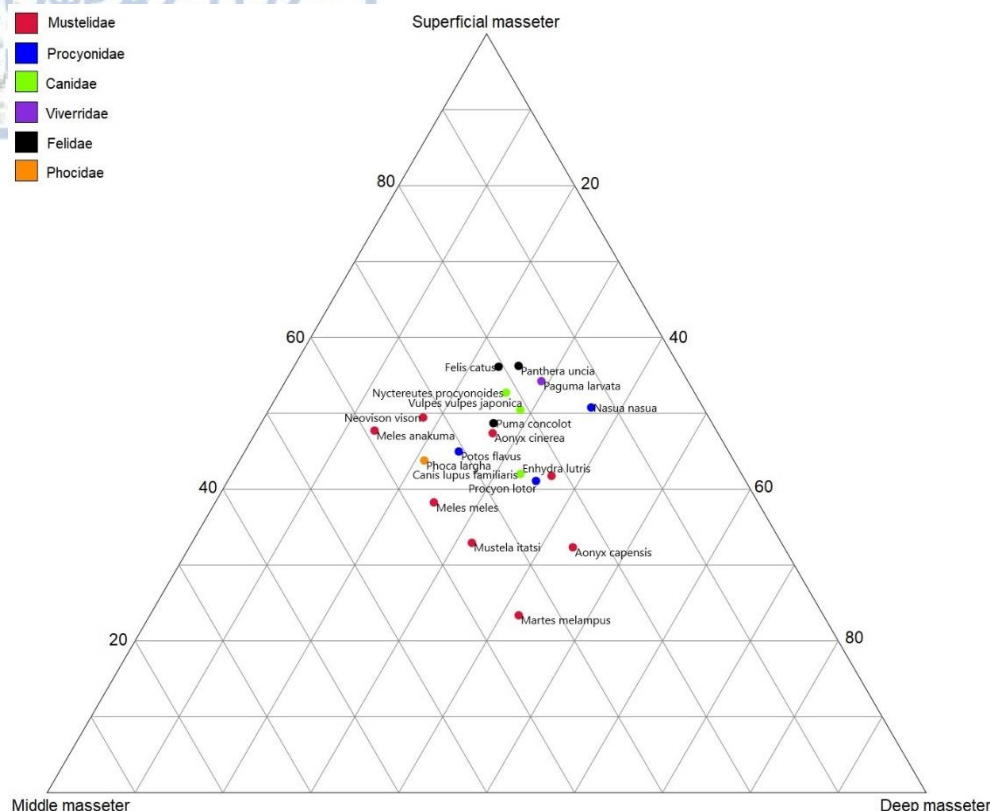


Figure 91. Ternary plot of percentages of PCSA of the layers of masseter of various carnivores (data for *Meles meles* computed from the dissection and data concerning the rest of the taxa adapted from Ito & Endo, 2016).

When isolating the mustelids, *M. meles* and *M. anakuma* present some differences. They mainly seem to differentiate at the pterygoids (Fig. 92) which are more developed in *M. meles*, while *M. anakuma* has slightly more developed temporalis. *Martes melampus* is the only mustelid which is distinctive from the rest with an increased masseter percentage. Furthermore, in *M. anakuma* the deep masseter appears more restricted (Fig. 93), when compared to the slightly more developed in *M. meles*.

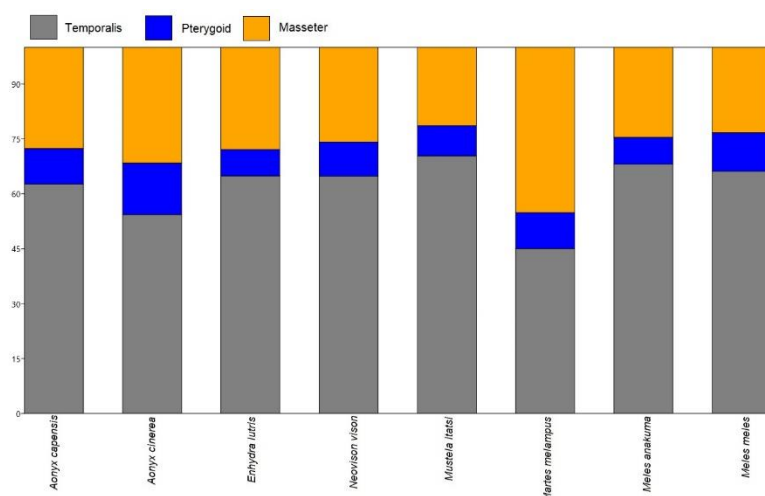


Figure 92. Percentages of PCSA of the adductor muscles of mustelids (data for *Meles meles* computed from the dissection and data concerning the rest of the taxa adapted from Ito & Endo, 2016).

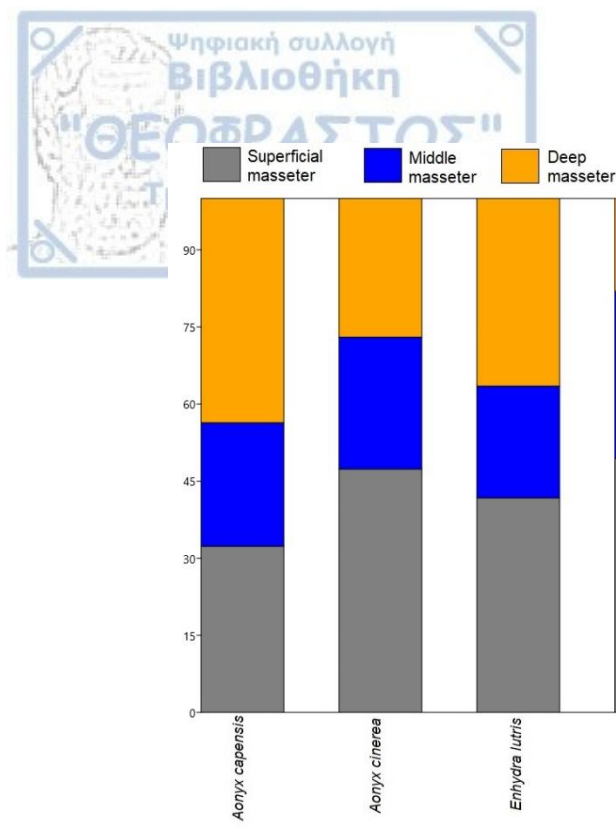


Figure 93. Percentages of PCSA of the layers of masseter of mustelids (data for *Meles meles* computed from the dissection and data concerning the rest of the taxa adapted from Ito & Endo, 2016).

PCSA, Bite force and comparison of wet and gross method

The PCSA of the muscles of the two dissected skulls was computed using the values of muscle mass (g) (from which the overall volume was computed along with muscle density) and fascicle length (cm) (Table 17). The overall produced force that the masticatory muscles can exert was computed by PCSA as well as by the dry skull method (Table 18). Moreover, bite force was estimated using the data inferred from the computation of the actual PCSA. Also, bite force of the same two dissected skulls was computed by the dry skull method in order to compare the results and observe the differences of these two methods (Table 19). The masseter was the only muscle where the layers were computed separately and added up in the end as the fascicles had a notably different direction. Data for the digastricus muscles are also available, however they are not used in the computation of bite force as only the adduction is of interest here.

As expected, the temporalis showed the largest values of PCSA, followed by the masseter and the pterygoids. The total forces that can be exerted from the muscles, present differences when the two methods (dry and PCSA) are used. The larger cranium presented increased forces in the gross method and the small cranium presented increased forces in the dry method even though the gross method considers the pterygoids as well, and better depicts the actual development of the muscles (Table 18). Computation of bite force using the formula of the dry method and correcting the area of masseter and temporalis using values from the PCSA, showed similar results with the computation of the total force. The gross method overestimated the force of the large cranium and underestimated that of the smaller cranium (Table 19).



Table 17. Mass, fascicle length, and PCSA of the masticatory muscles of the two dissected skulls of *Meles meles*.

		Masseter			Temporalis			Pterygoids			Digastricus		
		Mass (g)	FI (cm)	PCSA (cm ²)	Mass (g)	FI (cm)	PCSA (cm ²)	Mass (g)	FI (mm)	PCSA (cm ²)	Mass (g)	FI (cm)	PCSA (cm ²)
Cranium 1 (s)	Superficial	3.6005	3.836	0.885	29.344	4.571	6.056	1.7445	1.654	0.995	5.721	4.086	1.321
	Middle	1.673	1.846	0.855									
	Deep	1.2365	1.895	0.616									
	Total			2.356									
Cranium 2 (l)	Superficial	6.423	4.233	1.431	57.85	4.735	11.526	3.768	1.975	1.800	7.655	5.327	1.356
	Middle	4.095	2.801	1.379									
	Deep	2.16	2.377	0.857									
	Total			3.667									

Table 18. Total force computed with data from the dry method and the dissection of *Meles meles*.

	Total force of masseter and temporalis from dry skull (N)	Total force of masseter, temporalis and pterygoid from PCSA (N)
Cranium 1 (s)	425.961	348.057
Cranium 2 (l)	496.978	628.771

Table 19. Bite force computed by dry and gross method of *Meles meles*.

	Dry method bite force (N)	Gross method bite force (N)
cranium 1 (s)	316.55	227.03
cranium 2 (l)	433.08	472.93

Body mass

The estimation of body mass according to Van Valkenburgh (1990) is presented in Fig. 94. *Meles meles* has a range of approximately 9kg to 13kg, *M. canescens* (Crete) of 5.6kg to 8kg with a single exception of a specimen which weighs 10.5kg. *Meles anakuma* ranges between 4.9kg to 10kg and *M. leucurus* from 10kg to 14kg. The mainland species appear to be larger (*M. meles*, *M. leucurus*) than the insular ones. *Meles dimitrius* is close to the range of *M. meles* with a weight of 10.8kg. However, the species is represented by a single specimen which cannot be considered representative, as there is considerable variation, even in small insular populations, like that of *M. canescens* (Crete). The fact that the insular specimens have a notably reduced size should be noted. While *M. meles* and *M. leucurus* appear to be similar in size, *M. canescens* from Crete and *M. anakuma* from Japan are smaller, with the latter being the smallest of all. *Meles dimitrius* has an intermediate size placed between the mainland and insular specimens, not far from the single value estimated for *M. m. atavus* and significantly smaller than that of *M. thoralis*. *Meles dimitrius* (specimen APL – 544) was found to have a weight of 10.8kg, a result which seems to be near the

minimum of the body mass range estimated for *M. dimitrius* by Kargopoulos (2019) (~11-17kg).

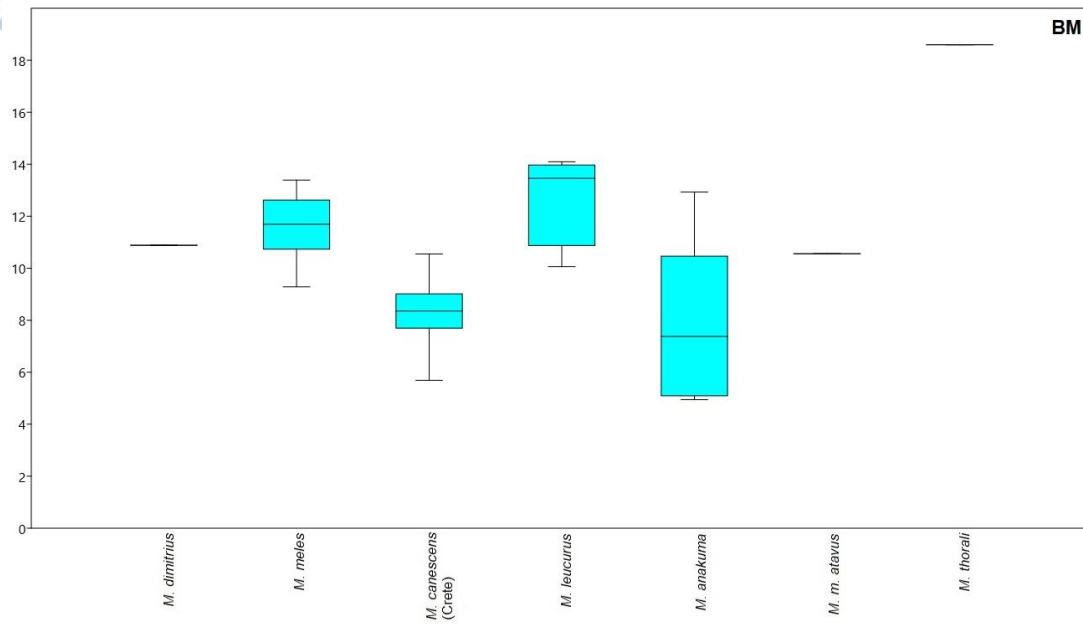


Figure 94. Body mass of Meles based on Van Valkenburgh (1990) estimation method.

DISCUSSION

The purpose of the study was to investigate the ecomorphology of the genus *Meles* by examining the extant European [*M. meles*, *M. canescens* (Crete)] and Asian (*M. leucurus*, *M. anakuma*) species, as well as the fossil representative, *Meles dimitrius* from Greece. Comparisons were made in order to infer whether different ecomorphs exist.

The observation of the masticatory system by dissecting two skulls of *M. meles* lead to the creation of a muscle map for both the extant *M. meles* and extinct *M. dimitrius*. The relative accommodation of the muscles was also examined, and temporalis was found to be the dominant adductor muscle. No significant differences were found in the extinct *M. dimitrius*, except for a possibly more enhanced superficial temporalis and a less developed superficial and middle masseter. Quantitative analyses (PCA, boxplots, computation of bite force by the dry skull method, PCSA by gross method, endocranial volume and body mass) supplemented by non – metric descriptive comparisons of extant and extinct species, show common traits between *M. dimitrius* and the insular badgers [*M. canescens* (Crete), *M. anakuma*] in distinction from the mainland group (*M. meles*, *M. leucurus*).

The main traits characterizing the insular group and *M. dimitrius* concern the temporalis muscle, the computed bite force and the brain volume, which show increased development when compared to the mainland species. Additionally, increased interorbital distances, well – developed digastricus and dentition with enhanced blade morphology of the carnassials are also common features in these species. *Meles dimitrius* differentiates from the extant insular species by a larger size and having an enhanced neck musculature, as attachment sites of neck muscles (nuchal crest, mastoid process) are well-developed.

PCA, Non – metric descriptive and Myological remarks

Results of PCA along with descriptive osteological and myological observations support some inferences about the functional morphology of the examined species. A grouping of a more mainland ecomorph (*M. meles*, *M. leucurus*) and a second more isolated/insular [*M. canescens* (Crete), *M. anakuma*, *M. dimitrius*] is apparent. A secondary grouping of the European [*M. meles*, *M. canescens* (Crete), *M. dimitrius*] and the Asian (*M. anakuma*, *M. leucurus*) species is also obvious and could possibly be attributed to phylogenetic factors. The insular/isolated species seem to share some characteristics which differentiate them from the mainland population. However, insular carnivores do not present specific adaptations which would be considered as a rule for insular endemism worldwide (Lyras et al., 2010). On the contrary certain adaptations differ even from island to island (Nanova et al., 2017).

Cranium

One discriminative parameter among the two main groups of insular and mainland, is the length of the temporal fossa, which is indicative of the size and accommodation of the temporalis muscle (Anyonge and Baker, 2006; Radinsky, 1981). Therefore, increased values [as noted in *M. dimitrius*, *M. canescens* (Crete) and *M. anakuma*] suggest increased areas of attachment for the temporalis muscle which would lead to increased forces for these species. Temporal fossa length alone is not adequate to indicate increased areas of temporalis. This variable is usually examined in

combination with post orbital constriction (Sicuro and Oliveira, 2011) which along with temporal fossa length define the area of the muscle. Measurements of postorbital constriction show increased values in *M. canescens* (Crete) and *M. anakuma* (data for *M. dimitrius* were not available), which do not agree with the increased development of temporalis. However, it could be of lesser importance as the overall forces computed are increased in the isolated/insular species and other morphologies (mentioned below) could compensate for this trait. Nonetheless, another variable that should be considered when examining the development of temporalis is the maximum zygomatic width as the masseter arises from the lower part of the arch and temporalis passes through it. Widened zygomatic area is indicative of a more robust temporalis (Anyonge and Baker, 2006; Penrose et al., 2016; Sicuro and Oliveira, 2011, 2002; Van Valkenburgh, 2007). *Meles dimitrius*, *M. canescens* (Crete) and *M. anakuma* all seem to share this character. *Meles thoralis* also appears close to this group with increased zygomatic breadth. Nanova et al. (2017) and Nanova and Prôa (2017) compared mainland and insular foxes and found that insular ones possessed wider zygomatics. The more lateral placement of the zygomatic arches is indicative of larger cross-sectional areas and therefore greater forces of the temporalis muscle. Also, it could be an indicator to better withstanding induced forces as zygomatic arches placed more laterally have lower strains induced on them. As far as the masseter is concerned, wider zygomatics allow a more ventral placement of these muscles. Consequently, weaker forces of the masseter are apparent while force of temporalis would be increased (Hartstone-Rose et al., 2014). This adaptation could correlate with more extensive use of the temporalis rather than the masseter, which is characteristic in more carnivorous animals. Additionally, Miller's index is increased in the insular group supporting a wider zygomatic arch than in the mainland species. Miller's index also supports the non – metric observation of wider skulls for *M. dimitrius*, *M. canescens* (Crete) and *M. anakuma*. *Meles meles* and *M. leucurus* show a more elongated shape according to Miller's index, suggesting skulls which favor biting velocity rather than biting strength (Timm-Davis et al., 2015).

Braincase width is increased in *M. dimitrius*, *M. canescens* (Crete) and *M. anakuma*, a trait which correlates with the more widened than lengthened skull of these species. Wider braincases allow increased insertion areas for the temporalis muscle and therefore a more developed muscle (Timm-Davis et al., 2015; Tseng and Flynn, 2015). Braincase width is also combined with braincase length suggesting a larger overall braincase, which also differentiates European from Asian species, as the Asian ones present a more lengthened braincase than the European. Braincase size is also indicative of the endocranial volume which was computed with the dry skull method, according to Damasceno et al. (2013). The results indicate increased values for *M. dimitrius*, *M. canescens* (Crete) and *M. anakuma* when compared to the equivalent mainland species, which agrees with the increased values of braincase width. If these traits are combined, a compensation for the increased postorbital constriction could occur, favoring the development of the temporalis muscle. Additionally, when bite force was computed with the dry skull method, it was found that the insular species have slightly increased values, supporting the hypothesis of a more developed muscular system of mastication.

Non – metric observations on the examined skulls show a well – developed superficial layer of temporalis for *M. dimitrius*. The enhanced sagittal crest along with the extra

structure in the front part of it, suggest larger origin areas for the superficial temporalis. As far as neck strength and locomotion is concerned, the nuchal crest, mastoid process, occipital condyles, and magnum foramen provide some information. Non – metric observations related to the nuchal crest suggest larger attachment areas for neck muscles (Law, 2019; Van Valkenburgh, 2007) in *M. dimitrius* and therefore stronger neck musculature, medium in *M. meles* and *M. leucurus* and reduced in *M. canescens* (Crete) and *M. anakuma*. The structure of the mastoid process in *M. dimitrius* would also correspond to a more enhanced neck musculature as well as that of the occipital condyles. More robust occipital condyles indicate increased neck and head musculature and therefore stability, especially when the head moves in a lateral direction in order to capture and kill prey. Increased stability is needed so that dislocation is avoided (Dumont et al., 2016). The foramen magnum differentiates *M. dimitrius*, *M. canescens* (Crete) and *M. anakuma* from the mainland group. The narrower and more dorsoventrally developed opening could indicate increased head mobility as less constricted areas of the atlanto-occipital joint are possibly linked to more carnivorous diet preferences so that a wider range of movement is allowed in contrast to more herbivorous forms which do not require a broadened range (Vander Linden et al., 2019).

Structures related to the digastricus muscle include the mastoid and paroccipital process which are the areas where it originates. These structures in *M. canescens* (Crete) and *M. dimitrius* correspond to a more developed digastricus which would indicate powerful and wide opening of the mandible, a trait specifically useful for carnivores (Scapino, 1976).

The pterygoid bone structure related to the origin site of the pterygoid muscles and specifically of the medial pterygoid is better developed in *M. canescens* (Crete) rather than in *M. meles*. The medial pterygoid pulls the mandible medially (Ito and Endo, 2016), thus, a larger origin area could indicate a more developed medial pterygoid for *M. canescens* (Crete) and possibly a tendency to perform lateral movements of the mandible at an increased rate. The area of the pterygoids could not be observed in *M. dimitrius* as it was damaged.

Meles dimitrius presents a wider rostrum, a morphofunctional adaptation to decrease torsion during struggling with prey and consequently lessen the possibility of mandible dislocation (Meachen-Samuels and van Valkenburgh, 2009). The PCA analysis showed that *M. canescens* (Crete), as well as *M. anakuma*, also exhibit wide rostra, like *M. dimitrius*.

Another characteristic, which seems to similarly develop in the insular specimens, is interorbital distance which corresponds to the distance between the eye sockets. It is suggested that the eyes of nocturnal animals are placed closer to each other rather than those which are more diurnal, where they are placed wider apart (Dumont et al., 2016). Nocturnal animals exhibit such a behavior usually in order to avoid predators and danger. Since *M. dimitrius*, *M. canescens* (Crete) and *M. anakuma* have increased interorbital distance they could be characterized as less nocturnal, an adaptation which could be connected with the decreased competition and presence of predators on the islands. For example, *M. canescens* (Crete) is the largest predator on the island (Sfenthourakis and Triantis, 2017) so it would be less dangerous to search for food

and wander around during the day. Additionally, Sleeman et al. (2009) reports that insular badgers of British islands also feed during the day. This trait raises some interesting questions for *M. dimitrius*. Both the faunas of Apollonia and Gerakarou include possible predators and so a diurnal behavior due to their absence as in other insular environments cannot be supported. Could *M. dimitrius* possess a specific defense mechanism that allowed its activity during the day? Could it be that those predators did not prefer to hunt badgers neither as a food resource nor as a way to eliminate competition as their preys might not have overlapped or is it that this trait is connected to something else entirely?

Regarding the morphology of the auditory bullae, more developed structures (more inflated) are connected with better hearing and are usually present in animals residing in more open environments (Hunt, 1974). Furthermore, larger auditory bullae are a better adaptation to fossorial animals as low frequency sounds are received enhancing their hearing ability (Squarcia et al., 2007 and references therein). Badgers being semi fossorial and living in burrows as well as hunting down small prey in their burrows, require such a trait. *Meles canescens* (Crete) and *M. anakuma* could therefore, possess a better sense of hearing. The auditory bullae of *M. dimitrius* were damaged and could not be observed.

Other characteristics were found to differentiate the various species of *Meles* not always agreeing with the mainland/insular grouping. This is not unexpected as insular species from different islands are deemed to have dissimilarities from each other (Nanova et al., 2017). This seems to be the case for *M. canescens* (Crete) and *M. anakuma* (Japan). If we consider the fact that the former is of European origin and the latter of Asian we may expect such differences of likely phylogenetic inheritance. Thus, certain measurements (braincase length, palate length, palate width, mastoid width) separate European from Asian species as well as mainland from insular. Values of the insular specimens were compared with the analogous mainland ones (from the same continent). Insular species present increased dimensions of the palate (palate length, palate width), which suggest larger areas for the processing of food, an adaptation possibly related to consumption of mixed or larger prey (Meachen-Samuels and van Valkenburgh, 2009). Furthermore a larger palatine is also related to mammals where the temporalis is the dominant masticatory muscle (Cox, 2008). Consumption of larger prey is also related to the increased tooth row length which corresponds to the functional bite space of an organism (Sicuro and Oliveira, 2011). Increased tooth row length could be connected with increased rostrum length. Tooth row length was found to correlate well with rostrum length ($r=0.59641$, $r^2=0.35571$, $p=0.0065$). Increased values were noted in *M. dimitrius*, *M. canescens* (Crete) and *M. anakuma*, compared to their mainland congeners (*M. meles* and *M. leucurus* accordingly). A possible suggestion is that the lengthened rostrum could be related to the semi fossorial behavior of the species, where it is used for digging and acquiring food. Consequently, a lengthened rostrum could indicate extensive use of this behavior.

Mastoid width is also increased at the insular specimens when compared with their mainland ones. The mastoid region is where the digastricus muscles originate and so increased areas correspond to more vertically placed muscles. Increased mastoid width values correspond to consumption of larger prey as well as increased bite forces (Law et al., 2018; Prevosti et al., 2012). Additionally, Ercoli et al. (2013) suggest that

animals which prefer larger prey are characterized by wider and more laterally placed mastoid processes. This arrangement of the mastoids allows increased mechanical advantage especially for lateral movements of the cranium. Paroccipital process area is also an origin area of the digastricus muscles. Thus, variation in their arrangement could correspond to differences in mandible opening (Echarri et al., 2017). Nonetheless, the results do not show extreme differentiation. Similar results are noted in the development of condylar breadth but with more obvious differentiation, with *M. dimitrius*, *M. leucurus* and *M. anakuma* showing increased values. Increased condylar breadth indicates increased lateral stability of the cranium useful when dealing with struggling prey. Lower values indicate increased head mobility (Dumont et al., 2016 and references therein). Furthermore, animals which prefer mixed prey are characterized by narrower condylar breadth (Meachen-Samuels and van Valkenburgh, 2009).

Ercoli et al. (2017) suggest that lower skull height and lengthened palate and rostrum indicate a preference in chasing down prey in burrows. *Meles canescens* (Crete) and *M. dimitrius* seem to combine these characters corresponding to an increased preference to this particular hunting behavior.

Mandible

The mandible of the genus *Meles* appears quite robust as a structure, indicative of the high bite forces applied. The working side lever arm is increased in all the species while the balancing side lever arm decreased, indicating a greater development of the part of the mandible closer to the temporomandibular joint which would correspond to generally increased forces. Biknevicius and Ruff (1992) suggest that shorter balancing side lever arm is related with greater contribution of contralateral masticatory muscle forces to hard material processing (bone cracking) and bite forces shifting at the working side premolars.

Outer lever moment arm appears decreased in *M. dimitrius* and *M. canescens* (Crete). Outer lever moment arm is indicative of the distance where force is applied during mastication but should always be considered in relation to the moment arm of the muscles (moment arm of temporalis, moment arm of masseter) which apply the force. If increased outer lever moment arm is not paralleled with increased moment arms of the muscles, lower mechanical advantage occurs as the load is moved further away from the fulcrum (temporomandibular joint in this case). Lower outer lever moment arm values and increased moment arms indicate increased mechanical advantage and therefore increased or better applicable forces (Grossnickle, 2020; Penrose et al., 2020). Indeed, mechanical advantage is increased in *M. canescens* (Crete), *M. dimitrius* and *M. anakuma*. Increased mechanical advantage correlates to increased bite forces (Figueirido et al., 2013) which seems to agree with the forces computed for *M. dimitrius*, *M. canescens* (Crete) and *M. anakuma* by the dry skull method. Increased mechanical advantage is related to higher forces. On the contrary decreased mechanical advantage is related to increased jaw velocity and faster opening and closing of the mouth for capturing fast moving prey (Timm-Davis et al., 2015).

Dentary length is also important, and short jaws as in *M. dimitrius*, and *M. canescens* (Crete) are better adapted to cope with increased forces and loads. On the contrary, longer mandibles indicate reduced force but increased velocities for capturing fast

moving prey (Romaniuk, 2018; Timm-Davis et al., 2015). Shorter mandibles relate to higher bite forces as the tooth row (and specifically the carnassials where the crushing and slicing of food takes place) moves closer to the temporomandibular joint increasing the bite force of the teeth closer to it contrary to those placed further away (Timm-Davis et al., 2015 and references therein). This is due to the increased mechanical advantage when closest to the temporomandibular joint.

The increased mandible depth (jaw depth at c1, jaw depth at m1, dentary depth at the junction p3p4) could indicate greater forces induced at these specific parts of the mandible (Meloro, 2011). Regarding the indices of the dentary bending at p3/p4 junction and m1/m2 junction (IXP4, IXM2) no conclusive observations can be made, except for *M. thoralis*, which has increased resistance. The range of values of *M. dimitrius* is extensive. *Meles meles* and *M. canescens* (Crete) have similar values. *Meles leucurus* has increased resistance in the junction of m1 – m2 and reduced in the junction p3 – p4. The opposite (reduced IXM2 and increased IXP4) is noticed in *M. anakuma*. This could indicate an extensive use of the molar teeth (m1 – m2) in *M. leucurus* where increased forces would be induced and a preferable use of the premolar teeth (p4) at *M. anakuma* shifting the bite force more anteriorly.

Non – metric observations concerning structures related to the masseter and the mandible indicate that the angular process, which is the insertion area of the superficial masseter, is quite restricted in *M. dimitrius*, corresponding to smaller attachment areas and therefore to a weaker superficial layer. The superficial masseter pulls the mandible forward (Ewer, 1986). The middle masseter is more developed in the mainland group, as its insertion area appears more enhanced than in the rest of the species. The middle masseter contributes to basic closing action (Ewer, 1986). The masseteric fossa, where the deep masseter attaches, has a different arrangement in *M. dimitrius* and the insular species when compared with the mainland ones. This arrangement could correspond to the same quantity of the deep masseter accommodated differently and being placed at a wider area at the insular species and to a more constricted space at the mainland ones without changing the total muscle mass.

In general, a tendency for more developed structures concerning the masseter and the mandible is marked in the mainland species. Higher mandibular ramus and coronoid process elevation suggest increased moment arm of the masseter and pterygoids and therefore induced forces in the vertical plane (Timm-Davis et al., 2015). Wider mandibular ramus also corresponds to more developed masseter. These observations could possibly indicate a preference in the development of the masseter rather than temporalis in the more mainland species, which could correspond to more herbivorous trends (Sicuro and Oliveira, 2011).

Dentition

Increased surfaces of the molars rather than of the premolars indicate a greater adaptation to omnivory or herbivory (Popowics, 2003), as the function of grinding is favored. The dentition of the genus *Meles* is indicative of an omnivorous diet. Badgers show a peculiar adaptation of the first upper and lower molar which are developed in such a way so as to allow them to slice (three rows of cusps at M1) as well as to grind (enlarged area) efficiently. Blunter dentition with increased surfaces could correspond to increased consumption of plant material. A smaller premolar carnassial P4, shifts

the bite force at the back of the tooth row thus increasing bite force as mastication is moved backwards in the toothrow and closer to the temporomandibular joint (Timm-Davis et al., 2015).

Concerning the upper dentition, the area of M1 (M1a) is reduced in *M. dimitrius*, *M. anakuma* and possibly *M. canescens* (Crete) which shows a great range of values indicating a rather variable character. Relative upper grinding area (UGR) is decreased in *M. dimitrius*, intermediate in *M. anakuma* and again highly variable in *M. canescens* (Crete). Reduced M1a and UGR indicate teeth better adapted to processing meat. Upper carnassial shape (P4P) is increased in the insular group as well as *M. dimitrius*. This trait corresponds to a more developed P4 used in processing meat (Frischia et al., 2007; Sacco and Van Valkenburgh, 2004). Non – metric observations suggest a more triangular shape of P4 for *M. canescens* (Crete), *M. anakuma* and *M. dimitrius* in contrast to the more subquadrate shape of *M. meles* and *M. leucurus*. M1 is more elongated in *M. anakuma* and *M. canescens* (Crete). Additionally, *Meles canescens* (Crete) has a notably sharper dentition. Considering these traits, *M. dimitrius* could be better adapted to processing meat and possibly *M. anakuma* and *M. canescens* (Crete). The latter taxon also has the trait of the sharper dentition which could be attributed to a more carnivorous or even insectivorous diet (Ungar & Sues, 2019; Ewer, 1986).

Evidence from the lower dentition does not fully support the previous suggestion. *Meles dimitrius* and *M. anakuma* preserve the less developed areas of m1 and m2 which indicate a better adaptation to meat consumption rather than plant material. However, *M. canescens* (Crete) appears to have increased areas more comparable to the mainland group. The same trend is noted at the index of relative lower molar grinding area (LGR). Increased values correspond to teeth better adapted to grinding (Frischia et al., 2007; Sacco and Van Valkenburgh, 2004). However, M1BS, which corresponds to the development of the blade of m1 appears extremely increased in *M. canescens* (Crete), probably compensating for the increased relative lower molar grinding area. Possibly an adaptation to efficient processing of both meat and plant material for *M. canescens* (Crete) could be suggested or a compensation due to the blade like morphology.

These specific traits could possibly indicate an increased carnivorous preference for the insular species [*M. canescens* (Crete) and *M. anakuma*] and *M. dimitrius*, while the mainland *M. meles* and *M. leucurus* could have an increased preference to omnivory. *Meles canescens* (Crete) shows some mixed characters and an adaptation to better processing of meat cannot be fully supported.

Despite the fact that some possible differentiation concerning the dentition could exist, the generalist feeding ecology of the genus is still apparent and no distinction in food consumption among species could be inferred by HSB. The variety of the food consumed does not favor a specific development of HSB indicating mainly soft and medium hardness of preferred food. Only *M. dimitrius* slightly differentiates from the extant species, but with no significance. This could only be an indication that *M. dimitrius* consumed slightly harder material than the extant species. However, the difference in values is extremely small [138° in *M. dimitrius* and 144° in *M. canescens* (Crete), 143° in *M. meles*] despite the fact that the values of *M. dimitrius* place it at the

second category of HSB of acute angles ($70^{\circ} - 140^{\circ}$) and not in the first category of undulating HSB ($>140^{\circ}$). What should be noted is that Stefen (1997) suggests that along with feeding preferences, phylogeny could also play an important role in the development of HSB. This is supported by the fact that the mustelid *Gulo gulo* presents the same amount of bone consumption as the *Hyena*. However, the HSB of *Gulo gulo* appear less acute when compared to the HSB of *Hyaena* which has an extremely zigzagged structure. This case could explain why the species of *Meles* which are all part of the same genus show no significant differences of the HSB even if some did consume harder food material.

All things considered, the main differences detected concern cranial variables. Mandible and dentition present an overlap and discrimination is not always apparent. *Meles* is a generalist and adapts with relation to the available food resources and environmental conditions so increased overlap is rather expected. Some species present large ranges which could be attributed to sexual dimorphism. Nonetheless some inferences could be made supporting different ecologies mainly discriminating insular and mainland populations. The fossil taxon *M. dimitrius* was found to share certain features with the insular group but it also presents some unique traits.

Dry skull method / Endocranial volume

Our results indicated that insular forms have a slight tendency to be stronger in bite force than mainland ones. Damasceno et al. (2013) found that the species which present the most increased bite forces (bite force quotient) are more carnivorous, and also possess the more developed brain volumes (brain volume quotient). This suggests that adaptations of the skull concerning carnivory also influence the total brain volume. These assumptions are supported by our analysis, where the insular species, characterized by increased bite force quotient also possessed the increased brain volume quotient. Additionally, Penrose et al. (2016) support that increased braincase areas as well as wider zygomatic arches, correspond to an adaptation for accommodating increased temporalis muscles and thus increased bite forces.

Dissection / Muscle accommodation

As dissection was restricted to the mainland *M. meles*, there were not comparisons with different taxa and especially the insular *M. canescens* (Crete).

The muscle scars of the extant of *M. meles* and their identification by analogy on the fossil cranium of *M. dimitrius* do not show great differences, so a relatively reliable assumption of the muscle accommodation of the fossil specimen could be made.

Comparing our results with data from Ito and Endo (2016), the PCA grouped families together (Mustelidae, Canidae, Felidae) with only some specimens placed further away, probably because of their adaptations to specific killing strategies and related muscular correlates. Ito and Endo (2016) proposed that further specialization occurs to gain more precise carnassial biting aided by the masseter (which is also noticed more developed in these taxa). *Meles meles* does not appear to have such an obvious specialization, as it is placed within the generalist Mustelidae group. Moreover, in *Meles*, the middle masseter is the second largest layer, whereas in the majority of the Felidae and the Canidae, the deep masseter dominates. The superficial and deep masseters aid in the more lateral movements of the mandible, while the middle performs more vertical movements (Ewer, 1986; Ito and Endo, 2016).

When confined to the Mustelids, *M. meles* and *M. anakuma* show certain differences. The main distinction is the slightly more developed pterygoids of *M. meles*, which along with the more developed deep layer of masseter, could indicate a better adaptation to lateral sliding of the *M. meles* mandible than in *M. anakuma*. However, the more developed pterygoids of *M. meles* may be related to the inclusion of both lateral and medial in the analysis, contrary to Ito and Endo (2016), who used solely the medial pterygoid. Concerning the layers of the masseter, *M. anakuma* possesses a larger superficial layer while *M. meles* a more developed deep layer, which relates to the backward movement of the mandible (Ewer, 1986).

PCSA Bite Forces / Comparison of dry method and PCSA (gross) method

Computed PCSA showed increased values for the temporalis followed by the masseter and lastly by the group of pterygoids indicating an extensive development of the temporalis. The increased differences in the computed total force by dry method and gross method of the muscles is expected (see also Penrose et al., 2020) as the first one is based exclusively on cranial measurements and the second one uses the actual muscle mass. Increased values are found in the larger skull when using the gross method and lower values when using the dry method, while the small skull showed the opposite trend. This could be attributed to the fact that the smaller cranium belonged to a young adult individual. Thus, the muscle mass might not have fully developed because of the young age of the individual. On the contrary, when using the dry skull method, which is based on cranial measurements alone, increased values would be expected as cranial features could be more developed in order to accommodate the muscle that would be developed. Law et al. (2016) also mention that muscle mass is more important than theoretical computation of bite force. In general, the dry method seems to underestimate the bite force as muscle volume and fascicle length is not accounted for. However, when dealing with a young individual the opposite trend is observed as the relative development and muscle volume plays a crucial role.

Synthesis / Conclusion

The genus *Meles* is an omnivorous/generalist mustelid carnivoran, currently represented by four different extant taxa. This study aimed at identifying cranial differences between those taxa that could be functionally related to specific dietary preferences and use them to infer the paleoecology of the Greek fossil taxon *M. dimitrius*. After examining the skulls of the different species via various analyses, an ecological profile was reconstructed. Although, no extreme differences were expected within a generalist group, some interesting characters have been traced.

Meles canescens (Crete), the Greek insular representative of the genus, was found to be a species with developed masticatory musculature system and increased bite forces even though it is one of the smallest *Meles* species (estimated mass: 5-10 kg). The temporalis, in particular, appears strengthened, especially the suprazygomatic and deep layers, while the less developed superficial layer does not seem to severely affect the overall produced forces (if it is supposed that sagittal crests affect the attachment area of superficial temporalis at such extent). Brain volume had a tendency for higher values. *Meles canescens* (Crete) displayed resistance to torsion when dealing with struggling prey, while it is adapted to mixed or even larger prey consumption. Evidence of a more diurnal behavior (possibly due to limited presence

of predators) and a better hearing are apparent, as well as a possible inclination to chasing down prey in burrows. As far as dietary preferences are concerned, an omnivorous and opportunistic character is obvious, while there could be some better adaptation to meat or even insect consumption. Nonetheless, a clearly carnivorous diet cannot be supported as the results concerning the dental traits are controversial. Blade – like morphology and grinding areas especially of the lower dentition are developed. On the contrary the overall sharper and more elongated outline of the dentition would support better processing of meat rather than plant material. The more developed temporalis when compared to masseter, found in more carnivorous taxa, could be an extra evidence for increased carnivory. Additionally, the more developed digastricus could indicate a powerful abduction of the mandible, crucial when hunting and consuming prey.

Meles anakuma, the Asian insular representative, is quite similar to *M. canescens* from Crete. Besides its small size and body mass (4-10 kg), high bite forces are also apparent. The temporalis and brain volume are well developed. *Meles anakuma* also presents increased resistance to torsion, more diurnal behavior, enhanced hearing, and a preference to mixed or large prey. Concerning the diet, *M. anakuma* shows some evidence of a better adaptation to processing meat (LGR, M1BS), indicating a well-developed blade morphology and more constricted grinding areas.

Meles meles, the European mainland representative, is characterized by traits which differentiate it from the insular species. It has a slightly less developed masticatory system than the insular representatives, with smaller computed bite forces, but with increased biting velocity. It is one of the largest species, with body mass ranging between 9-13 kg. It possibly prefers smaller and faster prey than the insular species as denoted by its adaptation to a rapid but not strong bite. Brain volume was also the smallest in the genus. It retains a rather developed masseter than temporalis and has constricted neck mobility which limits the range of head movements. No specific diet preferences are noted, and the generalist nature is extremely enhanced. The dental traits do not indicate a specific type of food preference. On the contrary, omnivory is greatly supported with slightly decreased percentage of meat material as the blade like morphology is not as apparent as in the insular species.

Meles leucurus, the Asian mainland representative, is not greatly differentiated from *M. meles*. Bite forces and brain volume could not be computed but the rest of the features indicate similarities with *M. meles*. Body mass ranges from 10 to 14kg. The more elongated skulls and the dentition suggest lowered forces but increased biting velocity. Increased lateral stability of the head could also be one of its adaptations. Finally, the dentition suggests an omnivorous diet with increased grinding areas and no tendency to more efficient processing of meat. Diurnal activity and enhanced hearing are not evident, and neither is a specialized hunting behavior.

Meles dimitrius, the fossil representative from the Early Pleistocene of Greece, is marked by a set of traits which seem to place it closer to the insular group. It is characterized by increased strength and a quite developed temporalis as well as neck musculature, while the masseter appears to be less favored (superficial layer). The brain volume is rather high, and the body mass was estimated near 10 kg. As in insular species, it shows good resistance to torsion when dealing with struggling prey. Mixed

or larger prey may have been consumed, while it possesses a good adaptation to hunting prey in burrows and has a powerful opening of the mandible due to the developed digastricus. As in the Japanese and the Cretan badger, a more diurnal behavior is assumed as well. Concerning the dietary preferences, dental traits possibly support more carnivorous trends when compared to the rest of the species without suggesting that *M. dimitrius* was mainly carnivorous. The omnivorous / generalist character is still highly present. HSB structures could indicate processing of slightly harder food material as the teeth were better adapted to endure high forces.

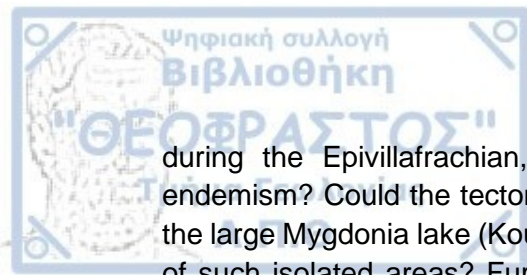
In this study, we identified a set of characters that groups together the insular species, differentiating them from the mainland ones. These 'insular' traits may represent adaptations to more isolated environments (islands in this case). The particular unbalanced ecosystems of the islands may have affected badgers in a specific way. The restricted space, limited food resources, and absence of predators could play an important role in the overall development of the organisms. Smaller size (due to the island rule), diurnal behavior (due to the absence of predators), increased bite forces, consumption of larger or mixed prey (due to the island rule where small taxa increase in size) as well as better hearing could all represent adaptations to a more isolated environment, despite the fact that no standard pattern is observed in insular carnivores.

Hypothesis for the fossil *Meles dimitrius*

When all data are considered, *M. dimitrius* seems to share more traits in common with the insular than with the mainland extant representatives of the genus.

On the one hand, one possible explanation could be that *M. dimitrius* resembles the insular species in many characters which are related to an increased musculature system and head/neck movements, as well as with a good adaptation in processing meat material. Thus, the reason for this resemblance could be due to the more extensive use of the temporalis muscle with some evidence of increased carnivory but for different reasons in each species. For the case of *M. dimitrius* the increased biodiversity of the area at that time and the consequent increased competition could play an important role. The still primitive *M. dimitrius* compared to the extant *Meles*, would not be so specialized in the processing of plant material and this would lead it to be a more active predator. Consequently, it would have to antagonize other medium sized carnivores and the enhanced musculature system as well as the more active head movements would be essential for fighting and defense.

On the other hand, another possible explanation could be that *M. dimitrius* might have represented an isolated population, following similar 'insular' ecomorphological paths. Despite the fact that APL – 544 is not one of the smallest specimens, *M. dimitrius* could still represent an endemic form, as the shared characters with the insular badgers remain, but could present an increased size as a certain adaptation created by the special environmental conditions. The fauna of Apollonia includes several other predators and so *M. dimitrius* would have faced severe competition, unlike its insular congeners. Thus, size could be affected by factors related to the rest of the present taxa as competition would hinder size reduction. This case poses the question whether this fossil representative of the extant badger was part of a more isolated population in the Greek Epivillafranchian and thus presenting characteristics found in insular badgers. Could the palaeogeography of Mygdonia Basin or the wider Northern Greece



during the Epivillafrachian, create locally isolated groups leading to a form of endemism? Could the tectonic activity of the Middle Pleistocene and the drainage of the large Mygdonia lake (Koufos et al., 1995 and references therein) allow the creation of such isolated areas? Further research of the palaeogeography and fauna of the Northern Greece could shed light on these questions. Other taxa of the Apollonia locality could be examined in order to concur whether such isolated systems existed, creating a form of local endemism and if other species were also affected.

REFERENCES

- Abramov, A. V., Puzachenko, A.Y., 2013. The taxonomic status of badgers (Mammalia, Mustelidae) from Southwest Asia based on cranial morphometrics, with the redescription of *Meles canescens*. Zootaxa 3681, 44–58.
<https://doi.org/10.11646/zootaxa.3681.1.2>
- Anyonge, W., Baker, A., 2006. Craniofacial morphology and feeding behavior in *Canis dirus*, the extinct Pleistocene dire wolf. J. Zool. 269, 309–316.
<https://doi.org/10.1111/j.1469-7998.2006.00043.x>
- Argant, A., 2004. Les Carnivores du gisement Pliocène final de Saint-Vallier (Drôme, France) The Carnivores of the late Pliocene site of Saint-Vallier (Drôme, France). Geobios 37, S133–S182.
- Barea-Azcon, J.M., Ballesteros-Duperon, E., Gil-Sanchez, J., Virgos, E., 2010. Badger *Meles meles* feeding ecology in dry Mediterranean environments of the southwest edge of its distribution range. Acta Theriol. (Warsz). 55, 45–52.
- Baryshnikov, G.F., Puzachenko, A.Y., Abramov, A. V., 2003. New analysis of variability of cheek teeth in Eurasian badgers (Carnivora, Mustelidae, *Meles*) Gennady. Russ. J. Theriol. 1, 133–149.
- Biknevicius, A.R., Ruff, C.B., 1992. The structure of the mandibular corpus and its relationship to feeding behaviours in extant carnivores. J. Zool. 228, 479–507.
<https://doi.org/10.1111/j.1469-7998.1992.tb04450.x>
- Boesi, R., Biancardi, C., 2002. Diet of the Eurasian badger *Meles meles* (Linnaeus, 1758) in the natural reserve of Lago di Piano, northern Italy. Mamm. Biol. 67, 120–125. <https://doi.org/10.1078/1616-5047-00018>
- Bryden, M., Halnan, C.R.E., 2017. Nomina Anatomica Veterinaria. Aust. Vet. J. 47, 433–433. <https://doi.org/10.1111/j.1751-0813.1971.tb02174.x>
- Byrne, A.W., Paddy Sleeman, D., O’Keeffe, J., Davenport, J., 2012. The ecology of the European badger (*Meles meles*) in Ireland: A review. Biol. Environ. 112, 105–132. <https://doi.org/10.3318/BIOE.2012.02>
- Carpenter, P.J., Pope, L.C., Greig, C., Dawson, D.A., Rogers, L.M., Erven, K., Wilson, G.J., Delahay, R.J., Cheeseman, C.L., Burke, T., 2005. Mating system of the Eurasian badger, *Meles meles*, in a high-density population. Mol. Ecol. 14, 273–284. <https://doi.org/10.1111/j.1365-294X.2004.02401.x>
- Christiansen, P., Adolfssen, J.S., 2005. Bite forces, canine strength and skull allometry in carnivores (Mammalia, Carnivora). J. Zool. 266, 133–151.
<https://doi.org/10.1017/S0952836905006643>
- Christiansen, P., Wroe, S., 2007. Bite Forces and Evolutionary Adaptations to Feeding Ecology in Carnivores. Ecology 88, 347–358.
[https://doi.org/10.1890/0012-9658\(2007\)88\[347:BFAEAT\]2.0.CO;2](https://doi.org/10.1890/0012-9658(2007)88[347:BFAEAT]2.0.CO;2)
- Cox, P.G., 2008. A quantitative analysis of the Eutherian orbit: Correlations with masticatory apparatus. Biol. Rev. 83, 35–69. <https://doi.org/10.1111/j.1469-185X.2007.00031.x>

- Curtis, A.A., Santana, S.E., 2018. Jaw-Dropping: Functional Variation in the Digastric Muscle in Bats. *Anat. Rec.* 301, 279–290. <https://doi.org/10.1002/ar.23720>
- Daiiana, B. De, 1995. Seasonal variation in the food habits of badgers in an Alpine valley. *Hystrix, Ital. J. Mammal.* 7, 165–171. <https://doi.org/10.4404/hystrix-7.1-2-4067>
- Damasceno, E.M., Hingst-Zaher, E., Astúa, D., 2013. Bite force and encephalization in the Canidae (Mammalia: Carnivora). *J. Zool.* 290, 246–254. <https://doi.org/10.1111/jzo.12030>
- de Lahunta, A., Evans, 2010. *Guide to the Dissection of the Dog*, Seventh. ed. Elsevier Saunders.
- Del Cerro, I., Marmi, J., Ferrando, A., Chashchin, P., Taberlet, P., Bosch, M., 2010. Nuclear and mitochondrial phylogenies provide evidence for four species of Eurasian badgers (Carnivora). *Zool. Scr.* 39, 415–425. <https://doi.org/10.1111/j.1463-6409.2010.00436.x>
- Druzinsky, R.E., Doherty, A.H., De Vree, F.L., 2011. Mammalian masticatory muscles: Homology, nomenclature, and diversification. *Integr. Comp. Biol.* 51, 224–234. <https://doi.org/10.1093/icb/ucr067>
- Dumont, M., Wall, C.E., Botton-Divet, L., Goswami, A., Peigné, S., Fabre, A.C., 2016. Do functional demands associated with locomotor habitat, diet, and activity pattern drive skull shape evolution in musteloid carnivorans? *Biol. J. Linn. Soc.* 117, 858–878. <https://doi.org/10.1111/bij.12719>
- Echarri, S., Ercoli, M.D., Amelia Chemisquy, M., Turazzini, G., Prevosti, F.J., 2017. Mandible morphology and diet of the South American extinct metatherian predators (Mammalia, Metatheria, Sparassodonta). *Earth Environ. Sci. Trans. R. Soc. Edinburgh* 106, 277–288. <https://doi.org/10.1017/S1755691016000190>
- Ellis, J.L., Thomason, J., Kebreab, E., Zubair, K., France, J., 2009. Cranial dimensions and forces of biting in the domestic dog. *J. Anat.* 214, 362–373. <https://doi.org/10.1111/j.1469-7580.2008.01042.x>
- Elmeros, M., Mikkelsen, D.M.G., Nørgaard, L.S., Pertoldi, C., Jensen, T.H., Chriél, M., 2018. The diet of feral raccoon dog (*Nyctereutes procyonoides*) and native badger (*Meles meles*) and red fox (*Vulpes vulpes*) in Denmark. *Mammal Res.* 63, 405–413. <https://doi.org/10.1007/s13364-018-0372-2>
- Ercoli, M.D., 2017. Morpho-functional analysis of the mastoid region of the extinct South American mustelid *†stipanicia pettorutii*. *Earth Environ. Sci. Trans. R. Soc. Edinburgh* 106, 337–349. <https://doi.org/10.1017/S1755691016000220>
- Ercoli, M.D., Álvarez, A., Busker, F., Morales, M.M., Julik, E., Smith, H.F., Adrian, B., Barton, M., Bhagavatula, K., Poole, M., Shahsavan, M., Wechsler, R., Fisher, R.E., 2017. Myology of the Head, Neck, and Thoracic Region of the Lesser Grison (*Galictis cuja*) in Comparison with the Red Panda (*Ailurus fulgens*) and Other Carnivorans: Phylogenetic and Functional Implications. *J. Mamm. Evol.* 24, 289–322. <https://doi.org/10.1007/s10914-016-9339-8>

- Ercoli, M.D., Echarri, S., Busker, F., Álvarez, A., Morales, M.M., Turazzini, G.F., 2013. The Functional and Phylogenetic Implications of the Myology of the Lumbar Region, Tail, and Hind Limbs of the Lesser Grison (*Galictis cuja*). *J. Mamm. Evol.* 20, 309–336. <https://doi.org/10.1007/s10914-012-9219-9>
- Evans, H.E., DeLahunta, A., 2013. *Miller's Anatomy of the Dog*, Fourth. ed. Elsevier Saunders.
- Ewer, R.F., 1973. *The carnivores*. Cornell University Press
- Ferretti, M.P., 2007. Evolution of bone-cracking adaptations in hyaenids (Mammalia, Carnivora). *Swiss J. Geosci.* 100, 41–52. <https://doi.org/10.1007/s00015-007-1212-6>
- Ferretti, M.P., 1999. Tooth enamel structure in the hyaenid *Chasmaporthetes lunensis lunensis* from the Late Pliocene of Italy, with implications for feeding behavior. *J. Vertebr. Paleontol.* 19, 767–770. <https://doi.org/10.1080/02724634.1999.10011189>
- Figueirido, B., Tseng, Z.J., Martín-Serra, A., 2013. Skull Shape Evolution In Durophagous Carnivorans. *Evolution* (N. Y). 67, 1975–1993. <https://doi.org/10.1111/evo.12059>
- Finarelli, J.A., 2011. Estimating endocranial volume from the outside of the skull in Artiodactyla. *J. Mammal.* 92, 200–212. <https://doi.org/10.1644/09-MAMM-A-391.1>
- Fischer, C., Ferrari, N., Weber, J.M., 2005. Exploitation of food resources by badgers (*Meles meles*) in the Swiss Jura Mountains. *J. Zool.* 266, 121–131. <https://doi.org/10.1017/S0952836905006576>
- Friscia, A.R., Van Valkenburgh, B., 2010. Ecomorphology of North American eocene carnivores: Evidence for competition between Carnivorans and Creodonts, in: Goswami, A., Friscia, A. (Eds.), *Carnivoran Evolution: New Views on Phylogeny, Form, and Function*. Cambridge University Press, pp. 311–341. <https://doi.org/10.1017/CBO9781139193436.012>
- Friscia, A.R., Van Valkenburgh, B., Biknevicius, A.R., 2007. An ecomorphological analysis of extant small carnivorans. *J. Zool.* 272, 82–100. <https://doi.org/10.1111/j.1469-7998.2006.00246.x>
- Gans, C., & Bock, W. J. (1965). The functional significance of muscle architecture-a theoretical analysis. *Ergebnisse der Anatomie und Entwicklungsgeschichte*, 38, 115.
- Gans, C., & de Vree, F. (1987). Functional bases of fiber length and angulation in muscle. *J. Morphol.*, 192, 63–85. <https://doi.org/10.1002/jmor.1051920106>
- Gittleman, J.L., 1986. Carnivore Brain Size, Behavioral Ecology, and Phylogeny. *J. Mammal.* 67, 23–36. <https://doi.org/10.2307/1380998>
- Gomes, D.J., Wierzbowska, I.A., Bevanger, K., O'Mahony, D.T., Rola, K., 2020. Diet of the European badgers (*Meles meles*) in urban and rural areas of Norway.

- Eur. J. Wildl. Res. 66, 1-11. <https://doi.org/10.1007/s10344-019-1347-6>
- Goszczyński, J., Jędrzejewska, B., Jędrzejewski, W., 2000. Diet composition of badgers (*Meles meles*) in a pristine forest and rural habitats of Poland compared to other European populations. J. Zool. 250, 495–505. <https://doi.org/10.1017/S0952836900004076>
- Grossnickle, D.M., 2020. Feeding ecology has a stronger evolutionary influence on functional morphology than on body mass in mammals. Evolution (N. Y). 74, 610–628. <https://doi.org/10.1111/evo.13929>
- Hall, R.E., 1926. The Muscular Anatomy of Three Mustelid Mammals, Mephitis, Spilogale and Martes. Univ. California, Publ. Zool. 30, 39.
- Hammer, Øyvind, Harper, David A.T., and Paul D. R., (2001). Past: Paleontological Statistics Software Package for Education and Data Analysis. Palaeontologia Electronica
- Hancox, M., 1988. Dental anomalies in the Eurasian badger. J. Zool. 216, 606–608. <https://doi.org/10.1111/j.1469-7998.1988.tb02460.x>
- Hartstone-Rose, A., Hertzog, I., Dickinson, E., 2019. Bite Force and Masticatory Muscle Architecture Adaptations in the Dietarily Diverse Musteloidea (Carnivora). Anat. Rec. 302, 2287–2299. <https://doi.org/10.1002/ar.24233>
- Hartstone-Rose, A., Perry, J.M.G., Morrow, C.J., 2012. Bite Force Estimation and the Fiber Architecture of Felid Masticatory Muscles. Anat. Rec. 295, 1336–1351. <https://doi.org/10.1002/ar.22518>
- Hartstone-Rose, A., Selvey, H., Villari, J.R., Atwell, M., Schmidt, T., 2014. The three-dimensional morphological effects of captivity. PLoS One 9, 1-15. <https://doi.org/10.1371/journal.pone.0113437>
- Heptner, V. G.; Sludskii, A. A. (2001). "Badger *Meles meles* Linnaeus, 1758". Mammals of the Soviet Union. Volume II, Part 1b, Carnivores (Mustelidae and Procyonidae). Washington, D.C.: Smithsonian Institution Libraries and National Science Foundation. pp. 1232–1282. ISBN 90-04-08876-8.
- Hunt, R.M., 1974. The auditory bulla in carnivora: An anatomical basis for reappraisal of carnivore evolution. J. Morphol. 143, 21–75. <https://doi.org/10.1002/jmor.1051430103>
- Ibiş, O., Tez, C., Özcan, S., Yorulmaz, T., Kaya, A., Mohradi, M., 2015. Insights into the Turkish and Iranian badgers (the genus *Meles*) based on the mitochondrial cytochrome b gene sequences. Vertebr. Zool. 65, 399–407.
- Ito, K., Endo, H., 2019. The effect of the masticatory muscle physiological cross-sectional area on the structure of the temporomandibular joint in Carnivora. J. Vet. Med. Sci. 81, 389–396. <https://doi.org/10.1292/jvms.18-0611>
- Ito, K., Endo, H., 2016. Comparative Study of Physiological Cross-Sectional Area of Masticatory Muscles among Species of Carnivora. Mammal Study 41, 181–190. <https://doi.org/10.3106/041.041.0403>
- Iurino, D.A., 2014. Body size reduction and tooth agenesis in Late Pleistocene *Meles*

- meles* (Carnivora, mammalia) from Ingarano (Southern Italy). Riv. Ital. di Paleontol. e Stratigr. 120, 109–118. <https://doi.org/10.13130/2039-4942/6053>
- Kahlke, R.D., García, N., Kostopoulos, D.S., Lacombe, F., Lister, A.M., Mazza, P.P.A., Spassov, N., Titov, V. V., 2011. Western Palaearctic palaeoenvironmental conditions during the Early and early Middle Pleistocene inferred from large mammal communities, and implications for hominin dispersal in Europe. Quat. Sci. Rev. 30, 1368–1395. <https://doi.org/10.1016/j.quascirev.2010.07.020>
- Kargopoulos, N., 2019. Carnivoran Dietary Adaptations A Multiproxy Study on the Feeding Ecology of the Fossil Carnivorans of Greece. Master Thesis, Department of Geology and Geoenvironment, National and Kapodistrian University of Athens, 214 pp.
- Kauhala, K., Ihalainen, A., 2014. Impact of landscape and habitat diversity on the diversity of diets of two omnivorous carnivores. Acta Theriol. (Warsz). 59, 1–12. <https://doi.org/10.1007/s13364-013-0132-2>
- Kieser, J.A., 1995. Gnathomandibular morphology and character displacement in the Bat - Eared Fox. J. Mamm. Evol. 76, 542–550.
- Kikuchi, Y., & Kuraoka, A. (2014). Differences in muscle dimensional parameters between non-formalin-fixed (freeze-thawed) and formalin fixed specimen in gorilla (*Gorilla gorilla*). Mammal Study, 39, 65–72. <http://doi.org/10.3106/041.039.0101>
- Konidaris, G.E., Kostopoulos, D.S., Koufos, G.D., 2020. *Mammuthus meridionalis* (Nesti, 1825) from Apollonia-1 (Mygdonia Basin, Northern Greece) and its importance within the Early Pleistocene mammoth evolution in Europe. Geodiversitas 42, 69–91.
- Konidaris, G.E., Kostopoulos, D.S., Maron, M., Schaller, M., Ehlers, T.A., Aidona, E., Marini, M., Tzouroukakis, V., Muttoni, G., Koufos, G.D., Harvati, K., 2021. Dating of the Lower Pleistocene Vertebrate Site of Tsiotra Vryssi (Mygdonia Basin, Greece): Biochronology, Magnetostratigraphy, and Cosmogenic Radionuclides. Quaternary 4, 1-18. <https://doi.org/10.3390/quat4010001>
- Konidaris, G.E., Tzouroukakis, V., Kostopoulos, D.S., Thompson, N., Giusti, D., Michailidis, D., Koufos, G.D., Harvati, K., 2015. Two new vertebrate localities from the Early Pleistocene of Mygdonia Basin (Macedonia, Greece): Preliminary results. Comptes Rendus - Palevol 14, 353–362. <https://doi.org/10.1016/j.crpv.2015.05.004>
- Kostopoulos, D.S., Maniakas, I., Tsoukala, E., 2018. Early Bison Remains from Mygdonia Basin (Northern Greece). Geodiversitas 40, 283-319.
- Koufos, G. D. 1992. The Pleistocene carnivores of the Mygdonia basin (Macedonia, Greece). Ann. de Paleontol. 78, 205–257.
- Koufos, G.D., 2006. The Neogene mammal localities of Greece: Faunas, chronology and biostratigraphy. Hell. J. Geosci. 41, 183–214.

- Koufos, G.D., 2014. The Villafranchian carnivoran guild of Greece: Implications for the fauna, biochronology and paleoecology. *Integr. Zool.* 9, 444–460. <https://doi.org/10.1111/1749-4877.12061>
- Koufos, G.D., 2018. New Material and Revision of the Carnivora, Mammalia from the Lower Pleistocene Locality Apollonia 1, Greece. *Quaternary* 1, 1-6. <https://doi.org/10.3390/quat1010006>
- Koufos, G.D., Kostopoulos, D.S., 1997. New Carnivore Material from the Plio-Pleistocene of Macedonia (Greece) with the Description of a new Canid. *Munchner Geowissenschaftliche Abhandlungen* 34, 33–63.
- Koufos, G.D., Kostopoulos, D.S., 2016. The Plio-Pleistocene Large Mammal Record of Greece: Implications for Early Human Dispersals into Europe, in: *Paleoanthropology of the Balkans and Anatolia, Vertebrate Paleobiology and Paleanthropology*. Springer Netherlands, pp. 2010–2012. <https://doi.org/10.1007/978-94-024-0874-4>
- Koufos, G.D., Syrides, G.E., Kostopoulos, D.S., Koliadimou, K.K., 1995. Preliminary results about the stratigraphy and the palaeoenvironment of Mygdonia Basin, Macedonia, Greece. *Geobios* 28, 243–249. [https://doi.org/10.1016/S0016-6995\(95\)80171-5](https://doi.org/10.1016/S0016-6995(95)80171-5)
- Law, C.J., 2019. Evolutionary shifts in extant mustelid (Mustelidae: Carnivora) cranial shape, body size and body shape coincide with the Mid-Miocene Climate Transition. *Biol. Lett.* 15, 1-6. <https://doi.org/10.1098/rsbl.2019.0155>
- Law, C.J., Duran, E., Hung, N., Richards, E., Santillan, I., Mehta, R.S., 2018. Effects of diet on cranial morphology and biting ability in musteloid mammals. *J. Evol. Biol.* 31, 1918–1931. <https://doi.org/10.1111/jeb.13385>
- Law, C.J., Young, C., Mehta, R.S., 2016. Ontogenetic scaling of theoretical bite force in southern sea otters (*Enhydra lutris nereis*). *Physiol. Biochem. Zool.* 89, 347–363. <https://doi.org/10.1086/688313>
- Lazaridis, G., Tsoukala, E., Maul, L.C., 2019. The earliest hystrix refossa: A new early villafranchian record from milia (Grevena, Macedonia, Greece). *Hystrix* 30, 12–18. <https://doi.org/10.4404/hystrix-00140-2019>
- Legendre, S., Roth, C., 1988. Correlation of carnassial tooth size and body weight in recent carnivores (mammalia). *Hist. Biol.* 1, 85–98. <https://doi.org/10.1080/08912968809386468>
- Li, F., Luo, Z.H., Li, C.L., Li, C.W., Jiang, Z.G., 2013. Biogeographical patterns of the diet of Palearctic badger: Is badger an earthworm specialist predator? *Chinese Sci. Bull.* 58, 2255–2261. <https://doi.org/10.1007/s11434-012-5650-9>
- Loy, A., 2018. Mustelidae Morphology, in: Vonk, J., Shackelford, T.K. (Eds.), *Encyclopedia of Animal Cognition and Behavior*. Springer International Publishing, pp. 1–13. https://doi.org/10.1007/978-3-319-47829-6_1210-1
- Lynch, J.M., Whelan, R., Il Frituri, A.I., Hayden, T.J., 1997. Craniometric variation in the Eurasian badger, *Meles meles*. *J. Zool.* 242, 31–44.

<https://doi.org/10.1111/j.1469-7998.1997.tb02927.x>

Lyra, G.A., van der Geer, A.A.E., Rook, L., 2010. Body size of insular carnivores: Evidence from the fossil record. *J. Biogeogr.* 37, 1007–1021.

<https://doi.org/10.1111/j.1365-2699.2010.02312.x>

Madurell-Malapeira, J., Alba, D.M., Marmi, J., Aurell, J., Moyà-Sola, S., 2011. The taxonomic status of European Plio-Pleistocene badgers. *J. Vertebr. Paleontol.* 31, 885–894. <https://doi.org/10.1080/02724634.2011.589484>

Maniakas, I., Kostopoulos, D.S., 2017. Morphometric-palaeoecological discrimination between Bison populations of the western Palaearctic. *Geobios* 50, 155–171. <https://doi.org/10.1016/j.geobios.2017.01.001>

Marmi, J., López-Giráldez, F., Macdonald, D.W., Calafell, F., Zholnerovskaya, E., Domingo-Roura, X., 2006. Mitochondrial DNA reveals a strong phylogeographic structure in the badger across Eurasia. *Mol. Ecol.* 15, 1007–1020. <https://doi.org/10.1111/j.1365-294X.2006.02747.x>

Martin, M.L., Travouillon, K.J., Fleming, P.A., Warburton, N.M., 2020. Review of the methods used for calculating physiological cross-sectional area (PCSA) for ecological questions. *J. Morphol.* 281, 778–789. <https://doi.org/10.1002/jmor.21139>

Martin, M.L., Warburton, N.M., Travouillon, K.J., Fleming, P.A., 2019. Mechanical similarity across ontogeny of digging muscles in an Australian marsupial (*Isodon fusciventer*). *J. Morphol.* 280, 423–435. <https://doi.org/10.1002/jmor.20954>

Masseti, M., 1998. Holocene endemic and anthropochorous wild mammals of the Mediterranean Islands. *Anthropozoologica* 9, 3–20.

Meachen-Samuels, J., van Valkenburgh, B., 2009. Craniodental indicators of prey size preference in the Felidae. *Biol. J. Linn. Soc.* 96, 784–799. <https://doi.org/10.1002/jmor.10712>

Meiri, S., Dayan, T., Simberloff, D., 2004. Body size of insular carnivores: Little support for the island rule. *Am. Nat.* 163, 469–479. <https://doi.org/10.1086/382229>

Meloro, C., 2011. Feeding habits of Plio-Pleistocene large carnivores as revealed by the mandibular geometry. *J. Vertebr. Paleontol.* 31, 428–446. <https://doi.org/10.1080/02724634.2011.550357>

Mendez, J., & Keys, A. (1960). Density and composition of mammalian muscle. *Metabolism*, 9, 184–188.

Murphy, R. A., & Beardsley, A. C. (1974). Mechanical properties of the cat soleus muscle in situ. *American Journal of Physiology*, 227(5), 1008–1013. <https://doi.org/10.1152/ajplegacy.1974.227.5.1008>

Nanova, O., Prôa, M., 2017. Cranial features of mainland and Commander Islands (Russia) Arctic foxes (*Vulpes lagopus*) reflect their diverging foraging strategies.

- Polar Res. 36, 1-7. <https://doi.org/10.1080/17518369.2017.1310976>
- Nanova, O., Prôa, M., Fitton, L.C., Evteev, A., O'Higgins, P., 2017. Comparison of cranial performance between mainland and two island subspecies of the arctic fox *Vulpes lagopus* (Carnivora: Canidae) during simulated biting. *Biol. J. Linn. Soc.* 121, 923–935. <https://doi.org/10.1093/biolinnean/blx029>
- Palombo, M.R., 2018. Insular mammalian fauna dynamics and paleogeography: A lesson from the Western Mediterranean islands. *Integr. Zool.* 13, 2–20. <https://doi.org/10.1111/1749-4877.12275>
- Penrose, F., 2018. Cranial morphology and masticatory biomechanics in the canidae. PhD Thesis, University of Liverpool 372 pp.
- Penrose, F., Cox, P., Kemp, G., Jeffery, N., 2020. Functional morphology of the jaw adductor muscles in the Canidae. *Anat. Rec.* 303, 2878–2903. <https://doi.org/10.1002/ar.24391>
- Penrose, F., Kemp, G.J., Jeffery, N., 2016. Scaling and Accommodation of Jaw Adductor Muscles in Canidae. *Anat. Rec.* 299, 951–966. <https://doi.org/10.1002/ar.23355>
- Perry, J.M.G., 2018. Inferring the Diets of Extinct Giant Lemurs from Osteological Correlates of Muscle Dimensions. *Anat. Rec.* 301, 343–362. <https://doi.org/10.1002/ar.23719>
- Pigozzi, G., 1991. The diet of the European badger in a Mediterranean coastal area. *Acta Theriol. (Warsz)*. 36, 293–306. <https://doi.org/10.4098/at.arch.91-31>
- Popowics, T.E., 2003. Postcanine dental form in the Mustelidae and Viverridae (Carnivora: Mammalia). *J. Morphol.* 256, 322–341. <https://doi.org/10.1002/jmor.10091>
- Prevosti, F.J., Turazzini, G.F., Ercoli, M.D., Hingst-Zaher, E., 2012. Mandible shape in marsupial and placental carnivorous mammals: A morphological comparative study using geometric morphometrics. *Zool. J. Linn. Soc.* 164, 836–855. <https://doi.org/10.1111/j.1096-3642.2011.00785.x>
- Proulx, G., 2016. World Distribution and Status of Badgers — A Review, in: Proulx, G., Do Linh San, E., (Eds.), *Badgers: Systematics, biology, conservation and research techniques*. Alpha Wildlife pp. 31–116.
- Radinsky, L.B., 1981. Evolution of skull shape in carnivores. *Biol. J. Linn. Soc.* 15, 369–388. <https://doi.org/10.1111/j.1095-8312.1981.tb01657.x>
- Revilla, E., Palomares, F., 2002. Does local feeding specialization exist in Eurasian badgers? *Can. J. Zool.* 80, 83–93. <https://doi.org/10.1139/z01-208>
- Romaniuk, A., 2018. Shape variation of Palearctic mustelids (Carnivora: Mustelidae) mandible is affected both by evolutionary history and ecological preference. *Hystrix, Ital. J. Mammal.* 29, 87–94. <https://doi.org/10.4404/hystrix>
- Roper, T.J., 2010. *Badger*. Collins, New York. <https://doi.org/10.1017/CBO9781107415324.004>

- Roper, T.J., 1994. The European badger *Meles meles*: food specialist or generalist? J. Zool. 234, 437–452. <https://doi.org/10.1111/j.1469-7998.1994.tb04858.x>
- Roper, T.J., Mickevicius, E., 1995. Badger *Meles meles* diet: a review of literature from the former Soviet Union. Mamm. Rev. 25, 117–129. <https://doi.org/10.1111/j.1365-2907.1995.tb00451.x>
- Rosalino, L.M., Loureiro, F., Macdonald, D.W., Santon-Reis, M., 2005. Dietary shifts of the badger (*Meles meles*) in Mediterranean woodlands: An opportunistic forager with seasonal specialisms. Mamm. Biol. 70, 12–23. <https://doi.org/10.1078/1616-5047-00172>
- Sacco, T., Van Valkenburgh, B., 2004. Ecomorphological indicators of feeding behaviour in the bears (Carnivora: Ursidae). J. Zool. 263, 41–54. <https://doi.org/10.1017/S0952836904004856>
- Sakamoto, M., Lloyd, G.T., Benton, M.J., 2010. Phylogenetically structured variance in felid bite force: The role of phylogeny in the evolution of biting performance. J. Evol. Biol. 23, 463–478. <https://doi.org/10.1111/j.1420-9101.2009.01922.x>
- Sasaki, M., Endo, H., Yamagiwa, D., Takagi, H., Arishima, K., Makita, T., Hayashi, Y., 2000. Adaptation of the Muscles of Mastication to the Flat Skull Feature in the Polar Bear (*Ursus maritimus*). J. Vet. Med. Sci. 62, 7–14. <https://doi.org/10.1292/jvms.62.7>
- Sato, J.J., 2016. The Systematics and Taxonomy of the World's Badger Species – A Review. Badgers Syst. Biol. Conserv. Res. Tech. 1–30.
- Scapino, R.P., 1976. Function of the digastric muscle in carnivores. J. Morphol. 150, 843–859. <https://doi.org/10.1002/jmor.1051500405>
- Schneider, C. A.; Rasband, W. S. & Eliceiri, K. W. (2012), "NIH Image to ImageJ: 25 years of image analysis", Nature methods 9(7): 671-675, PMID 22930834
- Sfenthourakis, S., Triantis, K.A., 2017. The Aegean archipelago: A natural laboratory of evolution, ecology and civilisations. J. Biol. Res. 24, 4-14. <https://doi.org/10.1186/s40709-017-0061-3>
- Sicuro, F.L., Oliveira, L.F.B., 2011. Skull morphology and functionality of extant Felidae (Mammalia: Carnivora): A phylogenetic and evolutionary perspective. Zool. J. Linn. Soc. 161, 414–462. <https://doi.org/10.1111/j.1096-3642.2010.00636.x>
- Sicuro, F.L., Oliveira, L.F.B., 2002. Coexistence of peccaries and feral hogs in the Brazilian pantanal wetland: An ecomorphological view. J. Mammal. 83, 207–217. [https://doi.org/10.1644/1545-1542\(2002\)083<0207:COPAFH>2.0.CO;2](https://doi.org/10.1644/1545-1542(2002)083<0207:COPAFH>2.0.CO;2)
- Sleeman, D.P., Davenport, J., Cussen, R.E., Hammond, R.F., 2009. The small-bodied Badgers (*Meles meles* (L.)) of Rutland Island, Co. Donegal. Irish Nat. J. 30, 1–6.
- Spassov, N., 2016. Paleoanthropology of the Balkans and Anatolia, in: Harvati, K., Roksandic, M. (Eds.), Paleoanthropology of the Balkans and Anatolia. Springer,

pp. 281–290. <https://doi.org/10.1007/978-94-024-0874-4>

Spassov, N., 2003. The Plio-Pleistocene vertebrate fauna in South-Eastern Europe and the megafaunal migratory waves from the east to Europe. *Rev. Paleobiol.* 22, 197–229.

Stefen, C. (1997). Differentiations in Hunter-Schreger bands of carnivores. In: Koenigswald, W.V. & Sander, P.M. (Eds.): *Tooth enamel microstructure*, Balkema, Rotterdam, pp. 123–136.

Stefen, C., 1999. Enamel microstructure of Recent and fossil Canidae (Carnivora: Mammalia). *J. Vertebr. Paleontol.* 19, 576–587.
<https://doi.org/10.1080/02724634.1999.10011166>

Squarcia, S.M., Sidorkewicz, N.S., Casanave, E.B., 2007. The hypertrophy of the tympanic bulla in three species of dasypodids (Mammalia, Xenarthra) from Argentina. *Int. J. Morphol.* 25, 597–602. <https://doi.org/10.4067/S0717-95022007000300021>

Thomason, J.J., 1991. Cranial strength in relation to estimated biting forces in some mammals. *Can. J. Zool.* 69, 2326–2333. <https://doi.org/10.1139/z91-327>

Timm-Davis, L.L., DeWitt, T.J., Marshall, C.D., 2015b. Divergent skull morphology supports two trophic specializations in otters (Lutrinae). *PLoS One* 10, 1–18.
<https://doi.org/10.1371/journal.pone.0143236>

Tseng, Z.J., 2012. Connecting Hunter-Schreger Band microstructure to enamel microwear features: New insights from durophagous carnivores. *Acta Palaeontol. Pol.* 57, 473–484. <https://doi.org/10.4202/app.2011.0027>

Tseng, Z.J., Flynn, J.J., 2015. Are cranial biomechanical simulation data linked to known diets in extant taxa? A method for applying diet-biomechanics linkage models to infer feeding capability of extinct species. *PLoS One* 10, 1–25.
<https://doi.org/10.1371/journal.pone.0124020>

Turnbull, W.D., 1970. Mammalian Masticatory Apparatus. *Fieldiana Geol.* 18, 147–356.

Ungar P.S., Sues HD. (2019) Tetrapod Teeth: Diversity, Evolution, and Function. In: Bels V., Whishaw I. (eds) *Feeding in Vertebrates. Fascinating Life Sciences*. Springer, Cham. https://doi.org/10.1007/978-3-030-13739-7_11

Van Valkenburgh, B., 1990. Skeletal and dental predictors of body mass in carnivores. In: Damuth, J., MacFadden, B.J. (Eds.), *Body Size in Mammalian Paleobiology: Estimation and Biological Implications*. Cambridge University Press, pp. 181–205.

Van Valkenburgh, B., 2007. Déjà vu: The evolution of feeding morphologies in the Carnivora. *Integr. Comp. Biol.* 47, 147–163. <https://doi.org/10.1093/icb/icm016>

Vander Linden, A., Campbell, K.M., Bryar, E.K., Santana, S.E., 2019. Head-turning morphologies: Evolution of shape diversity in the mammalian atlas–axis complex. *Evolution (N. Y.)*. 73, 2060–2071. <https://doi.org/10.1111/evo.13815>



Virgós, E., Mangas, J.G., Blanco-Aguilar, J.A., Garrote, G., Almagro, N., Viso, R.P., 2004. Food habits of European badgers (*Meles meles*) along an altitude gradient of Mediterranean environments: A field test of the earthworm specialization hypothesis. Can. J. Zool. 82, 41–51. <https://doi.org/10.1139/z03-205>

Vislobokova, I.A., Agadjanian, A.K., 2016. On the history of Early—Middle Pleistocene mammal faunas of the Central Balkans. Paleontol. J. 50, 187–201. <https://doi.org/10.1134/S0031030116020106>

Zhang, S., Pan, R., Li, M., Oxnard, C., Wei, F., 2007. Mandible of the giant panda (*Ailuropoda melanoleuca*) compared with other Chinese carnivores: Functional adaptation. Biol. J. Linn. Soc. 92, 449–456. <https://doi.org/10.1111/j.1095-8312.2007.00876.x>

APPENDIX

Table 1. Most important examined characters

	<i>M. dimitrius</i>	<i>M. canescens</i> (Crete)	<i>M. meles</i>	<i>M. anakuma</i>	<i>M. leucurus</i>
Sagittal crest	overdeveloped	underdeveloped	medium	underdeveloped	medium
Structure connected to sagittal crest	present	absent	absent	absent	absent
Nuchal crest	overdeveloped	underdeveloped	medium	underdeveloped	medium
Foramen magnum	narrow, more vertically placed	narrow, more vertically placed	wider, more horizontally placed	narrow, more vertically placed	wider, more horizontally placed
Auditory bullae	-	inflated	flattened	inflated	flattened
Insertion of middle masseter	underdeveloped	underdeveloped	well developed	underdeveloped	well developed
Angular process	underdeveloped	well developed	well developed	well developed	well developed
M1 shape	wider, more rectangular	more elongated talonid	wider, more rectangular	more elongated talonid	wider, more rectangular
P4 blade	well developed	well developed	underdeveloped	well developed	underdeveloped
m1 shape	constricted	wider	constricted	constricted	constricted
HSB	acute	undulating	undulating	-	-
TFL	increased	increased	constricted	increased	constricted
BCW	increased	increased	constricted	increased	constricted
MSW	increased	increased	constricted	increased	constricted
IOD	increased	increased	constricted	increased	constricted
BCL	increased	increased	constricted	increased	increased
PL	increased	increased	increased	constricted	constricted
PW	constricted	constricted	constricted	increased	increased
RW	increased	increased	constricted	increased	constricted
MI & MI'	wider	wider	longer	wider	longer
DL	short	short	elongated	elongated	elongated
MRH	constricted	constricted	increased	increased	increased
CPr elevation	constricted	constricted	increased	increased	increased
Mechanical advantage	increased	increased	decreased	increased	decreased
M1a	constricted	medium (wide ranges)	increased	constricted	increased
UGR	constricted	wide ranges	increased	medium	medium
P4 shape	wider	wider	medium values	medium values	wide ranges
m1a	constricted	increased	increased	constricted	increased
m2a	constricted	wide ranges	increased	constricted	increased
LGR	constricted	increased	medium	constricted	medium
m1 blade	increased	increased	medium	increased	medium
Body mass	increased	increased	smaller	-	increased
Bite force	increased	increased	lower	-	increased
Endocranial volume	increased	increased	smaller	-	increased
Temporalis muscle	well developed	well developed	less developed	well developed	less developed
Pterygoid muscle	-	well developed	underdeveloped	-	-
Masseter muscle	less developed	less developed	well developed	less developed	well developed
Digastricus muscle	well developed	well developed	less developed	-	-



Plate I. *Meles dimitrius*

- (1) Cranium (APL – 544)
 - A. Dorsal view
 - B. Ventral view
 - C. Lateral view
- (1) Partial premaxilla, sin (APL 545)
 - D. Ventral view
 - E. Lateral view
 - F. Dorsal view
- (2) Mandible
 - A. Lateral view external, sin (APL – 772)
 - B. Dorsal view, sin (APL – 772)
 - C. Lateral view external, dex (APL – 546)
 - D. Dorsal view, dex (APL – 546)
 - E. Lateral view internal, dex (APL – 546)
 - F. Lateral view external, sin (APL – 15)
 - G. Dorsal view, sin (APL – 15)
 - H. Lateral view internal, sin (APL – 15)
- (3) Mandible
 - A. Dorsal view, sin (GER – 161)
 - B. Lateral view external, sin (GER – 161)
 - C. Lateral view internal, sin (GER – 161)
 - D. Dorsal view (GER – 162)
 - E. Lateral view external, sin (GER – 162)
 - F. Lateral view external, sin (GER – 162)
- (4) A. Partial Cranium (GER – 164)
 - B. Upper Canine (GER – 163)
 - C. Partial premaxilla (GER – 160)



